The Swift “Dragoon”

2021 AIAA Austere Field Light Attack Aircraft Design

Presented by: Team Swift Dragoon

Team Members				
				
Isaiah Cacka 1230402	Joseph Coldiron 1230703	Cody Cost 1230908	Taylor Hicks 1230887	Nathan Wolf 998647
Team Advisor: Dr. Ronald Barrett, 022393				

The University of Kansas Aerospace Engineering Department

Acknowledgements

The team would like to take this opportunity to thank several groups of people and individuals who have influenced the design work completed in this project. Firstly, we would like to thank our parents and families for supporting us in our youth and for encouraging us to pursue our dreams in the field of Aerospace Engineering. Secondly, we would like to thank the subject matter experts who provided insight into the various aspects of this design. We would especially like to thank the members of the Nebraska Army National Guard, Colonel Roger Disrud, Professor Adrian Lewis, Captain Emily Thompson, and Captain James Allen for providing insight into the deployment, desired characteristics, and effectiveness of the proposed design from an Air Force, Army and Navy perspective. We would also like to thank the underclassmen that volunteered their time to help us complete the project, including Matthew Berkshire who helped to render high quality images. Finally, we would like to acknowledge Dr. Ron Barrett for his support throughout this project, specifically in the munition's studies conducted.

Table of Contents

Page #

Acknowledgements ii

Table of Contents ii

List of Tables iv

List of Figures vi

List of Symbols ii

1 Introduction: Mission Specification and Profile 5

1.1 Design Requirements 5

1.2 Mission Profile 6

2 Historical Review of Aircraft, Ordnance, and Delivery Methods 6

2.1 Historical Review of Aircraft 6

2.2 Historical Review of Ordnance and Delivery Methods 10

3 Design Optimization Function, Class I Economics Model, Life-Cycle Cost Minimization, and Weights Establishment 16

3.1 Design Optimization Function 16

3.2 Class I Economic Analysis and Weight Establishment 17
4 STAMPED Analysis of Light Attack Market 18
5 Weight Sizing Code Generation 20
5.1 Empty Weight to Takeoff Weight Ratio 20
5.2 Preliminary Design Weights & Engine Type Selection 21
6 Wing and Powerplant Sizing 22
6.1 Wing Sizing 22
6.2 Powerplant Sizing 23
7 Class I Design Configuration Down Selection 26
7.1 Configuration Matrix 26
7.2 Configuration Down Selection 26
8 Class I Design 28
8.1 Fuselage Layout 29
8.2 Engine Installation 29
8.3 Wing Layout 30
8.4 Empennage 31
8.5 Landing Gear 31
8.6 Drag Polar Analysis 32
9 Hard-Launch Ballistics Analysis 34
10 Review of Target Engagement Methods with Conventional and Advanced Hard-Launched Ordnance 36
11 Stability and Control 42
12 Class II Layout of Major Systems 47
12.1 Flight Control and Electrical Systems 47
12.2 Fuel System 49
12.3 Hydraulic System 49
12.4 Targeting Systems and Optics 50
12.5 Cockpit Instrumentations, RF, and Sat Coms 51
12.6 De-Icing and Anti-Icing Systems, Window Rain, Fog, and Frost Control 51

12.7 Gun System, Round Handling and Loading 52
12.8 Missile Accommodation, Loading and Launch 59
12.9 Bomb Accommodation, Loading and Launch 62
12.10 Internal Weapon Release and Egress 64
12.11 Safety and Survivability: Fault-Tree Analysis, Ejection Seats, Crashworthiness and Armor 66
12.12 Ground Equipment, Ergonometrics and Vehicle Compatibility 67
13 Class II Landing Gear 68
14 Class II Performance 69
14.1 Takeoff 69
14.2 Climb 69
14.3 V-n Diagram 70
14.4 Payload-Range Diagram + Utilization Analysis 70
14.5 Maneuvering 71
14.6 Landing 71
15 Class II Weight and Balance 71
16 Class II 3-View, Advanced CAD, Situational Rendering, and Exploded Views 74
17 Advanced Technologies and Risk Mitigation 77
17.1 Remote Crew 77
17.2 Observables Mitigation 77
17.3 MASS Rounds 78
17.4 Pod 78
17.5 Cross-shafting 78
18 Class II Cost Analysis 79
19 Manufacturing Plan 79
20 Compliance to Design Specification and TRL Considerations 83
References 84

List of Tables

Table 1.1: Light Attack Aircraft General Requirements [1] 5

Table 2.1: 0.50 BMG Rounds [33] 11
Table 2.2 20mm Shells [37] 12
Table 2.3: 25mm Shells [40] 13
Table 2.4: Gravity Weapons Categorized by Weight Class [38-41] 14
Table 2.5: U.S Guided Missiles [55-62] 15
Table 2.6: U.S. Unguided Rockets [52,53] 15
Table 3.1: Table of Design Requirements, Objectives, and Additional Objectives 16
Table 3.2: GOF Results of Dragoon Aircraft Compared to Competitors and the A-10 17
Table 3.3: Economic Comparison of Competitive Aircraft in the Market [19,21,64,65] 18
Table 5.1: Important Values Used for Sizing 21
Table 8.1: Aircraft Salient Characteristics 28
Table 8.2: Engine Characteristics 30
Table 8.3: Wing Characteristics 30
Table 8.4: High Lift Device Sizing Values 31
Table 8.5: Wetted Area 32
Table 8.6: Class I Drag Polar 33
Table 10.1: Reference Aircraft Weapons Installments 36
Table 11.1: Stability and control regulations and calculations 43
Table 11.2: Stability and control derivatives 45
Table 12.1: Control Surface Actuator Requirements 47
Table 12.2: Electrical Requirements 48
Table 12.3: Main Landing Gear Pressure Requirements 50
Table 12.4: Main Landing Gear Pressure Requirements with Spring System 50
Table 12.5: Wescam MX-20D Sensors 50
Table 12.6 Gun Platforms Considered for Use in Design [34,36,38,39,41,179,180,181] 52
Table 12.7 Shell Effectiveness Against Targets Based on Armor Level 53
Table 12.8 Kill Mechanism Costs 53
Table 12.9: Combat Turn Rearmament Time Budget 58

Table 12.10: Single Aileron Control Surface Fault Tree Analysis Probabilities 66

Table 13.1: Landing Gear Strut and Tire Load Force and Ratios 68

Table 13.2: Salient Tire Characteristics 68

Table 13.3: Landing Gear Strut Sizing 68

Table 15.1: Class II Component Weight Breakdown 72

Table 18.1: RDT&E Costs 79

Table 18.2: Manufacturing, Acquisition, Operating, and Life Cycle Costs (50 Units) 79

Table 19.1: Wing Material Selection 80

Table 19.2: Empennage Material Selection 81

Table 19.3: Fuselage Material Selection 81

Table 20.1: Specification Compliance Matrix 83

Table 20.2: TRL for Critical Aircraft Systems 83

List of Figures

Figure 1.1: Design Mission Profile at Full Payload & Ferry Mission Profile with Full Crew & 60% Payload 6

Figure 2.1: Junker Ju-87 [2] 7

Figure 2.2: HS 129 [4] 7

Figure 2.3: P-40 [6] 8

Figure 2.4: P-47 Thunderbolt [8] 8

Figure 2.5: Hawker Typhoon [10] 8

Figure 2.6: A-1 Skyraider [14] 9

Figure 2.7: Il-2 [12] 9

Figure 2.8: OV-10 Bronco [16] 9

Figure 2.9: EMB 314 Super Tucano [20] 9

Figure 2.10: A-10 Thunderbolt II [18] 10

Figure 2.11 Scaled View of Ground Attack Gun Platforms [15-19] 11

Figure 2.12 M791 APDS-T [40] 12

Figure 2.13: GAU-8 Installed in A-10 Nose [42] 13

Figure 2.14: M230 Installed on AH-64 [43] 13

Figure 2.15: Relative Shell Sizes [44] 14
Figure 2.16: Scaled Munitions 15
Figure 4.1: W_E with respect to W_{TO} [59-159] 18
Figure 4.2: W_E and W_{TO} with respect to time [59-159] 19
Figure 5.1: W_E/W_{TO} with respect to time [59-159] 20
Figure 6.1: Preliminary Sizing Drag Polar 23
Figure 6.2: L/D Ratio over Airspeed at FL3 23
Figure 6.3: L/D Ratio over Airspeed at FL350 24
Figure 6.4: L/D Ratio over Airspeed 24
Figure 6.5: Specific Range over Wing Loading 24
Figure 6.6: Wing Sizing Chart 25
Figure 7.1: Configuration 1 26
Figure 7.2: Configuration 2 26
Figure 7.3: Configuration 3 26
Figure 7.4: Configuration 4 26
Figure 7.5: Configuration 5 27
Figure 7.6: Configuration 6 27
Figure 7.7: Configuration 7 27
Figure 7.8: Configuration 8 27
Figure 7.9: Configuration 9 27
Figure 8.1: Isometric View of Fuselage Structure. Scale: 1:100 in. 29
Figure 8.2: Side Cutout View of Fuselage. Scale: 1:100 in. 29
Figure 8.3: Isometric View of Powerplant and surrounding Boom Structure. Scale: 1:60 in. 29
Figure 8.4: Rolls-Royce M250 [193] 30
Figure 8.5: Isometric View of Wing and Wing Structure 30
Figure 8.6: Isometric View of Empennage and Empennage Structure 31
Figure 8.7: Side, Front, and Isometric Views of Landing Gear Placement 31
Figure 8.8: Fuselage Perimeter Plot 32

Figure 8.9: Class I Drag Polar 33
Figure 9.1: Acceleration, Velocity, and Position Equations [171] 34
Figure 10.1 BASS Round Turn Avoidance [175] 36
Figure 10.2 Kinetic Energy (top) and Time (bottom) vs. Range (ft) 37
Figure 10.3 Armor Penetration Capabilities of Ground Attack Shells 38
Figure 10.4: Strafing Run CONOPS 39
Figure 10.5: Orbit Attack CONOPS 39
Figure 10.6 4 Mile Standoff Altitude Sweep Munitions Range Analysis 40
Figure 10.7 15,500 ft Altitude, 1 mi Orbit Direct Fire (BASS 2581/2583) 41
Figure 10.8 BASS Rounds Time of Flight for Indirect and Direct Fire 41
Figure 11.1: Class I longitudinal stability 42
Figure 11.2: Class I Directional Stability 43
Figure 11.3: Dutch roll characteristics graphed in AAA 44
Figure 11.4: Short period characteristics graphed in AAA 44
Figure 11.5: Trim diagram 46
Figure 12.1: Layout of Wiring and Placement of Flight Computers and Control Surface Actuators 47
Figure 12.2: Electrical System Layout 48
Figure 12.3: Fuel System Layout 49
Figure 12.4: Hydraulic System Layout 49
Figure 12.5: Wescam MX-20D (Manufacturer Photo and CAD) [176] 50
Figure 12.6: Cockpit Instrumentation Layout 51
Figure 12.7: Graphene De-icing System [178] 51
Figure 12.8: Bleed Air De-icing System 52
Figure 12.9: Number of Rounds Carried VS Caliber 53
Figure 12.10 M242 Bushmaster Dual Feed System 54
Figure 12.11 M242 Bushmaster 25mm Chain Gun 55
Figure 12.12 M242 Bushmaster Cannon Placement for Strafe Engagements 55
Figure 12.13 M242 Strafe Mode Armored Trough with Integrated Muzzle Break 56

Figure 12.14 M242 Bushmaster Aerodynamic Shroud Shown in Orbit Mode 56
Figure 12.15: Water Based Barrel Cooling System 57
Figure 12.16 M242 Bushmaster Integration and Spent Casing Ejection 58
Figure 12.17: Boresight Dynamics for Laser Guided Weapons [186] 60
Figure 12.18: Optional External Missile Hardpoints 61
Figure 12.19: Toss Bombing Engagement Diagram [187] 63
Figure 12.20 Ground Turn Pod Loading 64
Figure 12.21 Internal Stores Egress Diagram 65
Figure 12.22: Example Fault Tree Analysis Diagram 66
Figure 12.23: Armored Cockpit & Ejection Seats Bathtub 66
Figure 12.24: Refueling Reach 67
Figure 12.25: Engine Reach 67
Figure 12.26: Ground Services 68
Figure 14.1: Rate of Climb Envelope 69
Figure 14.2: V-n Diagram 70
Figure 14.3: Payload-Range Diagram 70
Figure 14.4: Sustained Turn Rate 71
Figure 15.1: Class II Center of Gravity Excursion Diagram 73
Figure 16.1: 3-View 74
Figure 16.2: Dragoon Exploded View 75
Figure 16.3: Situational Rendering at a Remote Airbase 76
Figure 17.1: Aircraft Exhaust and Chevrons 78
Figure 17.2: Cross-Shafted Engines 78
Figure 18.1: Aircraft Production Unit Costs 80
Figure 19.2: Wing Assembly Flow Chart 80
Figure 19.3: Empennage Assembly Flow Chart 81
Figure 19.4: Fuselage Assembly Flow Chart 81
Figure 19.5: Aircraft Final Assembly Flow Chart 82

List of Symbols

Symbol	Description	Units
A	aspect ratio	(~)
a	acceleration	(ft/s^2)
a_0	speed of sound	(ft/s)
c.g.	center of gravity	(~)
c_j	specific fuel consumption	(lbf/lbf-hr)
c_p	specific fuel consumption	(lbf/hp-hr)
C_A	axial coefficient	(~)
C_{A0}	adjusted axial coefficient	(~)
C_D	coefficient of drag	(~)
C_{D_0}	zero lift drag coefficient	(~)
C_f	friction coefficient	(~)
C_f/C	flap chord to wing chord ratio	(~)
C_l	rolling moment coefficient	(~)
C_L	coefficient of lift	(~)
C_m	pitching moment coefficient	(~)
C_n	yawing moment coefficient	(~)
C_y	sideslip coefficient	(~)
d	diameter	(ft)
D	drag	(lbf)
e	Oswald's efficiency factor	(~)
k	gain	(~)
l	length	(ft)
l_p	propeller loading factor for k2	(~)
L	lift	(lbf)
M	Mach number	(~)
m	mass	(lbm)
n	loading factor	(~)
N	number of components	(~)
P	power	(hp)
$\bar{q}$	dynamic pressure	(lbf/ft^2)
RC	rate of climb	(ft/min)
RCP	rate of climb parameter	(ft/min)
s	length	(ft)
S	wing area	(ft^2)
S_b	Ballistic Reference Area	(ft^2)
t	time	(s)
t/c	thickness to chord ratio	(~)
T	thrust	(lbf)
T_r	roll mode time constant	(s)
T_{2s}	spiral time to double amplitude	(s)
V	velocity	(ft/s)
W	weight	(lbf)
X_i	position in x-direction at time i	(ft)
Y_i	position in y-direction at time i	(ft)

Greek Symbols	Description	Units
α	angle of attack	(°)
β	sideslip angle	(°)
δ	deflection	(~)
γ	flight path angle	(°)
η_p	propeller efficiency	(~)
λ	taper ratio	(~)
μ_g	California bearing ratio	(~)
ρ	air density	(slug/ft^3)
σ	density ratio	(~)
τ	ratio of tip t/c to root t/c	(~)
ω_n	natural frequency	(~)
ζ	damping ratio	(~)

Subscripts	Description	Units
A	approach	(~)
aero	aerodynamic	(~)
CL	climb	(~)
E	empty	(~)
f	fuselage	(~)
F	fuel	(~)
FL	field	(~)
h	horizontal tail	(~)
L	landing	(~)
P	propeller	(~)
r	root	(~)
SL	stall	(~)
t	tip	(~)
tot	total	(~)
TO	takeoff	(~)
TOG	takeoff ground	(~)
w	wing	(~)
x	x-direction	(~)
y	y-direction	(~)
0	initial	(~)

Acronyms	Description
AB-MBD	Air Burst, Motor-Burnout Delay
AMP	Average Market Price
AP	Armor Piercing
APDS-T	Armor Piercing Discarding Sabot-Tracer
APEI	Armor Piercing Explosive Incendiary
APEX	Armor Piercing Explosive
APFSDS-T	Armor Piercing Fin-Stabilized Discarding Sabot-Tracer
API	Armor Piercing Incendiary
API-DT	Armor Piercing Incendiary Dim Tracer
API-T	Armor Piercing Incendiary-Tracer
APKWS	Advanced Precision Kill

Weapon System
APU ..... Auxiliary Power Unit
BASS ..... Ballistic Aeromechanically Stable Sabot
BCM ..... Ballistic Coefficient Multiplier
BMAB-MBD ..... Base Mount, Air Burst, Motor-Burnout Delay
BMRC-PD-PS ..... Base Mount, Resistance Capacitance, Payload Discharging Pilot-Selectable
CAS ..... Close Air Support
CCD ..... Charge Coupled Device
CEB ..... Combined Effects Bomb
CG ..... Center of Gravity
CGD ..... Command Guidance Datalink
CONOPS ..... Concept of Operations
CSO ..... Combat Systems Officer
DT ..... Dim Tracer
EO ..... Electro-Optical Guidance
F ..... Frangible
FAPDS-T ..... Frangible Armor Piercing Discarding Sabot-Tracer
FFAR ..... Folding-Fin Aerial Rocket
FL ..... Flight Level
FMJ ..... Full Metal Jacket
FMJBT ..... Full Metal Jacket with Boat Tail
GOF ..... General Optimization Function
GPS ..... Global Positioning System
HEDP ..... High Explosive Dual Purpose
HEI ..... High Explosive Incendiary
HEIAP ..... High Explosive Incendiary Armor Piercing
HEI-T ..... High Explosive Incendiary-Tracer
HEI-T-SD ..... High Explosive Tracer with Self-Destruct
HE-SF ..... High Explosive Semi-Fixed
I ..... Incendiary
IIR ..... Imaging Infrared
INS ..... Inertial Navigation System
JAGM ..... Joint Air-to-Ground Missile
JSOW ..... Joint Standoff Weapon
LR-HPBT ... Long Range Hollow Point Boat Tail
KEAS ..... Knot Equivalent Airspeed
LE ..... Leading Edge
MCG ..... Mean Geometric Chord
MMWR ..... Millimeter Wave Radar Seeker
MPLD-T ..... Multi-Purpose Low Drag-Tracer
MP-T ..... Multi-Purpose-Tracer
MPT-SD ..... Multi-Purpose Tracer with Self-Destruct
NMPD ..... Nose Mount, Point Detonating
NMPD-HSP Nose Mount, Point Detonating-High Speed Platforms
NMPD-SSP ..... Nose Mount, Point Detonating-Low Speed Platforms
NMRC ..... Nose Mount, Resistance Capacitance
PAB ..... Proximity Air Burst
PABM-T ..... Programmable Air Burst Munition-Tracer
PD ..... Point Detonating
RFP ..... Request for Proposal
SALH ..... Semi-Active Laser Homing
SAPHEI ..... Semi-Armor Piercing High Explosive Incendiary
SAPHEI-T Semi-Armor Piercing High Explosive Incendiary-Tracer
SLAM-ER ..... Standoff Land Attack Missile Expanded Response
SLAP ..... Saboted Light Armor Penetrator
SLAP-T ..... Saboted Light Armor Penetrator-Tracer
SPT-FMJ ..... Spitzer Pointed Full Metal Jacket
SSR ..... Sea Skimming Radar
T ..... Tracer
TE ..... Trailing Edge
TP ..... Training Purpose
TP-T ..... Training Purpose-Tracers
TRL ..... Technology Readiness Level
TSFC ..... Thrust Specific Fuel Consumption
WSO ..... Weapons System Officer

1 Introduction: Mission Specification and Profile

Direct support of troops with close air support (CAS) requires aircraft of high quality – a priority common across all military services. Fixed-wing light attack aircraft have proven effective as ground-attack CAS and date back to as early as WWI. The American Institute of Aeronautics and Astronautics (AIAA) released a Request for Proposal (RFP) for an affordable light attack aircraft capable of operating from short, austere fields near the front lines to provide CAS to ground forces on short notice and of completing some missions currently only feasible with attack helicopters [1]. This report was constructed to fulfill the requirements set forth by AIAA. To provide this air support, strafing runs, orbit, traditional bombing, and stand-off bombing were considered in the design of the aircraft.

1.1 Design Requirements

Table 1.1 provides the target mission specifications as given by AIAA in the RFP [1].

Table 1.1: Light Attack Aircraft General Requirements [1]

Design Mission Requirements	
Crew	2 crew members (zero-zero ejection seats)
Range	Minimum 2,500 nmi (Ferry Mission)
Additional Considerations	Survivability measures (Low Observables) Complete missions currently feasible only with attack helicopters
Certifications	Critical technologies TRL 8 or above MIL-STD-516C and JSSGs
Performance Requirements	
Austere Field Performance	Take-off & Landing over 50ft obstacle ≤ 4000ft
Density Altitude of Austere Field	Up to 6000 ft
Runway Conditions	California Bearing Ratio of 5 (grass or dirt surfaces)
Service Ceiling	≥ 30,000ft
Minimum Cruise Speed	310 kts per the mission profile
Service Life	
Production Run Duration	Service Life of +25 years or 15,000 hours
Hourly Cost	Less costly than current market
Entry into Service	2025
Ordnance Requirements	
Payload	3000 lb. armament
Weapons Provisions	Integrated gun, ability to carry rail-launched missiles, rockets, and bombs (500 lb. max)

1.2 Mission Profile

The following mission profiles were derived from the RFP. The aircraft design must be capable of performing both a design mission at full payload as well as a long-range ferry mission with full crew and 60% of the payload requirement. A requirement of both mission profiles, the aircraft designed must take-off and land over a 50 ft obstacle within 4,000 ft when operating from austere fields at a density altitude up to 6,000 ft with semi-prepared runways such as grass or dirt surfaces with California Bearing Ratio of 5. Additionally, for the design mission there is an inherent cruise speed from the requirement that the aircraft complete a 100 nmi cruise and descend to station within a period of 20 minutes. A cruise speed of 310 kts, as shown later, was chosen by the team to ensure the aircraft can complete the cruise and descent in the allotted time [1].

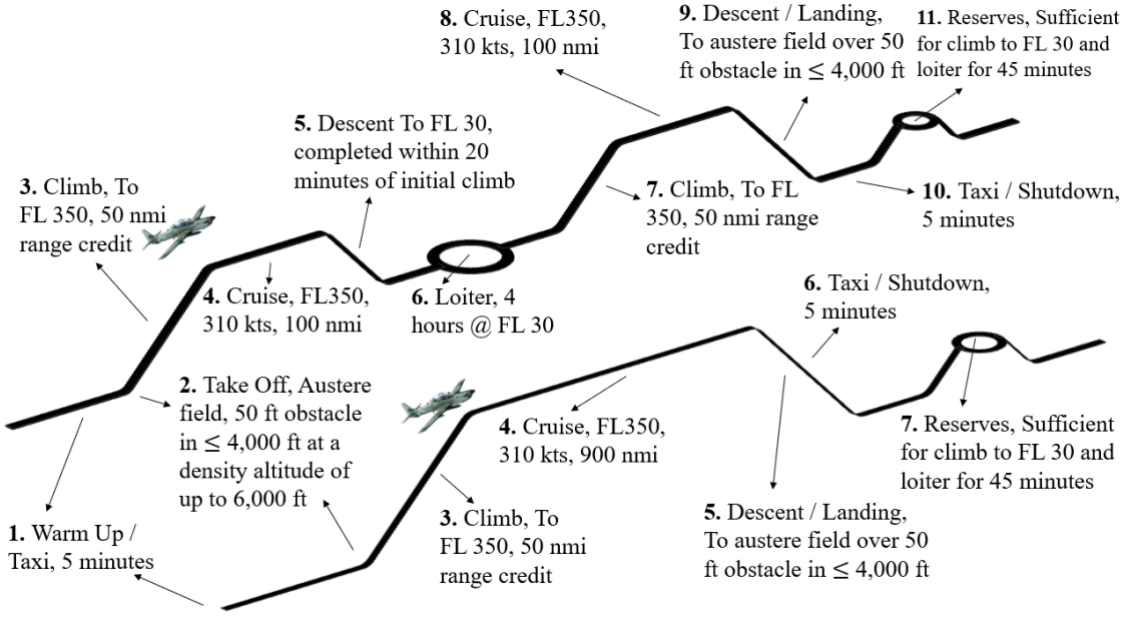

Figure 1.1: Design Mission Profile at Full Payload & Ferry Mission Profile with Full Crew & 60% Payload

2 Historical Review of Aircraft, Ordnance, and Delivery Methods

This chapter will describe aircraft, ordnance, and delivery methods historically used for light attack aircraft.

2.1 Historical Review of Aircraft

The importance of light attack aircraft was understood as early as WWI where pilots dropped flechettes and small ordnance at ground forces in an attempt to disrupt enemy supply lines and attack enemy trenches in the hopes of

breaking the stalemates that often developed in them. However, the first true light attack aircraft were developed and extensively used in WWII.

The Germans, fearing the stalemates of WWI, developed a new method of warfare: Blitzkrieg or "lightning war," relying on fast mechanized units to push through an opponent's line of defense and get behind enemy lines before a proper defense could be mounted. To this end, light attack aircraft were developed to help ground forces.

Figure 2.1: Junker Ju-87 [2]

The first light attack aircraft fielded by German forces was the Ju 87, or Stuka, to great success. The Ju 87 first flew in 1935 with around 6,000 aircraft being produced. It had a crew of two (a pilot and a rear gunner) and was powered by a 1,200 hp V-12 inverted, liquid-cooled Jumo 211 piston engine. The aircraft had an empty weight of 5980 lb. and a max takeoff weight of 9560 lb. The Ju 87 was used throughout the war as a dive bomber and ground attack aircraft, with many modifications and configurations. The aircraft had two forward 7.92 mm MG 17 machine guns and one rear 7.92mm MG 15 machine gun. Additionally, the Ju 87 could carry up to a 500 lb. bomb or 4 x 110 lb. bombs under the wings. Two large 37 mm gun pods could also be mounted to points under the wing [3].

Figure 2.2: HS 129 [4]

Later in the war Germany required a new, more powerful light attack aircraft that could effectively take out armored vehicles, leading to the development of the HS 129. The HS 129 first flew in 1939 with 865 being produced. The HS 129 had a crew of one and had an empty weight of 8863 lb. with a max takeoff weight of 11,574 lb. The HS 129 was unique in that it was a heavily armored with the plane designed around a large "bathtub" of steel that encompassed the cockpit and nose of the aircraft. Even the canopy was steel with only small windows, slanted heavily to deflect bullets. The aircraft was continually up gunned as tank armor improved. The aircraft was originally equipped with 2 x 7.92 mm MG 17 machine guns in the nose, but later models equipped 2 x 13 mm MG 131 machine guns instead. The belly of the aircraft was originally configured to carry 4 x 110 lb. fragmentation bombs, but a belly gun pod soon replaced the bombs and mounted 2 x 20 mm MG 151/20 cannons then later a single 30 mm cannon, and finally a 75 mm Rheinmetall PaK 40 anti-tank gun theoretically capable of destroying any tank in the world at the time. In addition, the wings could accommodate 2 x 110 lb. bombs on underwing hardpoints. Unfortunately, the HS 129 was plagued with engine problems first using two low-power German Argus AS 410 V-12 air-cooled engines generating 459 hp each and later

two French 14-cylinder Gnome-Rhone 14M air-cooled radial engines generating 691 hp each, neither of which generated adequate power [5].

The United States also developed light attack aircraft in WWII, the first of which was the P-40 Warhawk. It first flew in 1938 with 13,738 aircraft being produced by the Allied Powers. The P-40 had a crew of one and was powered by a V-12 liquid-cooled Allison piston engine producing 1,240 hp. With an empty weight of 5,922 lb. and a max takeoff weight of 9,200 lb., the P-40 was equipped with 6 x 0.5 in. M2 Browning machine guns in the wings as well as the capability to mount up to 2,000 lb. of bombs across three hardpoints. The P-40 was also an exceptional fighter with over 200 Allied fighter pilots becoming aces flying the P-40 including at least 20 double aces [7].

Figure 2.3: P-40 [6]

The P-47 Thunderbolt was later developed as a light attack aircraft, with its first flight in 1941 and 15,636 being produced. The P-47 had a crew of one and was powered by an 18-cylinder air-cooled radial piston Pratt and Whitney R-2800-59 engine producing 2,000 hp. With an empty weight of 10,000 lb. and a max takeoff weight of 17,500 lb., it carried 8 x M2 Browning machine guns, up to 2,500 lb. of bombs across three hardpoints and 10 x 5-in unguided rockets. The P-47 was especially suited for ground attacks with an armored cockpit and radial engines which were more damage tolerant than comparable liquid-cooled engines [9].

Figure 2.4: P-47 Thunderbolt [8]

In addition to using designs produced by the United States, the United Kingdom used the Hawker Typhoon as a light attack aircraft. First flying in 1940 and with 3,317 being produced, the Hawker Typhoon had a crew of one and was powered by a liquid cooled 24 piston Napier Sabre IIA producing 2,180 hp. With an empty weight of 8,840 lb. and a max takeoff weight of 13,250 lb., the aircraft was equipped with 4 x 20 mm Hispano MK II cannons and could carry 8 x RP-3 unguided rockets as well as up to 2 x 1000 lb. bombs [11].

Figure 2.5: Hawker Typhoon [10]

Similarly, the Soviets developed the Il-2 as a light attack aircraft in addition to using aircraft developed by the United States. The Il-2 first flew in 1939 with 36,183 produced. The aircraft had a crew of two (a pilot and a rear gunner) and was powered by a liquid cooled V12 Mikulin AM-38F engine producing 1,720 hp with an empty weight

Figure 2.7: Il-2 [12]

of 9,755 lb. and a maximum takeoff weight of 14,021 lb. The Il-2 was equipped with 2 x forward firing 23 mm VYa-23 cannons, 2 x forward firing 7.62 mm ShKAS machine guns, and a single rear turreted 12.7 mm UBT machine gun. In addition, the Il-2 could be equipped with 8 x RS-82 rockets and 6 x 220 lb. bombs in wing bomb bays and underwing mounts [13].

After WWII the light attack aircraft role was taken by the carrier-based A-1 Skyraider in the United States. The first flight of the A-1 was in 1945 and it remained in service until 1985 with 3,180 being produced. The plane had a crew of one (although variants had up to a crew of three) and was powered by an 18-cylinder air-cooled radial Wright R-3350-26WA engine producing 2,700 hp, with an empty weight of 11,968 lb. and a max takeoff weight of 18,106 lb. The A-1 Skyraider was equipped with 4 x 20 mm AN/M3 cannons and 15 external hardpoints with a capacity of 8,000 lb. It had the ability to carry combinations of bombs, torpedoes, mine dispensers, unguided rockets, and gun pods [15].

Figure 2.6: A-1 Skyraider [14]

Later light attack aircraft include the OV-10 Bronco, a twin turboprop light attack and observation aircraft that first flew in 1965 and is still in limited service with 360 produced. The aircraft has a two-man crew and is powered by two Garrett T76-G-420 turboprop engines producing 1,040 hp each with an empty weight of 6,893 lb. and a max takeoff weight of 14,444 lb. The OV-10 is equipped with either a single 20 mm M197 cannon or 4 x 7.62 mm M60C machine guns in addition to having five fuselage and two underwing hardpoints capable of carrying combinations of 7 or 19 tube 2.75 in FFars rockets, AIM-9 Sidewinders, or up to 500 lb. of bombs [17].

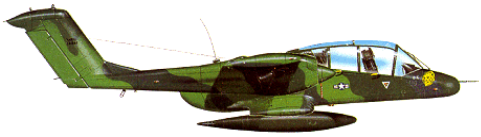

Figure 2.8: OV-10 Bronco [16]

Modern attack aircraft include the Brazilian EMB 314 Super Tucano, which is a light attack aircraft, and the United States' A-10 Thunderbolt II, which is not a light attack aircraft but has been an extremely successful attack aircraft. The EMB 314 Super Tucano first flew in 1999 with at least 200 produced and is still in production. The aircraft has a crew of two (a pilot and a navigator) and is powered by a Pratt and Whitney PT6-A-68C turboprop generating 1,604 hp with an empty weight of 7,055 lb. and a max takeoff weight of 11,605 lb. The EMB 314 is equipped with 2 x internal 12.7 mm FN Herstal machine

Figure 2.9: EMB 314 Super Tucano [20]

guns with 5 external hardpoints (two under each wing and one under fuselage) with a capacity of 3,300 lb. with the capability of carrying rockets, missiles, bombs, and electronics [21].

The A-10 first flew in 1977 and is still in wide service with 716 aircraft produced. The plane has a crew of one and is powered by two GE TF34-GE-100A turbofans producing 9,065 lbf with an empty weight of 24,959 lb. and a max takeoff weight of 50,000 lb. The A-10 is unique in that it is built around its massive 30 mm GAU-8/A rotary cannon, with an additional 11 hardpoints (8 underwing and 3 belly stations) providing a capacity of 16,000 lb. of rockets, missiles, bombs, and sensors in many combinations. The A-10 is extremely tough, surviving up to 23 mm armor piercing and high explosive rounds with a double redundant hydraulic flight system and a mechanical back up system if hydraulics are lost. The cockpit and critical parts of the aircraft are protected by 1,200 lb. of titanium aircraft armor similarly to the armored "bathtub" of the HS 129. In addition, the front windscreen and canopy are built to resist small arms fire [19].

Figure 2.10: A-10 Thunderbolt II [18]

"The A-10's gun could turn your house to toothpicks."
-Col. Roger Disrud, USAF,A-10 Pilot, Top Gun

2.2 Historical Review of Ordnance and Delivery Methods

The history of munitions deployed via light attack aircraft is as varied as the history of the aircraft that have delivered them. The following sections highlight the variety of hard launch, gravity, and rocket munitions fielded by United States Air Force and Army light attack aircraft. Figure 2.11 below, shows scaled images of ground attack gun platforms designed for, and used by the United States Military.

Shortly after the Army adopted the 5.56 NATO round as the standard infantry round in 1963 [22], development began on the XM214 Microgun, a platform capable of firing the standard issue rounds deployed by the infantry; however, the XM214 fell short of expectation as the gun was plagued by reduced accuracy caused by high volumes of fire and a lack of effective range compared to other cartridges and platforms [23].

Adopted in 1957 and Chambered in 7.62 NATO, the M60 machine gun has served all branches of the military. The M60 saw service over the jungles of Vietnam as a defensive weapon aboard search and rescue helicopters [24], and the role revealed one of the major flaws of single barreled weapons, as the intense suppressive fire frequently led to overheating guns and subsequent failures. In 1963 General Electric designed the M314 Minigun, a six-barreled

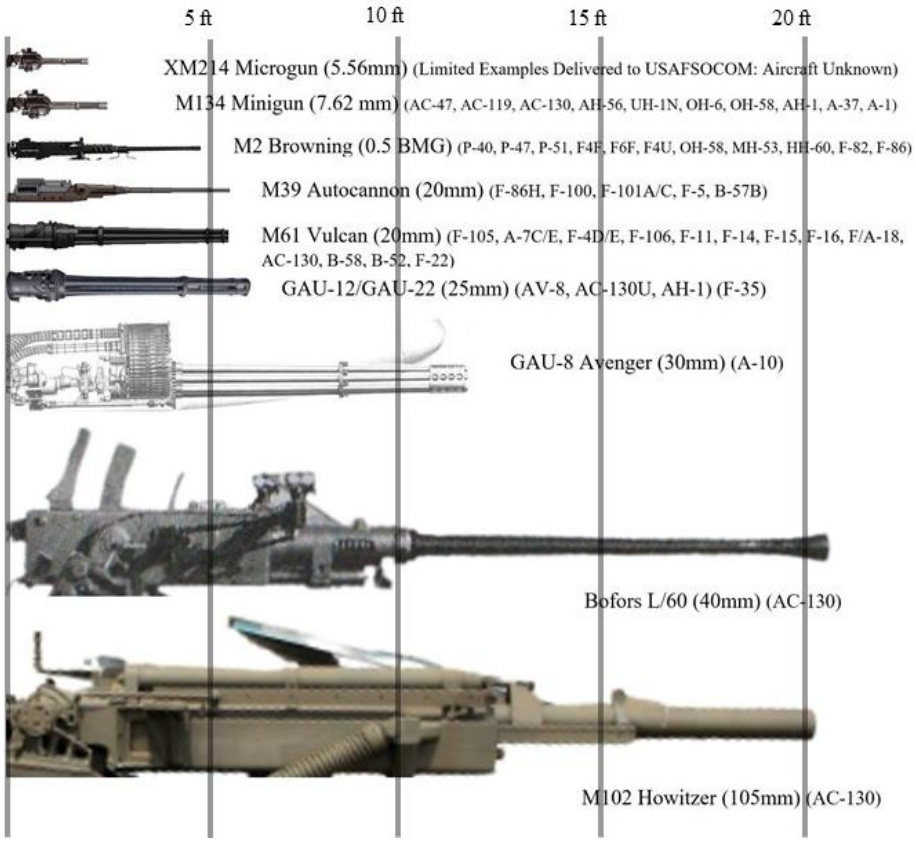

Figure 2.11 Scaled View of Ground Attack Gun Platforms [15-19]

rotary gun, to act as a replacement platform that could deliver high volumes of fire without reliability issues and gave aircrews a much-needed increase in firepower [31]. Both the M60 and M314 platforms continue service in multiple branches of the military, though the M60 is currently being phased out of service in favor of the M240 machine gun. Developed as a replacement gun for the coaxial mounted machine guns onboard tanks, the M240 was adopted by the Army in 1977, and in many other roles since then. Equipped with a quick-change barrel design, the M240 is more resilient to sustained fire than its predecessor [32].

Designed in the closing days of World War One, the M2 Browning is possibly the most recognized of United States heavy machine guns. Chambered in .50 BMG, the M2 and its descendants have seen constant service with all branches of the United States Military since 1933. The M2 flew combat missions onboard Allied fighters and bombers throughout the Second World War. Aboard the P-47 and other aircraft, the M2 flew ground attack missions into the heart of Germany, harassing axis supply lines and protecting allied ground forces. Service aboard fighter and ground attack aircraft continued into the Korean War, but eventually the M2 was replaced

Table 2.1: 0.50 BMG Rounds [33]

Designation	Effect
M1	T
M1	I
M2	Ball
M2	AP
M8	API
M10	T
M20	API-T
M21	T
M23	I
M903	SLAP
M962	SLAP-T
Mk211	HEIAP
Mk257	API-DT
Mk263	AP

by larger caliber cannons as the primary armament onboard United States ground attack aircraft. Firing a range of shells shown in Table 2.1, the M2 has continued to see action as a crew served weapon aboard a variety of military vehicles [34]. A continuation of the 0.50 BMG line, the Profense PF50, developed in 2018, features a remote-control Gun Control Unit (GCU), allowing for installation onboard unmanned vehicles [35].

"*The caliber of gun matters: If you have a 20mm, it's better than 0.50 cal. 25 is better than 20 and 30 gets all the jobs done.*"
-Prof. Adrian Lewis, US Army Special Forces Officer, Ret.

Designed in the late 1940s, the M39 autocannon offered a major advance in aircraft armament but was not without flaws. Chambered in 20mm, this platform delivered more powerful rounds than previous systems, and was quickly adopted for use in the ground attack role. Despite its effectiveness downrange, the revolver feed system used in the M39 was vulnerable to barrel wear, overheating, and parts reliability issues [36]. Further development of gun platforms capable of firing 20mm shells continued, and in 1959 General Electric launched the M61 Vulcan. A six barreled rotary cannon capable of firing at 6,000 rounds per minute, the design of the M61 addressed the issues present in revolver feed systems by rotating the barrels rather than the chamber, thus reducing wear on the barrels by increasing the time between shots and allowing the barrels to cool more effectively than single barrel platforms, without sacrificing the rate of fire of the cannon. Capable of firing a wide variety of cannon shells shown in Table **2.2**, the M61 has seen service as the primary weapon for most American fighter aircraft for the past 60 years [38].

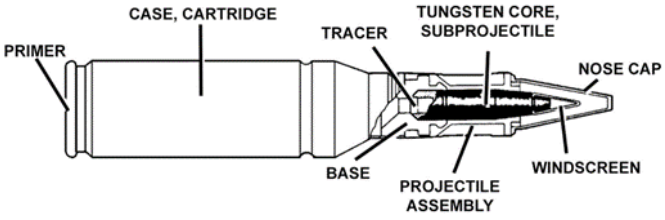

Figure 2.12 M791 APDS-T [40]

Table 2.2 20mm Shells [37]

Designation	Effect
M53	API
M56A3/A4	HEI
PGU-28A/B	SAPHEI
M242	HEI-T
M246	HEI-T
M940	MPT-SD
M775	API-T
M55A2	TP
M220	TP-T

A derivative of the M61, the M197, was adopted in 1967 for use in United States Army helicopter gunships. While the M314 Minigun had been an improvement over its single barrel counterparts, service in the jungles of Vietnam had revealed shortcomings, and the military was seeking an upgraded platform. General Electric lightened the M61 by removing three barrels, and the M197 gunnery system was accepted by the military and has seen service since. While the reduced number of barrels decreased the rate of fire of the M197 when compared to the M61, the lighter platform could fire the same ammunition as its larger parent system [39].

Developments in land-based vehicle armor have rendered smaller caliber munitions less effective, and the calibers of ground attack gun platforms have grown in response. A redesign of the GAU-8/A, mentioned later, the GAU-12/U was accepted by the United States Marine Corps for the AV-8B Harrier II attack aircraft in the late 1970s.

Firing a selection of 25mm shells shown in Table **2.3**, the five barreled rotary cannon GAU-12/U was also mounted to the United States Air Force AC-130 gunships, though in this configuration the rate of fire is limited to a fraction of the maximum to reduce wear on the barrels and to conserve ammunition. A derivative of the GAU-12/U, the GAU-22/A was developed for use in the F-35 Lightning II. With one barrel removed to save weight, the GAU-22/A has a reduced rate of fire but maintains the same diversity of ammunition and accuracy [41].

Table 2.3: 25mm Shells [40]

Designation	Effect
M919	APFSDS-T
M791	APDS-T
FAPDS	T
SAPHEI	T
M792	HEI-T-SD
MP	T
APEX	APEX
Mk210	HEI-T

Easily the most recognizable ground attack aircraft of the western world, the Fairchild Republic A-10 Thunderbolt II can deliver an enormous variety of munitions, but its chief method of attack is the incredibly powerful GAU-8/A rotary cannon. Chambered in 30mm rounds, the GAU-8/A was designed specifically to destroy tanks on the battlefield. Typical ammunition loads are a combination of PGU-14/B API and PGU-13/B HEI rounds designed to puncture and destroy armored targets. The firing rate of the GAU-8/A is fixed at 3,900 rounds per minute, and pilots are limited to one and two second bursts to conserve ammunition and minimize wear on the barrels. The GAU-8/A also has the unique feature of case capture, whereby spent cannon casings are captured and cycled back into the ammunition drum rather than ejected from the plane, a feature designed to prevent damage to the firing plane or sister craft, and to prevent potential injury to personnel on the ground. Additionally, the gun must be installed carefully on aircraft, as the recoil of the system is powerful enough to cause the aircraft to skew off target. The A-10 platform, shown in Figure 2.13, addresses this issue by aligning the firing barrel with the centerline of the aircraft, preventing adverse yawing effects [42]. The recoil of the GAU-

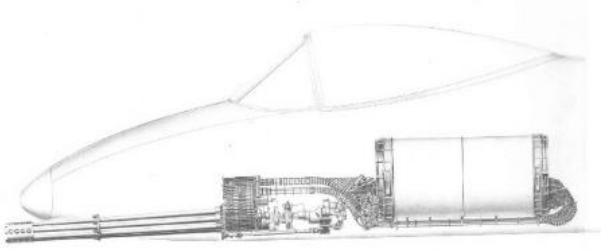

Figure 2.13: GAU-8 Installed in A-10 Nose [42]

Figure 2.14: M230 Installed on AH-64 [43]

8/A proved too high for helicopters, and in 1973 development of a helicopter compliant 30mm cannon led to the introduction of the M230 chain gun found on the AH-64 Apache attack helicopter, shown in Figure 2.14. Firing HEDP rounds, the M230 is highly effective against infantry, lightly armored vehicles, and buildings [43].

Table 2.4: Gravity Weapons Categorized by Weight Class [38-41]

500 Pounds	
Designation	**Description**
Mk82	Low-Drag General Purpose High Explosive
Mk82 Snakeye	Low-Drag Close Air Support High Explosive
BLU-111/B	Low-Drag General Purpose Stable High Explosive
BLU-111A/B	Thermal-Protective Coating on BLU-111/B (Navy)
BLU-126/B	Low Collateral Damage Bomb
BLU-129/B	Composite Low Collateral Damage Case
GBU-38(V)1/B	All-Weather Precision-Guided Mk82
GBU-38(V)2/B	All-Weather Precision-Guided BLU-111
GBU-38(V)3/B	All-Weather Precision-Guided BLU-126/B
GBU-38(V)5/B	All-Weather Precision-Guided BLU-129/B
250 Pounds	
Designation	**Description**
Mk81	Low-Drag General Purpose High Explosive
Mk81 Snakeye	Low-Drag Close Air Support High Explosive
GBU-29	Precision-Guided General Purpose High Explosive
GBU-39/B	Precision-Guided Glide Bomb
GBU-39A/B	Precision-Guided Glide Bomb

Figure 2.15: Relative Shell Sizes [44]

In 2012, the United States Air Force announced plans to outfit new generations of the AC-130 with 30mm Bushmaster II chain guns, designated the GAU-23/A. Firing HEI-T rounds, the Bushmaster II is also highly effective against personnel, lightly armored vehicles, and buildings [45]. The final gun platforms discussed in this report have, due to their size and weight, only been fielded as weapons systems onboard the AC-130. The first of these, the Bofors 40mm L/60 autocannon, developed in 1934, fires 120 rounds per minute [46].

The largest gun platform fielded on any aircraft, the M102 Howitzer, has been fitted to AC-130 aircraft to provide long range, heavy support fire. The gun is outfitted with HE-SF rounds, causing devastating damage over an adjustable range of engagements [47]. **Error! Reference source not found.** shows the sizes of a variety of ground attack hard launch munitions.

Gravity weapons originated in World War One, when pilots hand released flechettes, hand grenades, and even bricks from the cockpits of their planes in attempts to disrupt the enemies below. As aircraft rapidly developed and became more capable, munitions design accelerated, and gravity weapons grew larger and more

powerful. **Error! Reference source not found.** shows the applicable gravity weapons deployed by the United States military.

Table 2.5: U.S Guided Missiles [55-62]

Designation	Guidance System	Target
AGM-114K/K2/K2A Hellfire II	SALH	Land
AGM-114N Hellfire (MAC)	SALH, MMWR	Land
AGM-114R Hellfire II (Hellfire Romeo)	SALH	Land
AGM-114R9X Hellfire	SALH	Land
AGM-65(A-K) Maverick	EO, IIR,SALH,CCD	Land
AGM-84 Harpoon	SSR	Ship
AGM-84K SLAM-ER	INS,GPS,CGD	Land
AGM-88E AARGM	ARG	Land
AGM-88F HCSM	ARG	Land
AGM-88G AARGM-ER	ARG	Land
AGM-119 Penguin	SSR	Ship
AGM-176 Griffin	SALH,GPS,INS	Land
AGM-179 JAGM	SALH,MMWR	Land

Table 2.6: U.S. Unguided Rockets [52,53]

Zuni 5-in. (FFAR) (1957-Present)	
Warhead	**Effect**
Mk24	HE
Mk32	ATAP/HEAT-FRAG
Mk33	I
Mk63	HE-FRAG
Hydra 70 (1972-Present)	
Warhead	**Effect**
M151	HEDP
M156	WP
M229	HEDP
M247	HEAT/HEDP
M255	APERS
M255E1/A1	FI
M257	PI
M259	WP
M261	MPSM
M264	RP
M267	MPSM-P
M274	PS
M282	IR
WTU-1/B	P
WDU-4/A	APERS
WDU-4A/A	APERS
Mk84	CH

The final section of munitions that will be covered in this report is rockets and missiles. While these two types of munitions share powered travel to their target, they differ in that rockets are unguided on their path to the target after launch, while missiles are guided through one or more methods, typically using fins or gimballing engines, on their path to the target. Rocket pod technology saw extensive use in both the Korean and Vietnam wars, where pods were frequently fitted to attack aircraft and helicopters and continue to be a popular method of delivery for rockets in modern light attack aircraft. Guided missiles, larger by design due to tracking and guidance hardware, are typically carried in racks designed to carry small compliments of missiles that can be individually targeted at multiple enemy

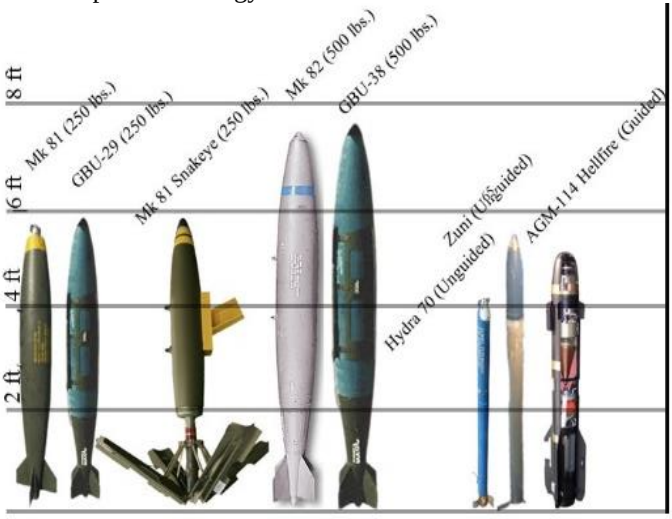

Figure 2.16: Scaled Munitions

combatants. **Error! Reference source not found.** shows a selection of unguided rockets used in United States ground attack aircraft.

Development on the next generation of the Hydra 70, the AGR-20A Advanced Precision Kill Weapon System (APKWS) began in 2012. This package fitted to the Hydra 70, reconfigures the unguided rocket into a precision-guided air to ground missile [54]. **Error! Reference source not found.** shows popular air to ground missiles and their guidance method, as well as intended targets.

3 Design Optimization Function, Class I Economics Model, Life-Cycle Cost Minimization, and Weights Establishment

This chapter includes the optimization function and brief study of Class I economics for the competitive market.

3.1 Design Optimization Function

Table 3.1: Table of Design Requirements, Objectives, and Additional Objectives

Design Requirement (R_i)	Number (n)	Design Requirement (R_i)	Number (n)
Certification:MIL-STD-516C & JSSGs	1	Integrated Gun	7
Entry into Service 2025	2	Service Life: 15,000 hrs over 25 yrs	8
Critical Technology TRL 8+	3	Service Ceiling > 30,000 ft	9
Take-off Field Length	4	Crew: 2 w/ zero-zero ejection seats	10
Survivability Measures	5	Mission Range 100 nmi, 4 hrs loiter	11
Payload 3,000 lb. w/ variety loadouts	6	Ferry Range 900 nmi	12

Design Objectives (O)	Number (j)	ROWF	Design Objectives (AO)	Number (i)	ROWF
"Best Value" (DOC, C_{aq})	1	20	Multiple engines	9	4
Mission Flexibility	2	40	Direct and orbital fire	10	4
Design Objectives (AO)	**Number (i)**	**ROWF**	Minimize gun gas ingestion	11	2.5
Gun w/ effective rounds	1	3	Weapons package flexibility	12	5
More ammo than A-10	2	1	Minimize gun CEP	13	5
Cruise faster than A-10	3	2	Low acoustic signatures	14	4
Ferry Range 2,500 nmi	4	3.5	Low tracer observability	15	2
Small hanger footprint	5	1	Indirect fire with low CEP	16	4
Low acquisition cost	6	4	Glass panel gunnery	17	2
Low operating cost	7	4	Remote 2nd seat capable	18	3.5
Cockpit visibility	8	3	Dmg. resistant control sys.	19	5

The generalized optimization function seen below was formulated to help assign a numeric value to potential designs based upon the RFP [1] design requirements and objectives, along with additional objectives proven to be important factors. The design requirements of the equation are shown in product operator, if all requirements are met the yield is one, if any single requirement is not satisfied the result is zero. The two sum operators use the design

objectives, and each have a relative objective weighting factor (ROWF) that allow for comparison of possible design configuration in chapter 7. Objectives are non-binary and vary depending on its comparison to the market. Table 3.1 shows these variables and weightings.

$$\textbf{General Optimization Function} = \textbf{GOF} = \prod_{1}^{n} R_n \left(\sum_{1}^{i} \textbf{ROWF}_i \times O_i + \sum_{1}^{j} \textbf{ROWF}_j \times AO_j \right)$$

Using the function shown above, the Dragoon was compared to its major competitors, the AT-6 and the A-29, as well as the A-10. The scores of the aircraft were calculated based on what extent they met the design objectives (O) and ancillary design objectives (AO). The scores were normalized to one and can be seen in Table 3.2. The first row of scores has zeros for both the AT-6 and the A-10. This is because the A-10 only has one crew member and the AT-6 does not have an integrated gun, both are violations of the RFP requirements. The second row of scores shows the scores for these aircraft under the assumption that they have met the RFP requirements.

Table 3.2: GOF Results of Dragoon Aircraft Compared to Competitors and the A-10

Aircraft	Dragoon	A-10 Thunderbolt II	AT-6 Wolverine	A-29 Super Tucano
GOF Score	0.94	0	0	0.68
GOF Score (Neglecting RFP Requirements)	0.94	0.74	0.70	0.68

3.2 Class I Economic Analysis and Weight Establishment

This section outlines the analysis of the economics and cost of aircraft within the market according to Jan Roskam's models in *Airplane Design Part VIII: Cost Estimation: Design, Development, Manufacturing, and Operating* [192]. The life cycle cost of an aircraft is composed of four pieces: the cost of research, development, tests, and evaluations, the acquisition costs operating costs, and the cos of disposal. In Appendix A of *Airplane Design Part VIII* is an equation model relating the takeoff weight of military aircraft to their cost as seen below [63] which accounts for inflation. Three of the current competitive aircraft in the market for ground attack fighters were selected and compared in Table 3.3 to get an idea how the takeoff weights and the direct operating cost affect the total life cycle cost for one aircraft of a specific type (note service life normalized to 15,000 hrs). The results show a lower takeoff weight, W_{TO} directly correlates to a lower acquisition cost.

$$\boldsymbol{AMP_{1989}} = \textbf{invlog}\left(\textbf{2.3341} + \textbf{1.0586}(\textbf{log}\boldsymbol{W_{TO}})\right)$$

Table 3.3 shows how the life cycle cost is mainly impacted by the operating costs of the aircraft over time, up to 6 times or more than the acquisition cost. Note in the following table the A-10's life cycle cost accounts for the current re-winging procedure, along with ranges for costs.

Table 3.3: Economic Comparison of Competitive Aircraft in the Market [19,21,64,65]

Aircraft	AT-6 Wolverine	A-29 Super Tucano	A-10 Thunderbolt II
W_{TO} (lbf)	10,000[64]	11,905[21]	50,000[19]
Cost of Acquisition "Roskam"[63]	$7.78 M	$9.35 M	$42.7M
Direct Operating Costs ($/hr)	$1,000 – $2,500[65]	$1,000[65]	$20,000[65] - $60,000[19]
Life Cycle Costs/ Unit (15,000hr)	~ $22.8 M - $45.2 M	~ $24.4 M	~ $343 M - $943 M

The results from the Class I economics model drives our design to try to minimize the maximum takeoff weight to below or around W_{TO} = 10,000 lb. It also proves to show how the direct operating cost can drive up the life cycle cost by huge margins; therefore, the design goal would be to minimize this cost. It can be noted that these operating costs are driven by fuel, maintenance, support for onboard systems crew personnel, storage, spare parts, depots, and other miscellaneous costs [63, 66]. Some of the main drivers are the crew and maintenance. The maintenance cost for a complex design of a wing or engine will significantly increase maintenance cost and overhaul time. The cost of training pilots is also another concern and cost for the survivability of an aircraft as it can cost around $5 million to fully train a fighter pilot on average [66]. This means the mission success rate should be high to lower chances for lost pilots and aircraft to drastically reduce cost but also increase pilot/military approval. This leads to the solution to have a remote pilot and decrease on duty cost and training needs.

4 STAMPED Analysis of Light Attack Market

Statistical Time and Market Predictive Engineering Design (STAMPED) Analysis Techniques are used in the initial sizing process to determine how specific engineering variables change throughout time by tracking them in historical and contemporary aircraft. Using this process, the design of the aircraft is manipulated to achieve both a reasonable design and a market competitive final concept. Figure 4.1 and Figure 4.2 show how this methodology is utilized to track changes in many variables including wing characteristics, weight, range, and payload. For the purposes of this report, light attack aircraft providing similar capabilities to those detailed in the RFP were analyzed and the information divided according to engine configuration.

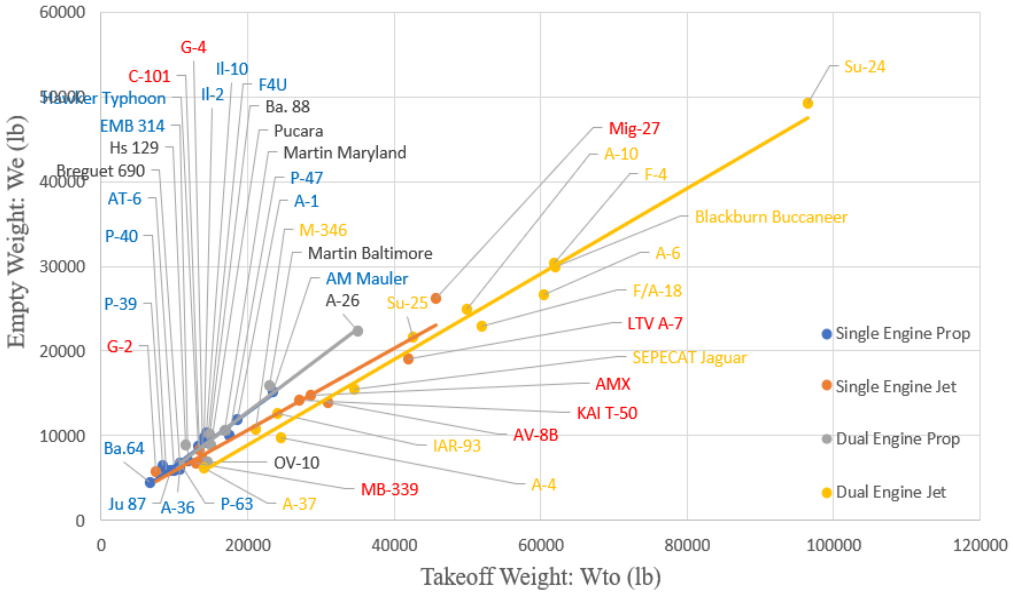

Figure 4.1: W_E with respect to W_{TO} [59-159]

Figure 4.2: W_E and W_{TO} with respect to time [59-159]

5 Weight Sizing Code Generation

The purpose of this chapter is to present the preliminary weight sizing of the aircraft.

5.1 Empty Weight to Takeoff Weight Ratio

The STAMPED data collected consists of both historical and contemporary light attack aircraft fielded across the world. Figure 5.1 contains a graph tracking the empty weight to takeoff weight ratio of known light attack aircraft. The data is divided into four sections based on engine number and type so that each possible configuration can be more closely tracked. It was determined that a dual engine configuration is preferred for the design as the redundancy safeguard should improve the survivability of the aircraft; however, all configurations were considered to provide a better analysis of the market. Figure 5.1 shows that the OV-10 Bronco and A-4 Skyhawk possess the most beneficial empty weight to takeoff weight ratios for dual engine propeller aircraft and dual engine jet aircraft respectively. While both of these aircraft were introduced prior to 1970, it is understood that technological advances in aerospace engineering over the past 50 years should be able to match the feats of previous aircraft designers.

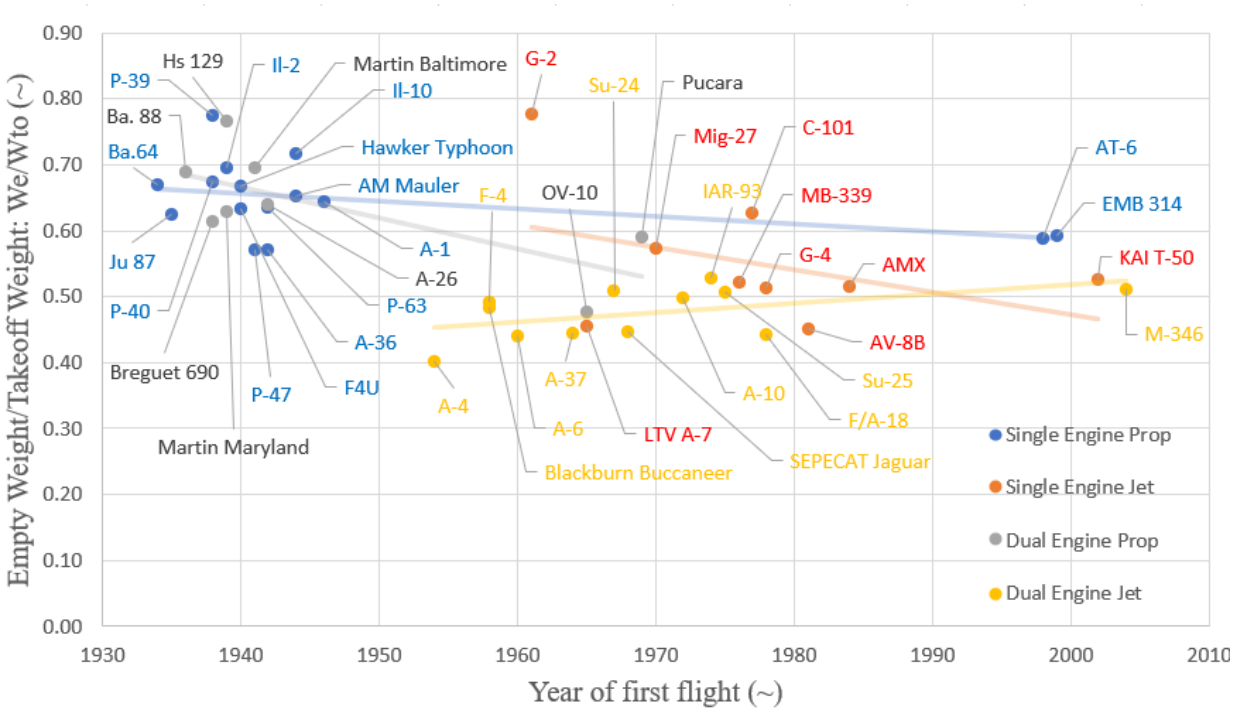

Figure 5.1: W_E/W_{TO} with respect to time [59-159]

5.2 Preliminary Design Weights & Engine Type Selection

Preliminary weight sizing methods used in this report follow the guidance of Jan Roskam as detailed in Chapter I of *Airplane Design Part I: Preliminary Sizing of Airplanes* [67]. Mission fuel weights were estimated as the sum of used fuel and reserved fuel, both of which were found using the fuel-fraction method. Within this method, each mission was broken into the phases as seen in Figure 1.1, and the fuel used during each phase was either estimated using Table 2.1 of *Airplane Design Part I* [67] or found using Breguet's range and endurance equations. When calculating cruise and loiter segments, optimistic values for lift-to-drag ratio, specific fuel consumption, and propeller efficiency were suggested (Table **5.1**), assuming technological advances in aircraft machinery and design.

After preliminary sizing was completed for both the design and ferry missions, it was determined that the design mission profile (Table **5.1**), will size the aircraft. The final preliminary weights are given in Table **5.1**. Using these sizing estimates, it was decided that a dual propeller configuration would be pursued for the final design concept as the lighter takeoff weight is more desirable.

Table 5.1: Important Values Used for Sizing

Configuration:	Dual Propeller	Dual Jet
L/D	18	22
c_j	~	0.5 lbf/lbf-hr[57]
c_p	0.4 lbf/hp-hr[67]	~
η_p	0.71[67]	~
W_{TO}	9,547 lbf	12,300 lbf
W_E	3,819 lbf	5,534 lbf
W_F	2,328 lbf	3,365 lbf

6 Wing and Powerplant Sizing

The purpose of this chapter is to present the methods and results of wing and powerplant sizing.

6.1 Wing Sizing

Indicated in the RFP, the requirements for this aircraft are a 4,000 ft takeoff ground roll from an austere runway. This information was used with sizing techniques from *Airplane Design Part I* [67] to generate takeoff sizing lines (Figure 6.6).

$$\left(\frac{W}{P}\right)_{TO} = \frac{l_p\left(\frac{\sigma N d_P^2}{P_{TO}}\right)^{1/3}}{\frac{\left(\frac{0.0376\left(W/S\right)_{TO}}{s_{TOG}(\rho)}\right) + 0.72C_{D_0}}{C_{L_{maxTO}}}}$$ [Eq. 3.9, Ref 67]

FAR 25 aircraft sizing techniques were used to generate the vertical landing sizing lines (Figure 6.6) using the following equations and relationships:

$\frac{W}{S} = \frac{1/2\,\rho V_{SL}^2 C_{L_{max}}}{W_L/W_{TO}}$	$V_A(\text{kts}) = s_{FL}\sqrt{\frac{s_{FL}(\text{ft})}{0.3}}$	$V_{SL}\left(\frac{\text{ft}}{\text{s}}\right) = \frac{V_A\left(\frac{\text{ft}}{\text{s}}\right)}{1.2}$
[Ref 67]	[Eq. 3.16, Ref 67]	[Eq. 3.15, Ref 67]

Although the RFP does not state a climbing requirement, it can be reasonably assumed that a light attack aircraft has a high chance of coming under fire from hostile ground forces, possibly losing control in an engine. For this reason, FAR 23.67 one engine inoperative requirements were followed. Therefore, the climb requirements were generated using the following equations from *Airplane Design Part I* [67].

$\frac{W}{P} = \eta_p * \left(\frac{\sqrt{W/S}}{19\sqrt{\sigma}\left(C_L^{3/2}/C_D\right)} + RCP\right)^{-1}$ [Eq. 3.24, Ref 57]	$RCP = \frac{RC}{33000} = \frac{\frac{dh}{dt}\left(\frac{\text{ft}}{\text{min}}\right)}{33000}$ $= \frac{60(0.012)V_{CL}}{33000}$ [Eq 3.23, Ref 67]
$C_L^{3/2}/C_D = \frac{1.345(Ae)^{3/4}}{C_{D_0}^{1/4}}$ [Eq. 3.27, Ref 67]	$V_{CL} = \sqrt{\frac{2\left(\frac{W}{S}\right)}{\rho C_{L_{climb}}}}$ [Ref 67]

As the RFP requires the initial decent to 3,000ft to conclude within 20 minutes of the initial climb, a cruise speed and a dash speed both of 310 knots were assumed. The sizing lines for these were generated using the following equation: $\frac{W}{P} = \frac{\eta_p}{\left(\frac{\bar{q}C_{D_0}}{W/S} + \frac{W/S}{\bar{q}\pi Ae}\right)V}$ [Ref 68]. Additionally, maneuvering requirements were based on a presumed circular

orbital engagement method with a one-mile radius and a turning speed of 180 knots based on subject matter expert input. The sizing line for this was generated using the following equation:

$$\frac{W}{P} = \frac{\eta_p}{\left(\frac{\bar{q}C_{D_0}}{W/S} + \frac{W/S}{\bar{q}\pi Ae}n^2\right)V}$$ [Eq. 3.45, Ref 67].

A dominant factor in wing sizing was wing fuel volume. As the preliminary weight sizing of the aircraft estimated a takeoff weight under 10,000 lbf and a lift-to-drag ratio of 18, the resulting wing characteristics limit available wing space for fuel. To acquire a favorable and competitive value for wing loading, fuel will need to be stored in alternative locations, such as in wingtip tanks or internally in the fuselage. Using desired salient characteristics, the equation to the right was used to calculate wing fuel volume.

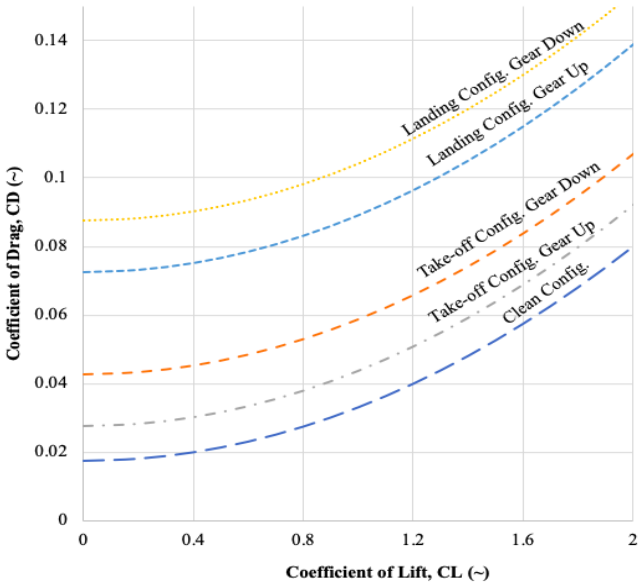

Figure 6.1: Preliminary Sizing Drag Polar

$$V_{wf} = 0.548\left(\frac{S^2}{b}\right)\left(\frac{t}{c}\right)_r\left(\frac{1+\lambda_w\sqrt{\tau_w}+\lambda_w^2\tau_w}{(1+\lambda_w)^2}\right)$$ [Eq. 6.3, Ref 188]

Using *Airplane Design Part I* [67] and values from preliminary sizing, initial drag polar lines were graphed for each configuration as seen in Figure 6.1

6.2 Powerplant Sizing

Once a preliminary wing loading value was determined, lift-to-drag ratios were calculated at varying altitudes, airspeeds, and aspect ratios using this relationship: $\frac{L}{D} = \frac{\bar{q}(W/S)}{\bar{q}^2 C_{D_0} + \frac{(W/S)^2}{\pi Ae}}$ [Ref. 68]

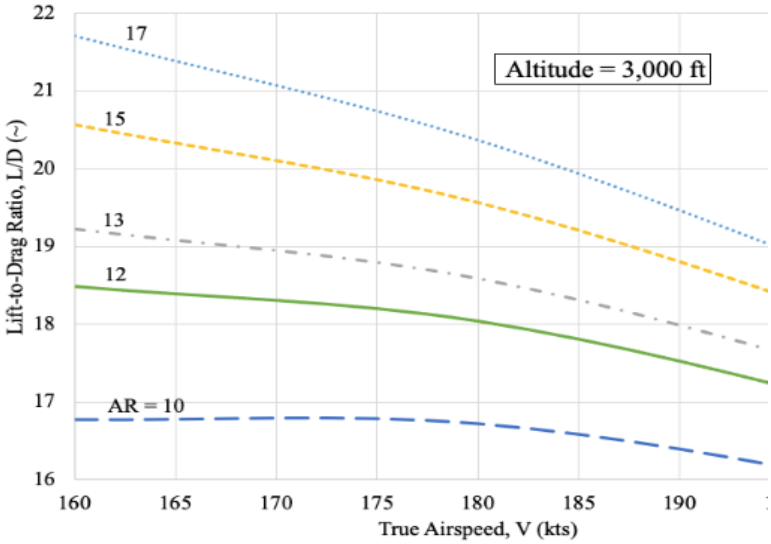

Figure 6.2: L/D Ratio over Airspeed at FL3

As the success of the preliminary weight estimate relies on a large lift to drag ratio, it is pertinent that the found values be plausible. Figure 6.2 and Figure 6.3 show the relationship between lift to drag ratio and true airspeed for varying aspect ratios at 3,000 ft and 35,000 ft, respectively. It was determined that an altitude of 35,000 ft yields the best results for the given wing loading and 310 kts cruise speed (Figure 6.3). The design aircraft will possess an aspect ratio of 12 to gain a lift to drag ratio of 18 at 35,000 ft.

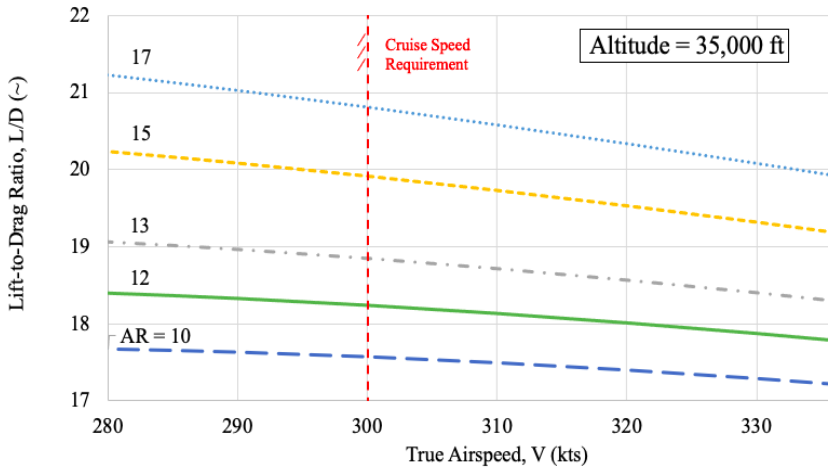

Figure 6.3: L/D Ratio over Airspeed at FL350

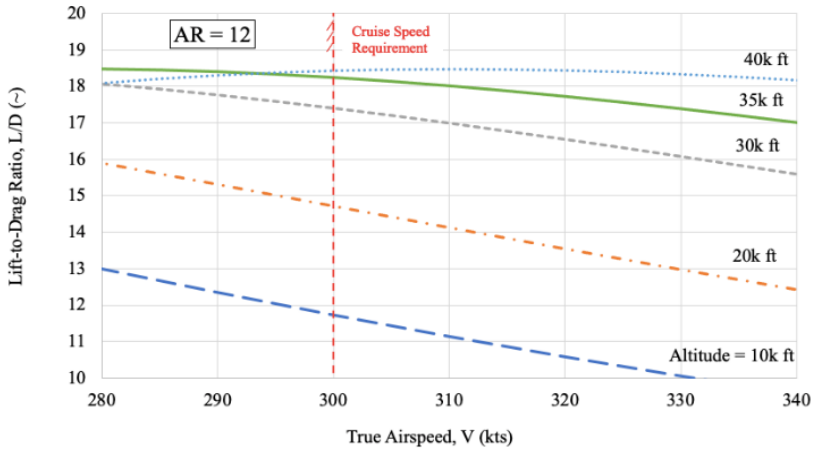

Figure 6.4: L/D Ratio over Airspeed

The relationship $SR = \frac{1}{W\left(\frac{c_p \dot{W}_F}{\eta_p \dot{W}_F + T_{core} c_p V}\right)\left(\frac{\rho V^2 C_{D_0}}{2(W/S)} + \frac{2(W/S)}{\pi A e \rho V^2}\right)}$ [Ref. 68] was used to determine specific ranges for varying aspect ratios, velocities, altitudes, and wing loadings. Figure 6.5 shows specific range as a function of wing loading and compares the most logical pairings.

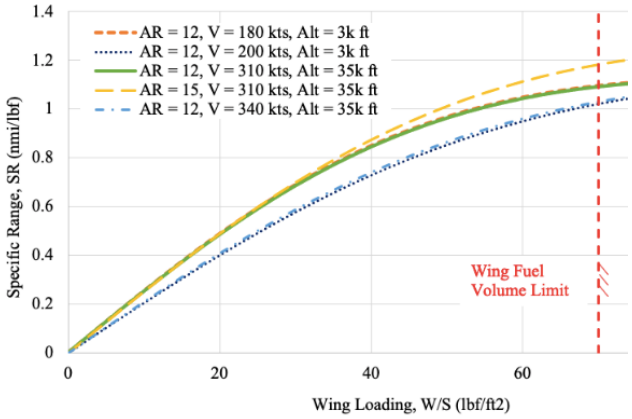

Figure 6.5: Specific Range over Wing Loading

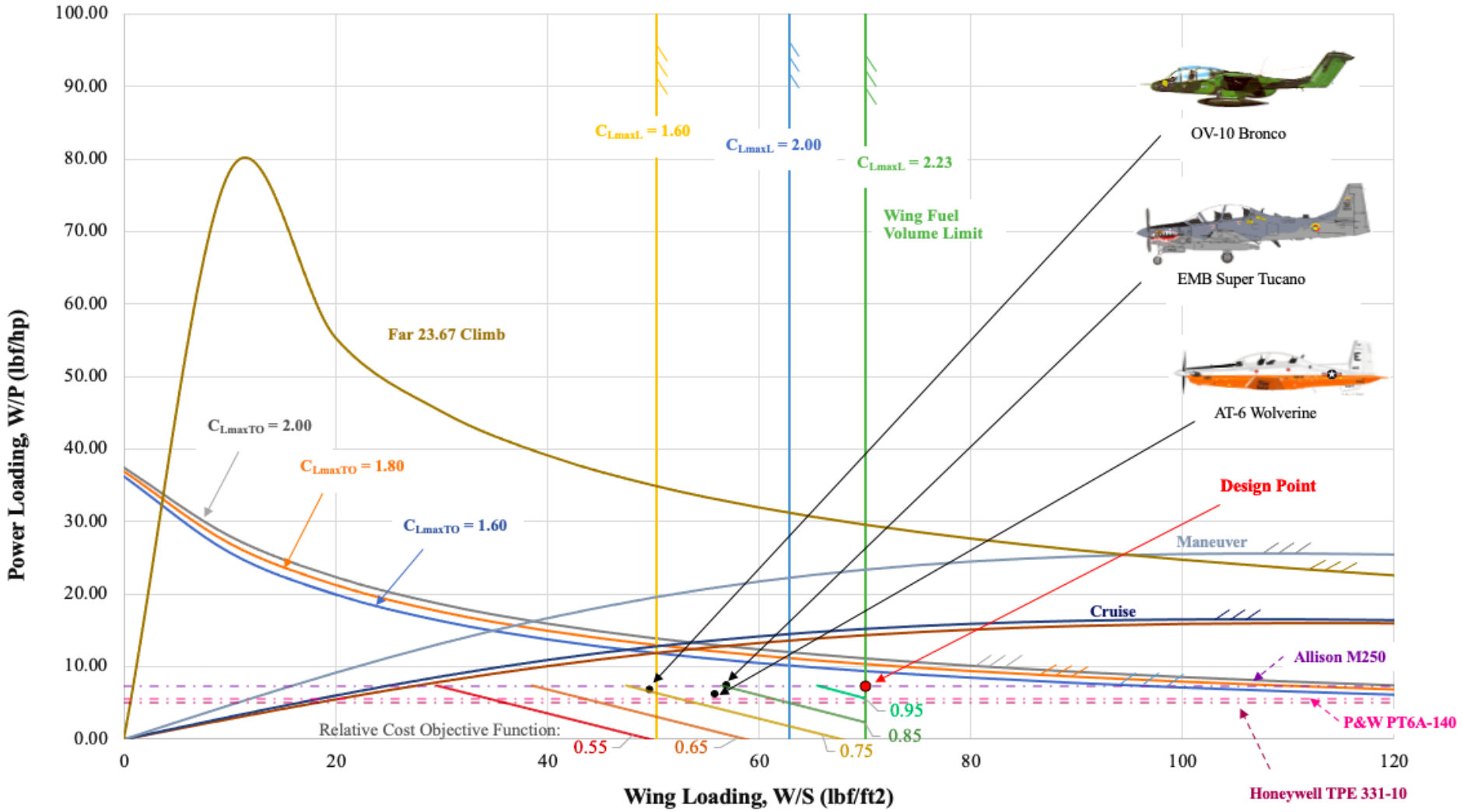

Figure 6.6: Wing Sizing Chart

7 Class I Design Configuration Down Selection

7.1 Configuration Matrix

The first step into the design of the Dragoon was the determination of the Class I Design configuration. A sweep of designs was modeled and compared based on their perceived characteristics seen on the right. Each design carries its own perks and drawbacks while trying to maximize a specific flight characteristic. Some notable configurations are Figure 7.1 being similar the Super Tucano and AT-6, Figure 7.8 being a similar configuration to the OV-10, and the A-10 being alike to Figure 7.9 layout.

Design 1:
+ Simple Design
- Single Engine
- No Center Mounted Gun
- Prop Ground Clearance
- Increase in CEP
- Landing Gear length grow

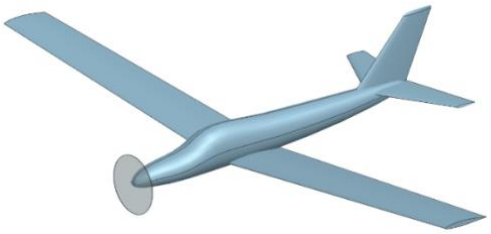

Figure 7.1: Configuration 1

Design 2:
+ Main Gun Placement
+ Large Internal Storage
- Prop Ground Clearance
- Decreased Visibility
- Landing Gear length grow

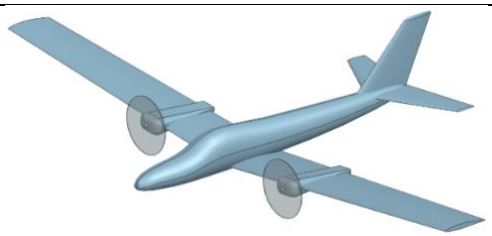

Figure 7.2: Configuration 2

Design 3:
+Prop Ground Clearance
+ Increased Visibility
+ Favorable Landing Gear
- Weight Savings
- Aft CG

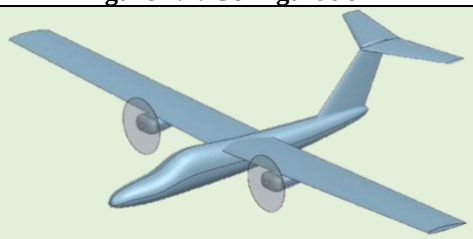

Figure 7.3: Configuration 3

Design 4:
+ Prop Ground Clearance
+ Reduced Wetted Area
- Reduced Controllability
V-Tail

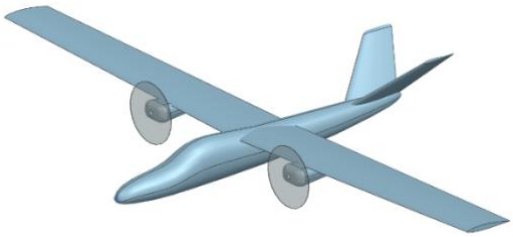

Figure 7.4: Configuration 4

7.2 Configuration Down Selection

Of the configurations presented above, some have inherent flaws or drawbacks that do not align with the RFP or design objectives of the team. Given the mission specifications, the aircraft will need to withstand active duty in rough environments and still be able to perform with a high level of fidelity. Designs therefore need to have an excellent quality of reparability, simplicity, combat performance, and cost. Specifically, for this design mission the need for

multiple engines was considered a high priority, as the survivability in cases of engine failure in combat ensures pilot safety and operation of aircraft. Similarly, the aircraft must be simple enough to repair in remote locations set up by military personnel and crew, also driving operational costs down. Propeller driven aircraft were seen as advantageous in terms of austere field performance due to the extra force generated by "prop-kick." The main drawback to a propeller versus a high bypass turbofan would be the increase in observables and noise. The solution to this issue would be to decrease the propeller loading on the turboprop. The comparisons of the aircraft lead to the decision between the configurations 3 and 8 above. Ultimately, configuration 8 (Figure 7.8) was chosen. Configuration 8 includes many advantages including: large propeller clearance to help reduce disk loading, ease of weapons egress with no fuselage or vertical tail for ordnance to hit, increased yaw controllability

Design 5:
+ Higher Cruise Speed
+ Reduced Wetted Area
- Foreign Object Debris
- Increased Runway Length (lower L/D)

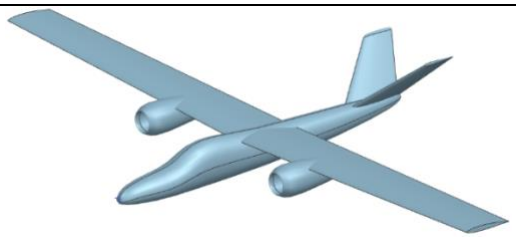

Figure 7.5: Configuration 5

Design 6:
+ Higher Cruise Speed
- Foreign Object Debris
- Gun Gas Ingestion
- Aft CG
- SARUS effect

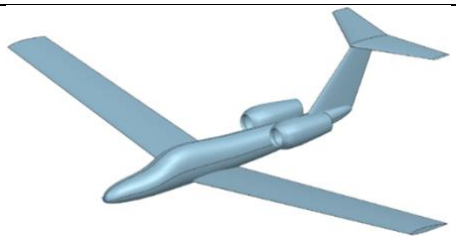

Figure 7.6: Configuration 6

Design 7:
+ Prop Ground Clearance
+ Payload Storage
- HT Placement
- Prop Wash over VT & HT

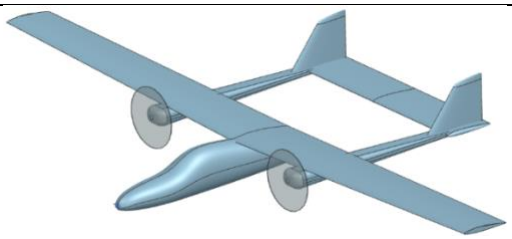

Figure 7.7: Configuration 7

Design 8:
+ Prop Ground Clearance
+ CL alpha bump in VT, end plate
+ Payload Storage
+ Weapon Egress
- Prop Wash over VT

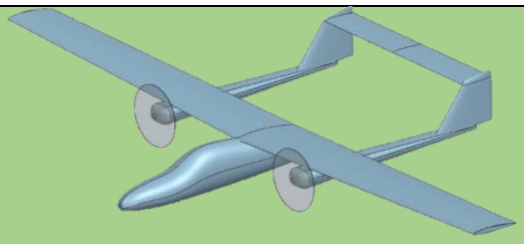

Figure 7.8: Configuration 8

Design 9:
+ Low Observability
+Increased Visibility
- Flow over HT
- Gun Gas Ingestion

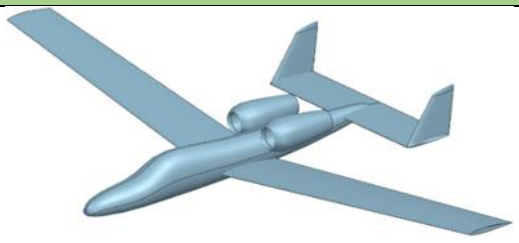

Figure 7.9: Configuration 9

during maneuvers from vertical tail placement with end plating. This specific design also works well with the synergism to keep the outside of the aircraft as clean as possible with the smallest wetted area.

8 Class I Design

The purpose of this chapter is to present the early modeling of the Dragoon as a Class I configuration design. Included are preliminary geometric characteristics as well as fuselage and empennage sizing. The methods used for analysis come from *Airplane Design Part I-II* [67,188].

Table 8.1: Aircraft Salient Characteristics

	Wing	**Horizontal Tail**	**Vertical Tail**
Area (ft^2)	136.4	20.0	18.0
Span (ft)	40.5	8.8	6
MGC (ft)	3.58	2.25	2.6
MGC LE, FS (ft)	22.5	50.0	42.5
A	12	3.87	2
Sweep Angle (°)	0	0	20
Taper Ratio	0.4	1	0.6
Thickness Ratio	0.17	0.15	0.15
Airfoil	LS 417	NACA 2315	NACA 0015
Dihedral Angle (°)	0	0	0
Incidence Angle (°)	0	0	10
Control Chord Ratio	0.2	0.2	0.2
Control Span Ratio	0.22	0.94	0.75
Flap Chord Ratio	0.2	~	~
Flap Span Ratio	0.15	~	~
	Fuselage	**Cabin Interior**	**Overall Aircraft**
Length (ft)	29.0	~	35.8
Max. Height (ft)	4.6	~	9.5
Max. Width (ft)	3.3	~	42.1

8.1 Fuselage Layout

The length of the fuselage is 30.7 ft assuming a length to diameter ratio, L_f/D_f, of 7.0. The placement of the cockpit provides sufficient visibility for stacked, level seating with 18 degrees in the front; it is assumed the WSO will use augmented vision and a series of instruments for target fire rather than direct line of sight. Adhering to the RFP, both crew members (50^{th} percentile female and 95^{th} percentile male) will be seated in zero-zero ejection seats, placed to prevent serious lower-body injury in the case of ejection. The fuselage was spaced to accommodate a completely internal weapons loadout as well as an integrated gun. The placement of both the gun as well as the hard-launched ammunition are confirmed in Class II Design. The design of the weapons housing and egress systems consists of a removable pod structure that comprises the underbelly of the fuselage. Ideally, this pod can be customized for a variety of missions, but for the purpose of this report, the pod is only fitted for the required design mission.

Figure 8.1: Side Cutout View of Fuselage. Scale: 1:100 in.

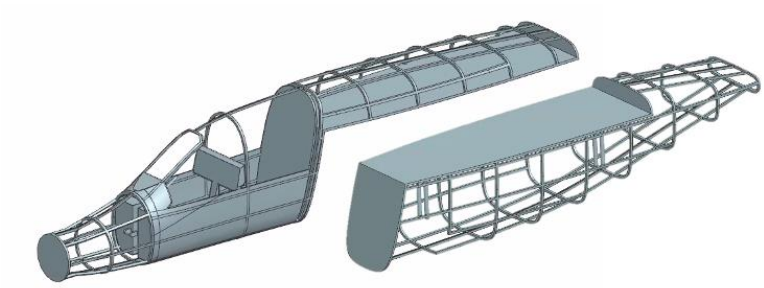

Figure 8.2: Isometric View of Fuselage Structure. Scale: 1:100 in.

8.2 Engine Installation

The configuration and installation of the powerplant is as seen in Figure 8.3. The powerplant was selected in Chapter 6 during the preliminary powerplant sizing. The selection of a turboprop engine over a turbofan was to improve takeoff and landing performance in austere conditions. The propeller sized to the aircraft measures 6 ft in diameter and has five blades. The selected engine is the Rolls-Royce (Allison) M250 C30R/3 because of favorable power loading (Figure 8.3 & Figure 8.4).

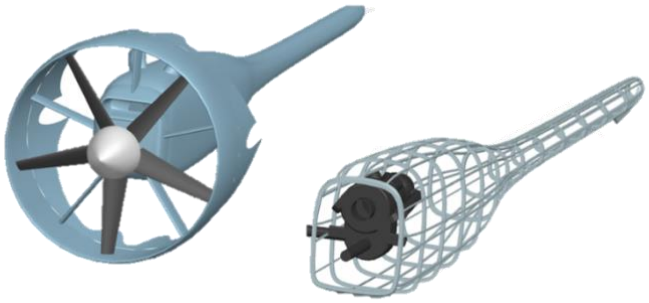

Figure 8.3: Isometric View of Powerplant and surrounding Boom Structure. Scale: 1:60 in.

Both engines are housed in booms connected to the wing. The placement of each powerplant in slightly forward the leading edge to allow proper spacing for the propeller and duct.

Table 8.2: Engine Characteristics

Engine	Rolls-Royce M250-C30R/3
Takeoff Power	650 shp
TSFC	0.6 lb/hp-hr
Length	41 in.
Diameter	21.9 in.
Weight	274 lbf

Figure 8.4: Rolls-Royce M250 [193]

8.3 Wing Layout

The aircraft was designed with a high wing in mind to increase visibility, raise the mounting of the engines, decrease disk loading, and decrease FOD. A LS 417 airfoil was selected for increased lift in austere conditions and to maximize wing thickness for fuel volume. No sweep, twist, or dihedral were deemed necessary for the success of the design, and a taper ratio of 0.4 was selected to lower wing weight. The wing control surfaces consist of inboard and outboard flaps, inboard and outboard ailerons, and leading-edge slats.

Table 8.3: Wing Characteristics

Span (ft)	40.5
Wing Area (ft2)	136.4
Aspect Ratio	12.0
Sweep Angle (deg)	0
Airfoil	LS 417
Taper Ratio	0.4
Twist Angle	0
Dihedral Angle	0
Root Chord	4.54
Tip Chord	1.82

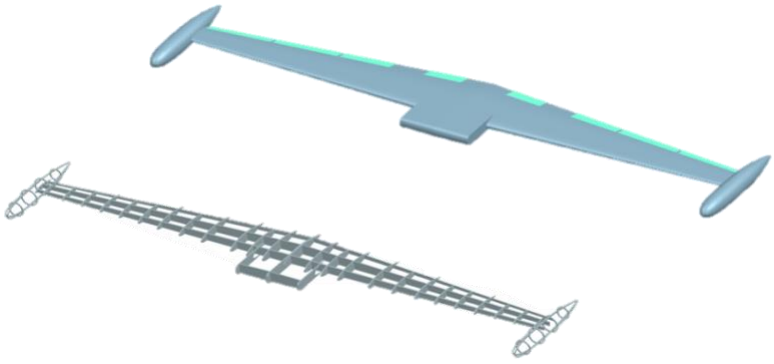

Figure 8.5: Isometric View of Wing and Wing Structure

8.3.1 High Lift Devices

The design of high lift devices follows the methods from *Airplane Design Part II* [188]. Flap sizing was performed for landing conditions which requires the highest maximum lift coefficient of 2.23. Single slotted Fowler flaps with leading-edge slats provide sufficient lift coefficient to meet the design C_{LmaxL}. The flap deflection angles required for takeoff and landing configurations are shown in Table 8.4.

Table 8.4: High Lift Device Sizing Values

Flap Type	Single Slotted Fowler	Flight Phase	δf
C_f/C	0.2	Takeoff	10
S_{wf}/S	0.36	Landing	40
η_i	0.08		
η_o	0.5		

8.4 Empennage

As seen in Figure 8.6 the empennage is designed with a boom tail configuration with a high vertical tail. The vertical tails are placed in propwash to improve stability; the horizontal tail is lifted above the wing and fuselage increase effectiveness. Additionally, the height of the empennage allows for improved weapons egress and loading on the ground. The vertical tails are tilted inwards to increase the structural integrity of the empennage, and the horizontal tail is modeled with a thicker airfoil for the same reason. The location of the connection of the vertical tails to the horizontal tail simulates an infinite airfoil resulting in better lift properties.

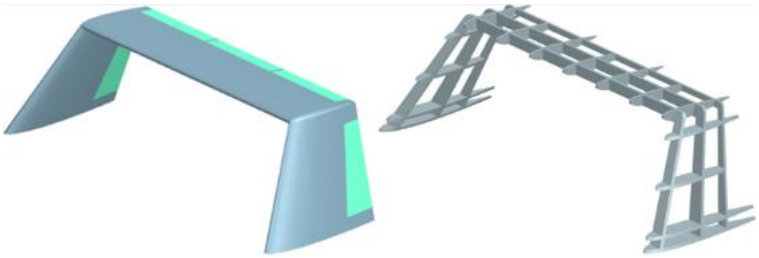

Figure 8.6: Isometric View of Empennage and Empennage

8.5 Landing Gear

The design of the landing gear follows the methods from *Airplane Design Part II* [188] and *Airplane Design Part IV* [190]. A tricycle configuration with retractable nose and main gear was selected. The nose gear was designed to retract into the nose of the aircraft, and the main gear was designed to retract into each boom aft the engines. Longitudinal and lateral direction considerations were adhered to when placing the landing gear in the fuselage. The main landing gear was placed at a 15° angle aft of

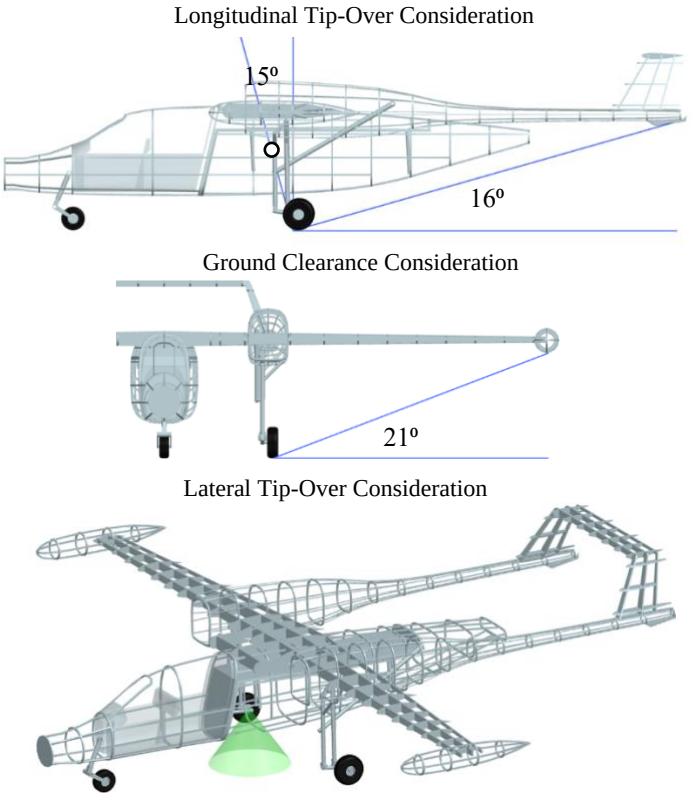

Figure 8.7: Side, Front, and Isometric Views of Landing Gear Placement

the most aft CG to prevent longitudinal tip-over (Figure 8.7). The tail ground angle and wingtip ground angles were greater than 15° and 5° respectively to adhere to ground clearance criterion (Figure 8.7). To prevent lateral tip-over, the nose and main landing gear were placed to accommodate a 35° cone within a triangular section centered at the most forward CG (Figure 8.7).

8.6 Drag Polar Analysis

This section provides a Class I drag polar analysis performed using the guidance from *Airplane Design Part II* [188] and *Airplane Design Part VI* [191]. The wetted area of the design aircraft was estimated and checked using the Siemens NX CAD model presented in previous sections. The fuselage perimeter plot seen in Figure 8.8 shows the curvature of the fuselage estimated at each fuselage station used for the estimation of wetted area. Using the values reported in Table 8.5 the parasite drag of the aircraft was determined to be 4 ft^2 assuming a conservative friction coefficient, C_f, of 0.005. Drag polars were then recalculated as seen in Table 8.6 and presented in Figure 8.3.

Table 8.5: Wetted Area

Component	S_{wet} (ft^2)
Wing	255
Horizontal Tail	41
Vertical Tail	35
Fuselage	289
Ducts	64
Booms	200
Total	**883**

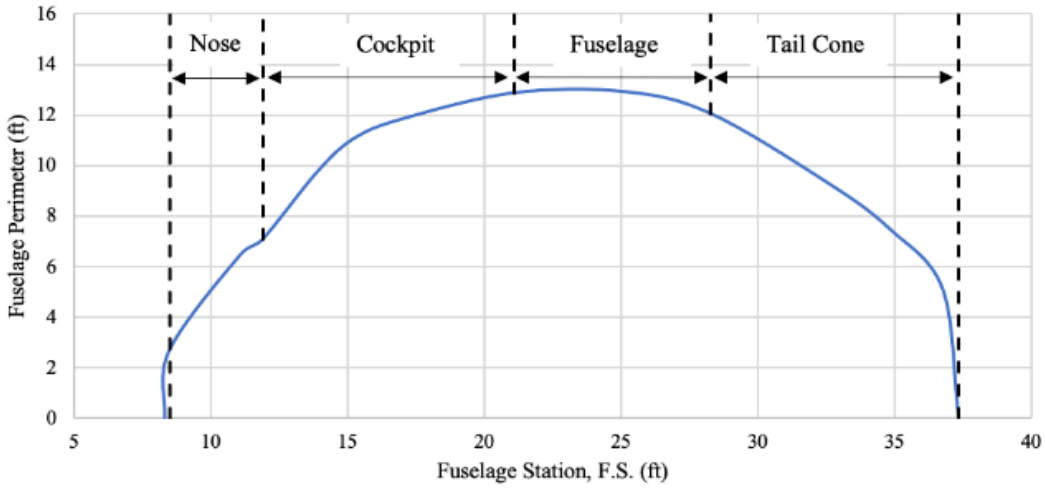

Figure 8.8: Fuselage Perimeter Plot

Table 8.6: Class I Drag Polar

Configuration	ΔC_{do}	C_{do}	$1/\pi Ae$	e	L/D_{max}
Clean	0.00	0.029	0.031	0.85	16.5
Take-off Flaps, Gear Down	0.025	0.054	0.033	0.80	11.8
Take-off Flaps, Gear Up	0.010	0.039	0.033	0.80	13.9
Landing Flaps, Gear Down	0.070	0.099	0.035	0.75	8.4
Landing Flaps, Gear Up	0.055	0.084	0.035	0.75	9.2

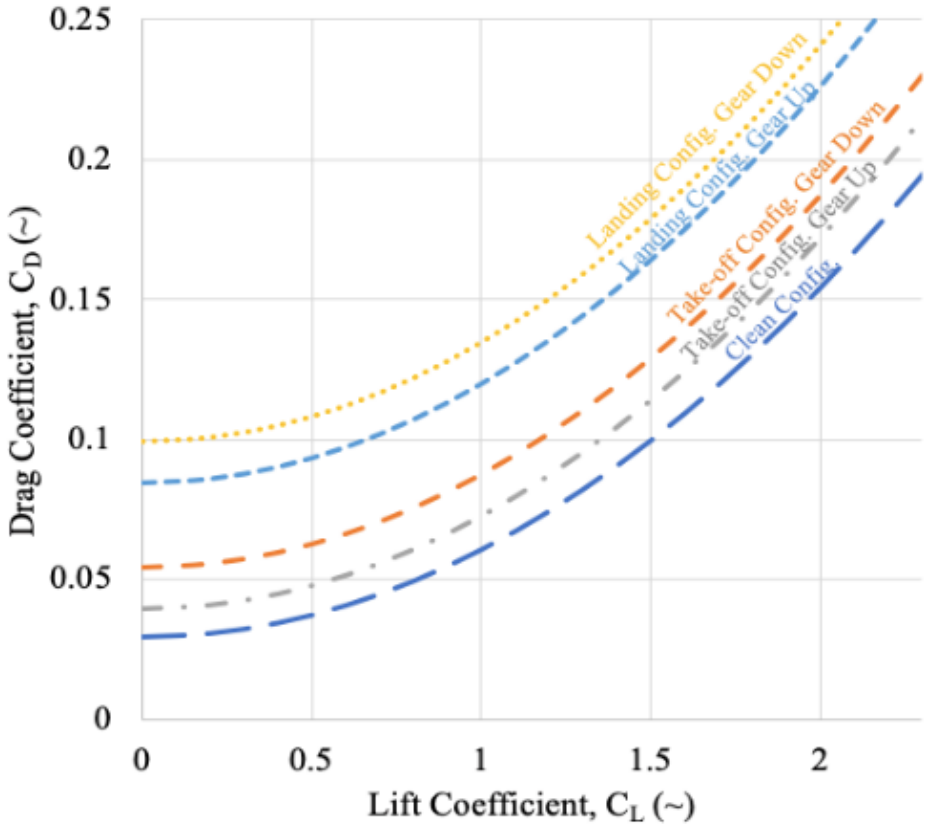

Figure 8.9: Class I Drag Polar

9 Hard-Launch Ballistics Analysis

For hard-launch ballistics analysis, a code was generated to compare various sizes and types of rounds as if they were fired at altitude and velocity from an aircraft to quantitively analyze guns, aircraft, and target engagement methods. With the initial states of the aircraft (speed, altitude, angle of attack, etc.) and publicly available round information [170] (designator, mass, caliber, & length), physics relationships were used to create a ballistics code. Once these initial states are inputted to the ballistics code, the equations below are used to calculate the reference area (S_b), initial total velocity (V_{0tot}), and initial Mach number (M_0) of the round [171]. Then, an appropriate drag trend is chosen. For the ballistics code, the axial coefficient of the PGU-28 is used. It is an appropriate trend for arial gunnery rounds, thus providing the values of the baseline axial coefficient ($C_{Abaseline}$). These values where found by using publicly available axial coefficient data with respect to Mach number trends [172] to develop polynomial expressions replicating the trend in the Ballistics Aerial Gunnery Solver (BAGS) for any Mach number required. Once the value for $C_{Abaseline}$ is calculated a new C_A with a Ballistic Coefficient Multiplier is calculated (C_{A0}) to adjust the axial coefficient to accommodate different types of round form factors [171].

$$S_b = \Pi d^2/4$$

$$V_{0tot} = \sqrt{V_{x0}{}^2 + V_{y0}{}^2}$$

$$M_0 = V_{0tot}/a_0$$

$$C_{A0} = BCM(C_{Abaseline})$$

With these values determined, force vectors of a round are calculated. Acceleration is calculated by dividing the force by the round's mass, then change in velocity for a specific time step is calculated, and position is calculated as seen in Figure 9.1. Once these values are calculated for a timestep, the flight path angle, pressure, temperature, and density are recalculated and the next timestep is analyzed [171]. This process is repeated until ground impact.

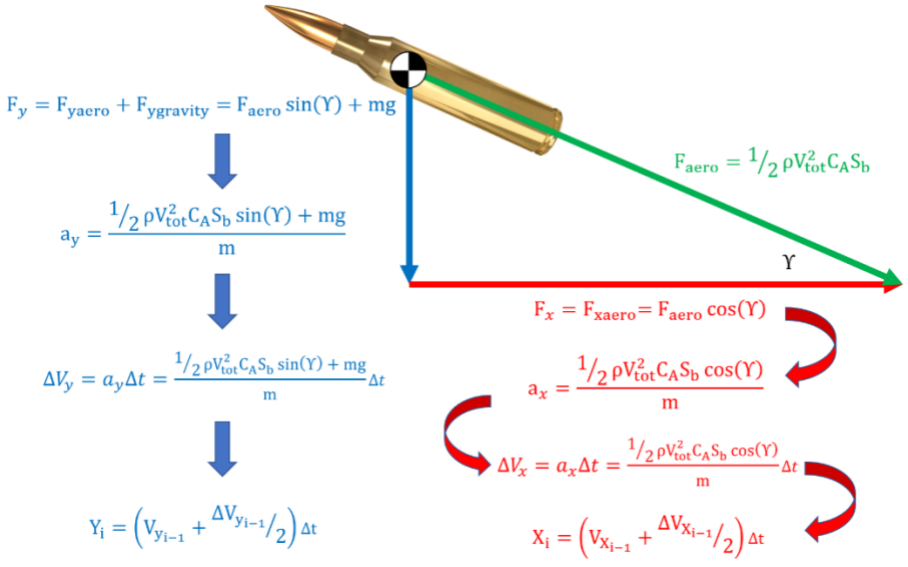

Figure 9.1: Acceleration, Velocity, and Position Equations [171]

Ballistic Aerial Gunnery Solver

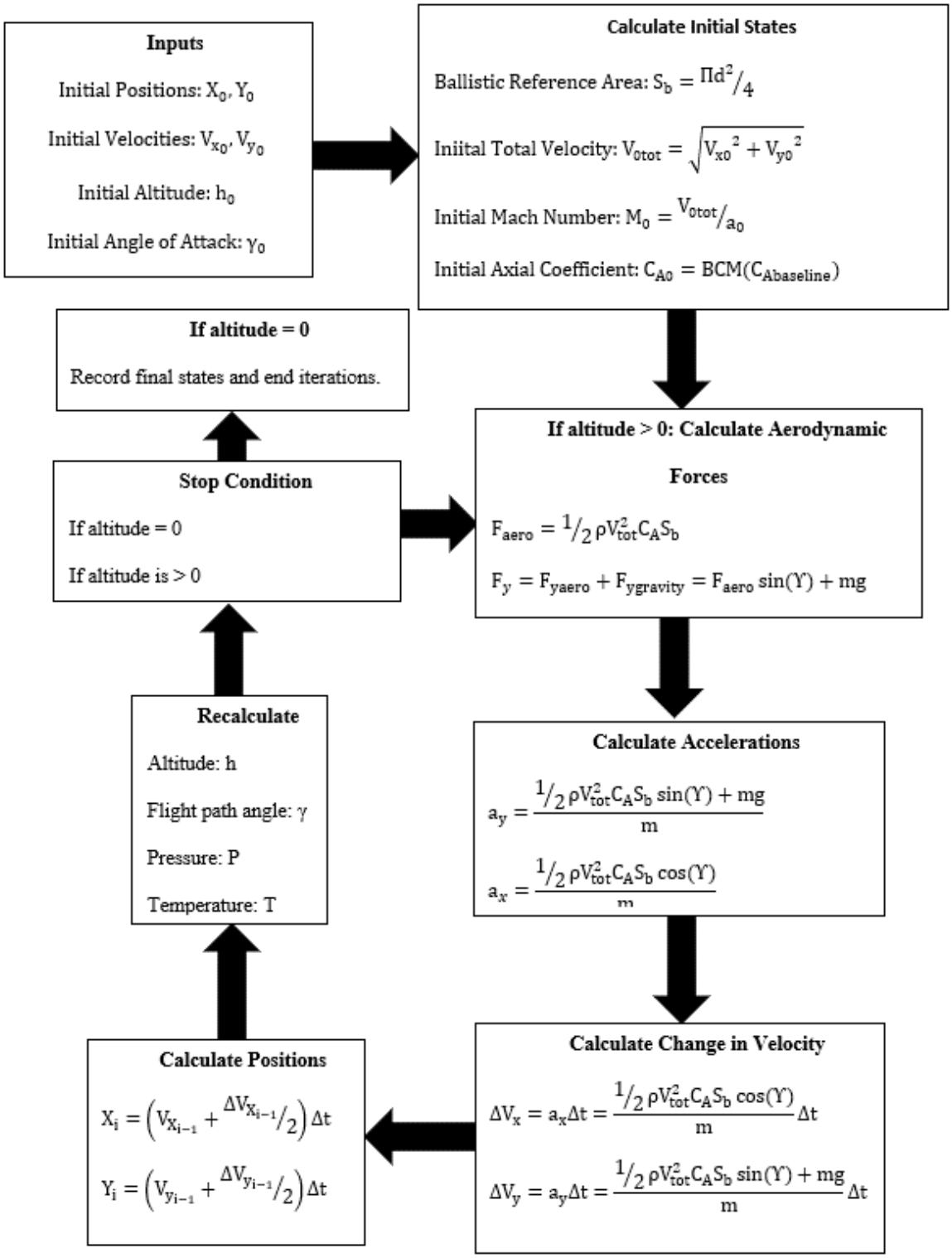

10 Review of Target Engagement Methods with Conventional and Advanced Hard-Launched Ordnance

Table 10.1: Reference Aircraft Weapons Installments

Aircraft	Gun	Penetration
EMB 314 Super Tucano	2 x internal M3P 12.7mm machine guns	19 mm at 550 m [163]
AT-6 Wolverine	2 x external M3P 12.7mm gun pods	19 mm at 550 m [163]
A-10	1 internal GAU-8 30mm cannon	69 mm at 500 m [164]

Since military forces have deployed aircraft, conventional hard-launch munitions have been the primary method of engagement of enemy targets. Armor growth onboard aircraft has been limited by weight, while ground vehicles have seen exponential advancements in armor capabilities. This increase in defensive capability has rendered small caliber ground attack munitions ineffective against hard targets. Historically, the higher kinetic energy required to pierce thicker armor has been achieved by fitting larger caliber guns to ground attack platforms, an effective strategy, but with a major increase in weight, the costs of doing so grow with the gun's performance. A recently developed munition, the Ballistic Aeromechanically Stable Sabot, or BASS, round addresses this problem. Sabot systems are found in many different military vehicles around the world, but none have been employed on aircraft before due to the dangers of damaging the host aircraft. In a conventional sabot system, the penetrator is surrounded in the casing by an expendable sleeve, allowing the transfer of nearly all the round's kinetic energy into the penetrator. Typically, upon exiting the barrel the sleeve breaks into multiple aeromechanically unstable fragments, creating a dangerous cloud for an aircraft. In BASS rounds, the sabot sleeve is one aeromechanically stable piece as shown on the left of Figure 10.1. Note that the CAD of the BASS rounds displayed in this report was generated using publicly available information cleared for export by the Department of Defense. After exiting the barrel, the sabot pulls a turn tighter than the aircraft is capable and removes itself from the flight path as shown at the right of Figure 10.1.

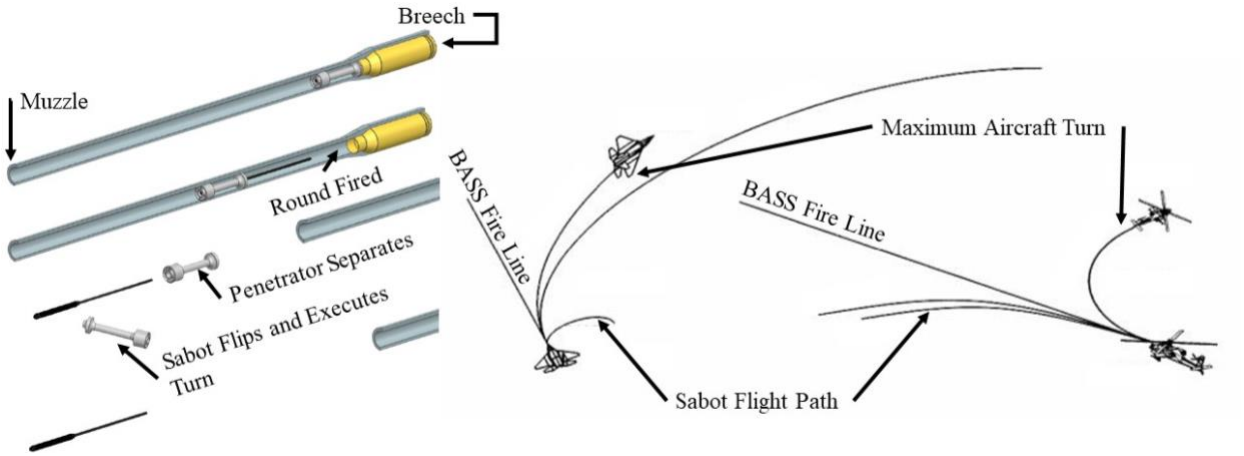

Figure 10.1 BASS Round Turn Avoidance [175]

The BASS round transfers nearly all the kinetic energy potential of the round into the small cross-section penetrator, and thus gains an advantage over similar caliber rounds. Figure 10.2 below shows a comparison of common ground attack rounds to 20 and 25mm BASS rounds generated with the ballistic code discussed in Chapter 8 of this report. The top chart tracks the kinetic energy of the round versus its distance downrange and shows that for typical engagement ranges of around 10,000 feet, the 25mm BASS2581 delivers more kinetic energy to the target than the 30mm PGU-13A/B and SAPHEI rounds fired by the A-10. The bottom chart, tracking range versus time, shows that the BASS rounds are capable of longer standoff ranges than conventional rounds.

"As a whole, if you want to keep your system low cost, investment in munitions development (in particular lethality and survivability) will far outweigh investments in platform development as evidenced in programs like the BASS"-Dr. Lauren Schumacher

Figure 10.2 Kinetic Energy (top) and Time (bottom) vs. Range (ft)

Continued analysis of common rounds employed in ground attack produced the chart shown in Figure **10.3** on the following page, tracking the Armor Penetration capabilities versus Range of Engagement of these rounds. Following the trends laid out in Figure **10.2**'s comparison of Kinetic Energy versus Range, this graph illustrates the increased anti-armor capabilities of the Dragoon when utilizing 25mm BASS rounds over the competing ground attack

aircraft, including the A-10. Figure **10.3** below shows that at typical engagement distances, the 25mm BASS rounds used onboard the Dragoon have better armor penetration than the 30mm cannon aboard the A-10.

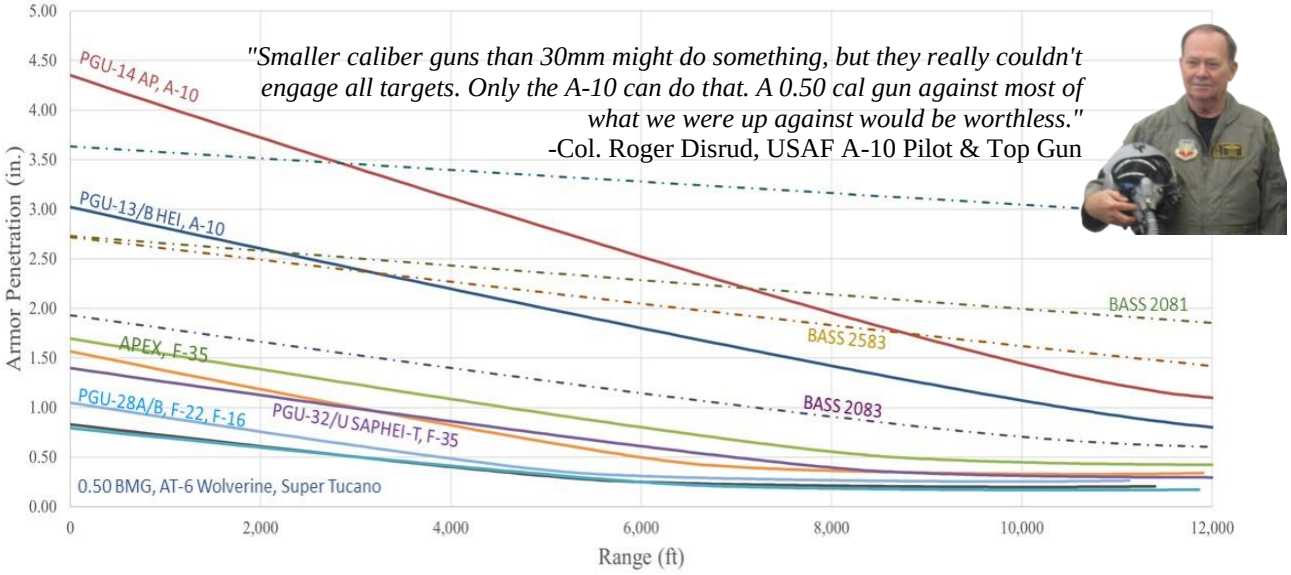

Figure 10.3 Armor Penetration Capabilities of Ground Attack Shells

There are two primary methods of delivering these hard-launched ordnances from attack aircraft, strafing runs and orbits. Strafing runs are the performed by aircraft with guns pointed in the direction of flight. The A-10 and EMB 314 Super Tucano deliver their hard-launched munitions via strafing runs. By approaching the target directly in front of the aircraft, strafing runs allow the pilot to see the target as they fly towards and shoot at it. The aircraft has to make a turn to be able to re-engage the target and provide its support to the ground troops. This tactic usually requires a second aircraft to provide cover fire as the first aircraft Even then, there are breaks in between the suppression fire and the aircraft can be left vulnerable to enemy fire. The other method of delivery, orbit fire, can help to eliminate this lack of suppressive fire. The AC-130 Gunship delivers its munitions while performing an orbit. An orbit attack requires a plane to have a gun mounted at 90 degrees, or a similar angle, to the direction of flight. This gun positioning allows the plane to fly in a circle around its target and allows the aircraft to continuously deliver munitions downrange. While the orbit allows for continuous delivery, a strafing run allows for repeated hits in the same spot of a target. Since both methods of delivery can provide advantages to an aircraft, the Dragoon will be able to deliver hard-launched ordnance both in strafe and orbit because of the rotating turret gun. This feature will give the aircraft strategic flexibility that

will allow one aircraft to do the job of two aircraft. As conditions in the battlefield change, the aircraft will even be able to switch modes during deployment.

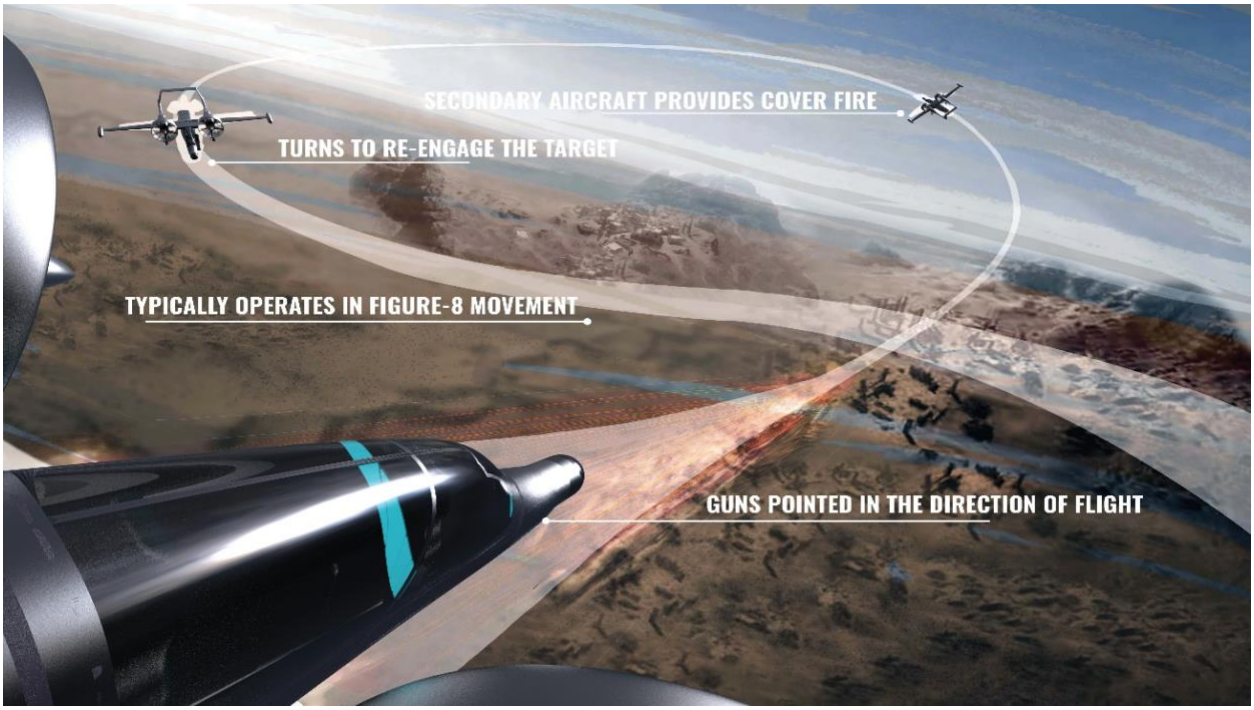

Figure 10.4: Strafing Run CONOPS

Figure 10.5: Orbit Attack CONOPS

While designing the orbit fire attack mode of this aircraft, consideration was given to crew survivability and safety. In the following analysis, solid pink lines are used to demarcate the effective range of the Russian-built SA-25 surface-to-air missile, indicating a no-fly zone for the aircraft, while analyzing the effective range of hard launched munitions employed by orbit engagement aircraft, specifically the AC-130 variants. Figure 10.6 below displays a sweep of these range analysis charts while firing at 3,000 ft increments between 3,000 and 15,000 ft.

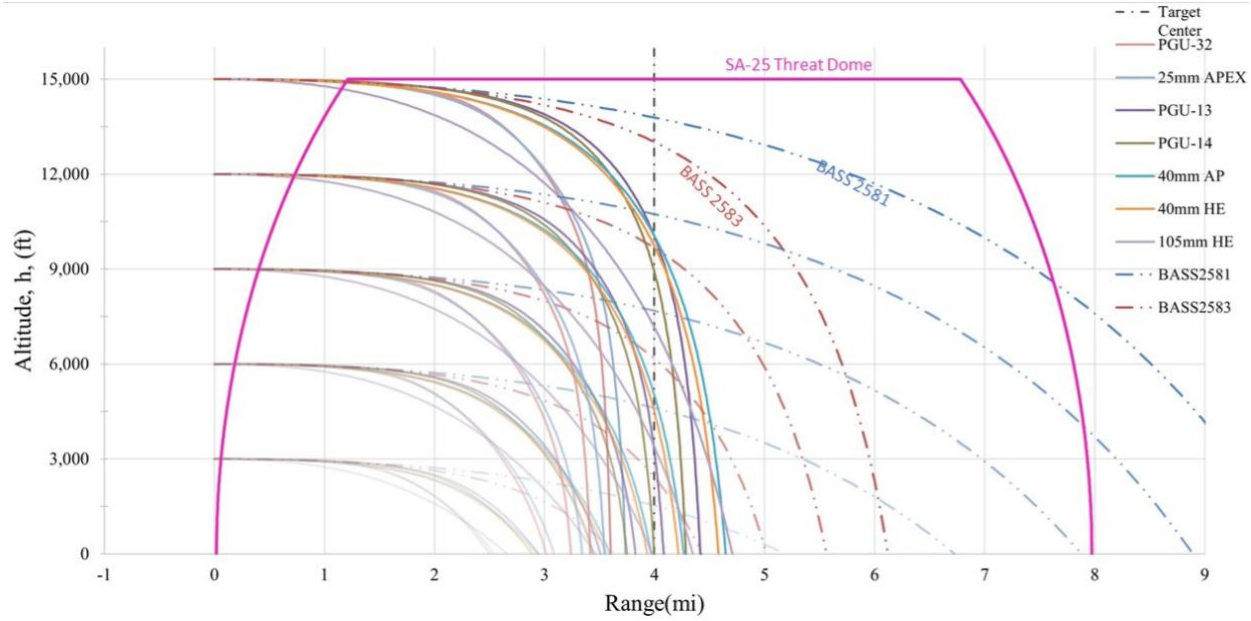

Figure 10.6 4 Mile Standoff Altitude Sweep Munitions Range Analysis

Following the analysis of the currently employed ground attack rounds and the range of the specified BASS rounds, Figure 10.7 shown on the next page, tracks the time of flight of the BASS 2581 AP rounds (blue) and BASS 2583 HE rounds (orange) when fired from 15,500-foot altitude and one mile standoff. The BASS 2581 round is smaller in diameter and heavier and is intended to function in the armor piercing function, while the lighter 2583 has a larger diameter and contains a hollow portion to facilitate the deployment of high explosive payloads.

"Orbiting fire is better than strafing fire. The reason is that orbiting fire can both suppress and engage. Strafing fire alone engages, then for the majority of the time the aircraft is circling around, the bad guys are able to return fire, move and engage friendly forces and aircraft. If an AC-130 was overhead and knew where both we and the bad guys were, we knew we would all be safe."
-Prof. Adrian Lewis, US Army Special Forces Officer, Ret.

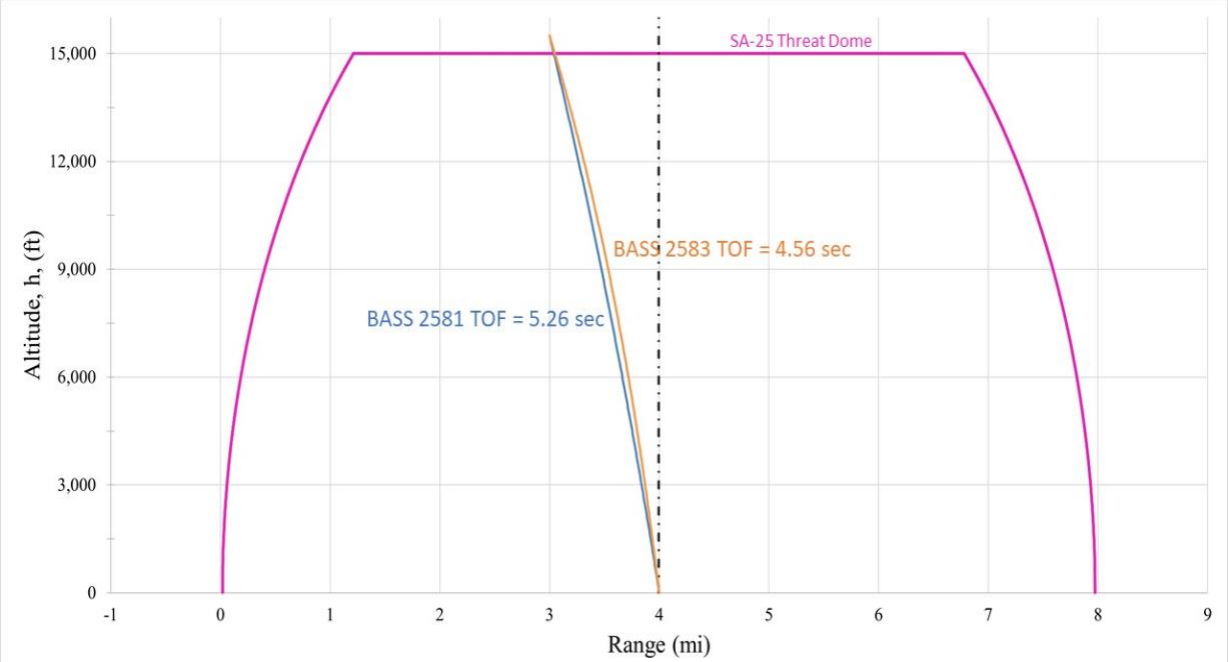

Figure 10.7 15,500 ft Altitude, 1 mi Orbit Direct Fire (BASS 2581/2583)

The final chart generated for this section, Figure 10.8, shown below, tracks the time of flight (TOF) of the rounds fired from orbit until their impact with the ground in both indirect and direct fire engagements.

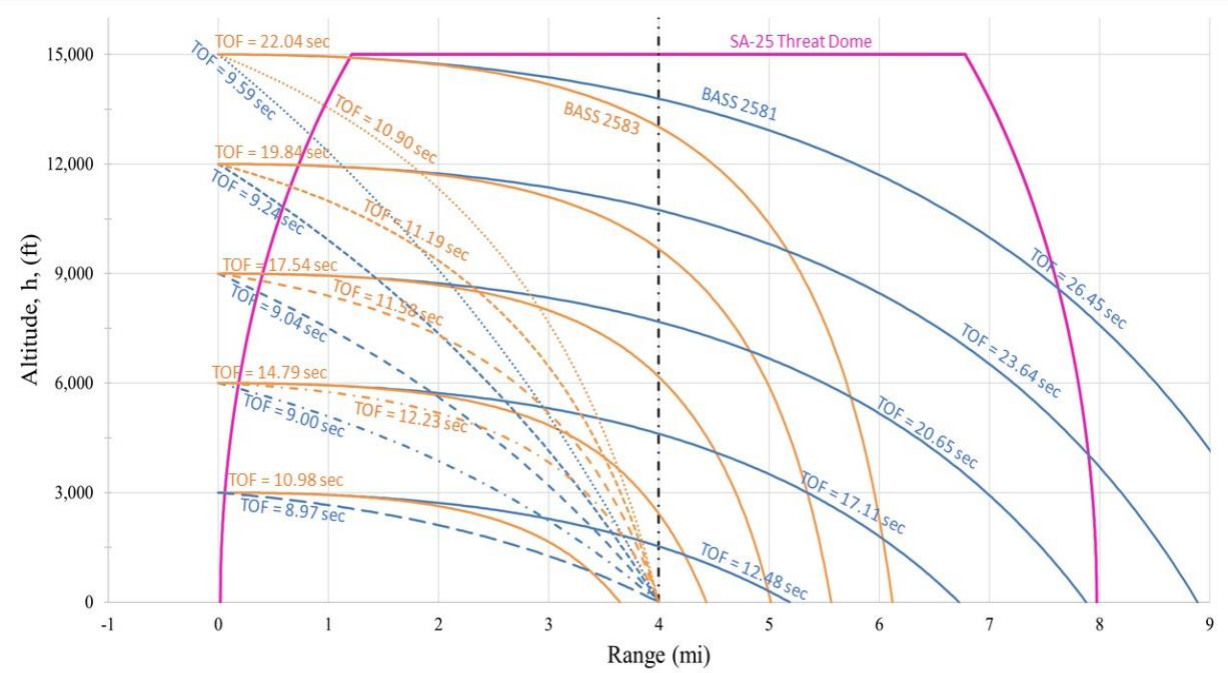

Figure 10.8 BASS Rounds Time of Flight for Indirect and Direct Fire

11 Stability and Control

Initial Class I Stability and Control was done using techniques found in *Airplane Design Part VI* [191] and Multhopp integration. Figure 11.1 shows the initial Class I longitudinal stability tracking the aerodynamic center and center of gravity with increasing horizontal tail area to the design area of 20 ft^2. This indicated that the design has a 13% static margin in the most aft center of gravity and a 35% static margin at the most forward center of gravity location.

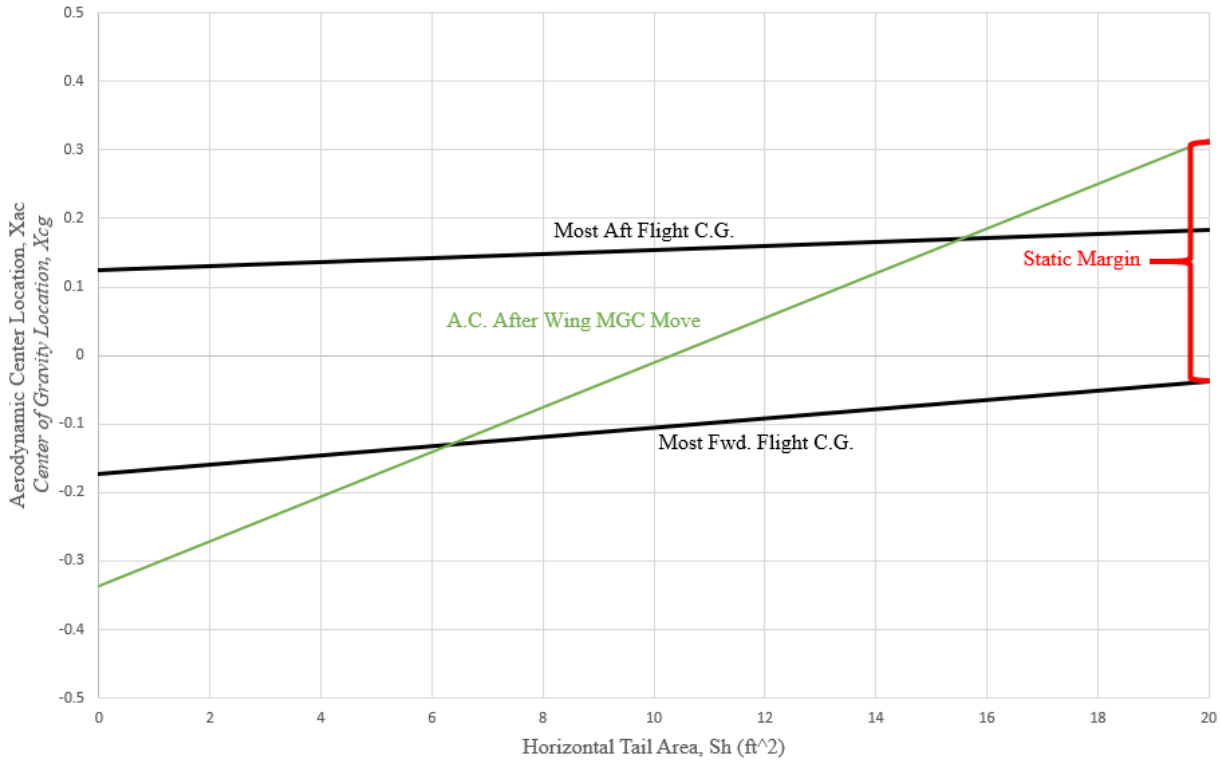

Figure 11.1: Class I longitudinal stability

Class I Directional Stability can be seen in Figure 11.2. To be directionally stable, the aircraft needs at least 0.001/degree yawing moment coefficient due to sideslip. This figure shows that the design is able to achieve a value of almost four times that. However, this is only do the dynamic pressure over the vertical tails caused by the propeller. Without this benefit, the design only provides a yawing moment coefficient of -0.0015/degree. This means that if the engines failed the aircraft would be directionally unstable. Fortunately, the engines are cross-shafted, so this scenario would only occur if both engines failed simultaneously. Therefore, the probability of this occurring is relatively low. Regardless, a feedback loop can be implemented in this scenario to keep the aircraft stable.

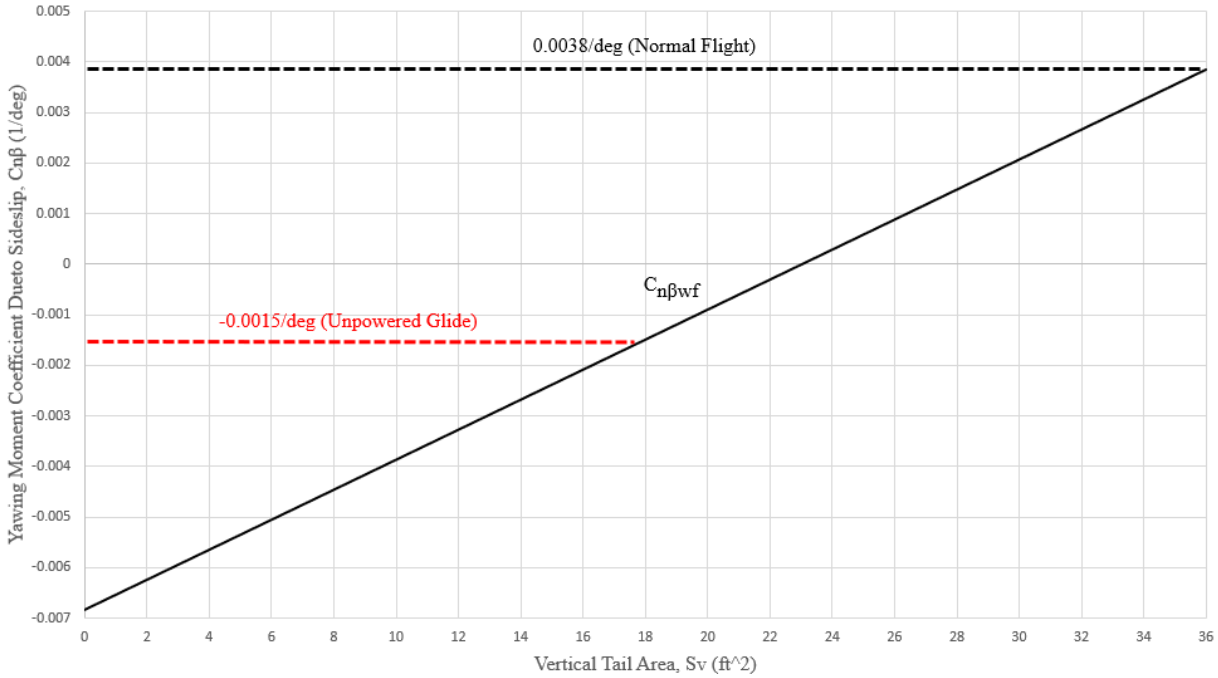

Figure 11.2: Class I Directional Stability

After Class I Stability and Control showed that the aircraft would be stable, a more in-depth Class II Stability and Control analysis was done using Advanced Aircraft Analysis (AAA) software from DARcorporation. To be adequately controllable, the aircraft must adhere to level-1, class IV stability and control regulations. These regulations as well as the aircraft stability calculated by AAA can be seen in Table 11.1.

Table 11.1: Stability and control regulations and calculations

Stability and Control Term	Level 1 Class IV Requirement	Dragoon Stability and Control	Flying Quality Dragoon Achieves
Phugoid Damping Ratio: ζ_p	$\zeta_p > 0.04$	0.004 rad/s (de-facto) 0.394 rad/s (with feedback)	**Level 1 (with feedback)**
Phugoid Natural Frequency: ω_{n_p}	~	0.12 rad/s	**Level 1**
Short Period Damping Ratio: ζ_{sp}	$0.35 < \zeta_{sp} < 1.3$	0.45 rad/s	**Level 1**
Short Period Natural Frequency: $\omega_{n_{sp}}$	$\omega_{n_{sp}}$	2.17 rad/s	**Level 1**
Dutch Roll Damping Ratio: ζ_d	$\zeta_d > 0.4$	0.99 rad/s	**Level 1**
Dutch Roll Natural Frequency: ω_{n_D}	$\omega_{n_D} > 1$	0.90 rad/s (de-facto) 1.03 rad/s (with feedback)	**Level 1 (with feedback)**
Roll Mode Time Constant: T_r	T_r < 1.4 seconds	1.2 seconds	**Level 1**
Time to Double Amplitude in Spiral: T_{2s}	T_{2s} > 12 seconds	16.6 seconds	**Level 1**

These can also be seen in Figure 11.4 and Figure 11.3. Figure 11.4 shows that the short period clearly satisfies level 1 flying qualities. However, Figure 11.3 indicates that the aircraft does not satisfy the Dutch roll frequency level-1 flying quality of 1 rad/s. In addition, the aircraft does not naturally satisfy the phugoid natural frequency

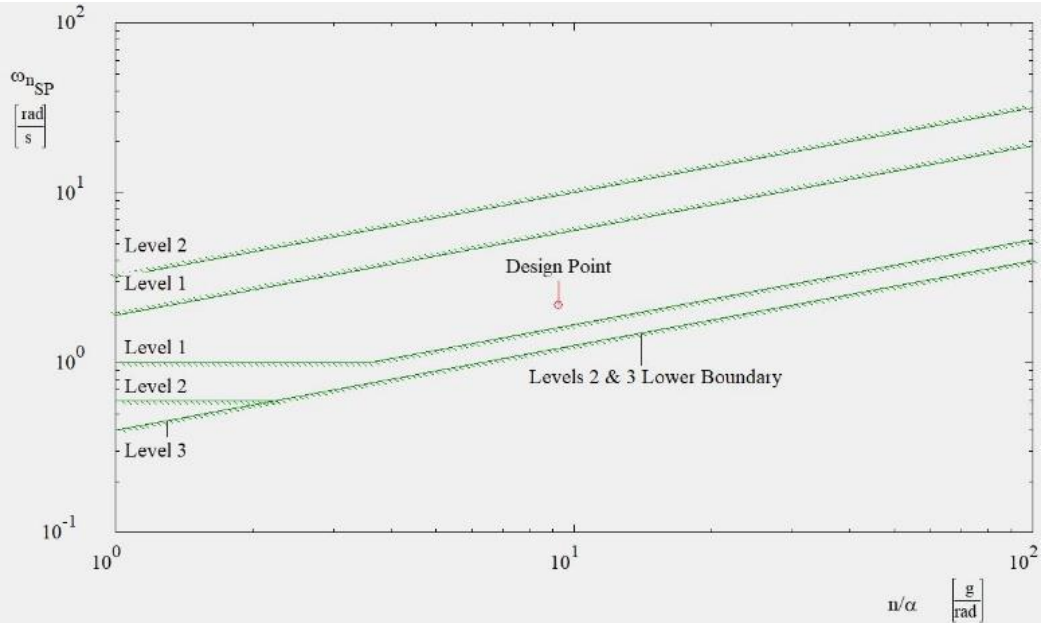

Figure 11.4: Short period characteristics graphed in AAA

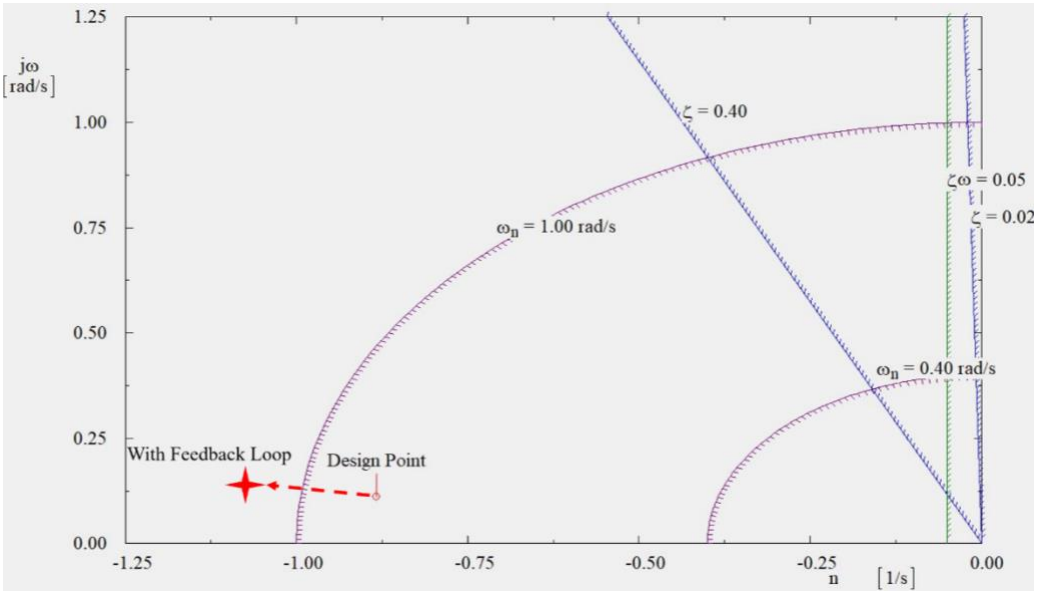

Figure 11.3: Dutch roll characteristics graphed in AAA

requirement. Therefore, a feedback system was created for both of these to satisfy the level-1, class IV flying qualities.

The feedback gain for Dutch roll is based on feedback to the rudder as seen in the following equation:

$$\mathbf{k_u/_{\delta_T}} = \frac{\mathbf{\Delta C_{T_{x_u}}}}{\mathbf{U_1 C_{T_{\delta_T}}}} \ [\mathbf{Ref.}\ 192\ \mathbf{eq.\ 3.18}]$$

$$k_u/_{\delta_T}\left(U_1 C_{T_{\delta_T}}\right) = C_{T_{x_u}}{}_{de-facto} - C_{T_{x_u}}{}_{required}$$

$$k_u/_{\delta_T}\left(U_1 C_{T_{\delta_T}}\right) = (-0.0501) - (-1.1)$$

$$k_u/_{\delta_T}\left(U_1 C_{T_{\delta_T}}\right) = 1.0499$$

The feedback gain for the phugoid mode is based on feedback to the engine as seen the following equation:

$$k_\beta/_{\delta_r} = \frac{C_{n_{\beta_{de-facto}}} - C_{n_{\beta_{required}}}}{C_{n_{\delta_r}}} \text{ [Eq. 3. 28, Ref 192]}$$

$$k_\beta/_{\delta_r} = \frac{(-0.0115) - (-0.02)}{-0.1059}$$

$$k_\beta/_{\delta_r} = -0.08$$

The stability and control derivatives found by AAA are given in Table 11.2, and the trim diagram can be seen in Figure 11.5. This diagram clearly shows that we have a stable pitch break and can operate with -20 to 20° of elevator deflection. The left side of the figure indicates the effect of elevator deflection on the aircraft coefficient of lift while the right side is the trim diagram with black lines indicating our most forward and aft C.G. locations while the red circle indicates the design point.

Table 11.2: Stability and control derivatives

Longitudinal		**Lateral**	
	Cruise		**Cruise**
$C_{m_\alpha}\left(1/_{rad}\right)$	-0.5451	$C_{y_\beta}\left(1/_{rad}\right)$	-0.3789
$C_{L_u}(\sim)$	0.3072	$C_{l_\beta}\left(1/_{ra\,d}\right)$	-0.0308
$C_{m_u}(\sim)$	0.0705	$C_{n_\beta}\left(1/_{rad}\right)$	-0.0115
$C_{L_q}\left(1/_{rad}\right)$	13.60	$C_{y_p}\left(1/_{rad}\right)$	0.0196
$C_{m_q}\left(1/_{rad}\right)$	-47.5	$C_{l_p}\left(1/_{rad}\right)$	-0.6367
$C_{L_{\dot\alpha}}\left(1/_{rad}\right)$	1.8795	$C_{n_p}\left(1/_{rad}\right)$	-0.0915
$C_{m_{\dot\alpha}}\left(1/_{rad}\right)$	-11.2475	$C_{y_r}\left(1/_{rad}\right)$	0.2020
$C_{L_{i_H}}\left(1/_{rad}\right)$	4.1678	$C_{l_r}\left(1/_{rad}\right)$	0.2082
$C_{m_{i_H}}\left(1/_{rad}\right)$	-3.8344	$C_{n_r}\left(1/_{rad}\right)$	-0.1059
$C_{L_{\delta_E}}\left(1/_{rad}\right)$	0.1107	$C_{y_{\delta_A}}\left(1/_{rad}\right)$	0
$C_{m_{\delta_E}}\left(1/_{rad}\right)$	-0.6627	$C_{l_{\delta_A}}\left(1/_{rad}\right)$	0.1091
		$C_{y_{\delta_R}}\left(1/_{rad}\right)$	0.038
		$C_{l_{\delta_R}}\left(1/_{rad}\right)$	0.0027
		$C_{n_{\delta_R}}\left(1/_{rad}\right)$	-0.0205

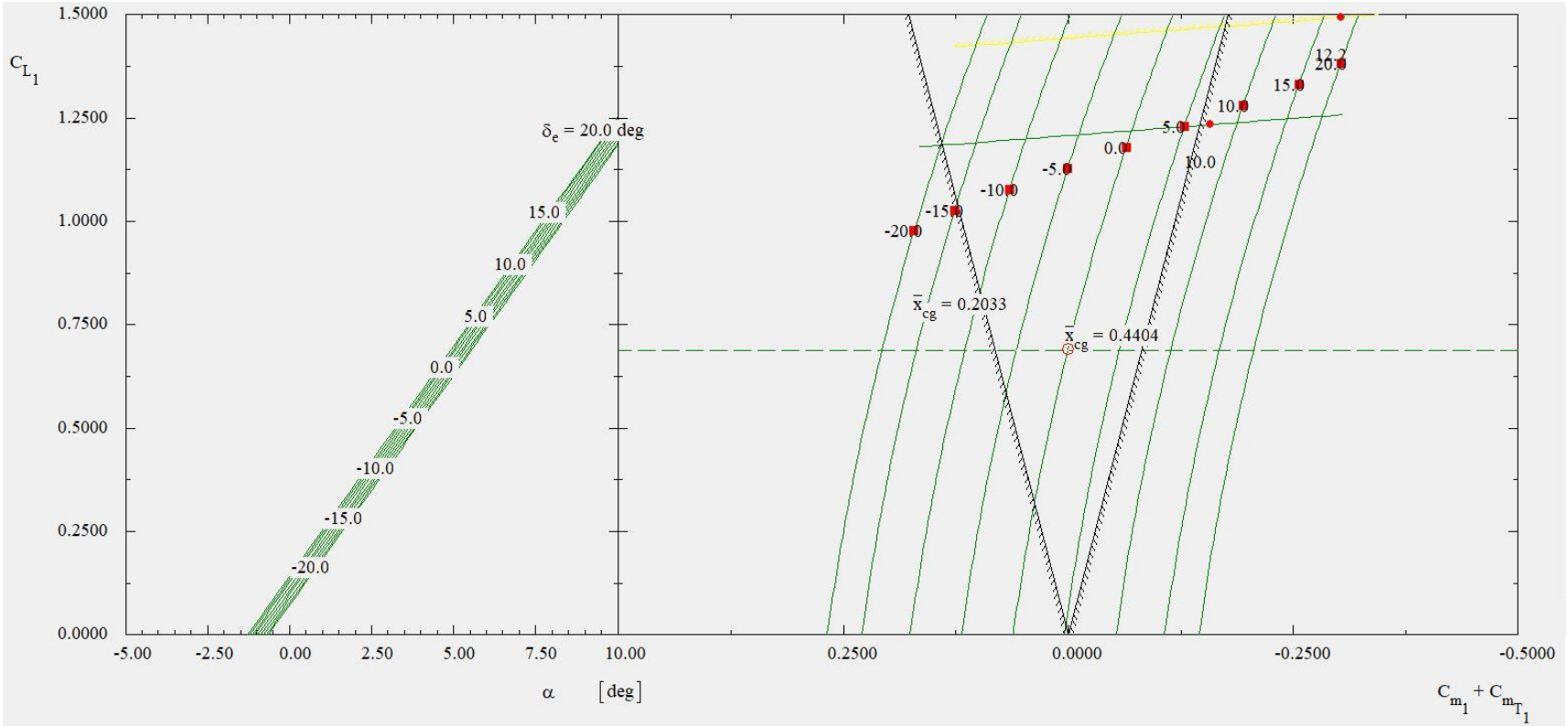

Figure 11.5: Trim diagram

12 Class II Layout of Major Systems

This chapter details the layout of the Dragoon systems.

12.1 Flight Control and Electrical Systems

This section describes the flight control and electrical systems of the Dragoon aircraft.

12.1.1 Layout of Wiring and Control Surface Actuators

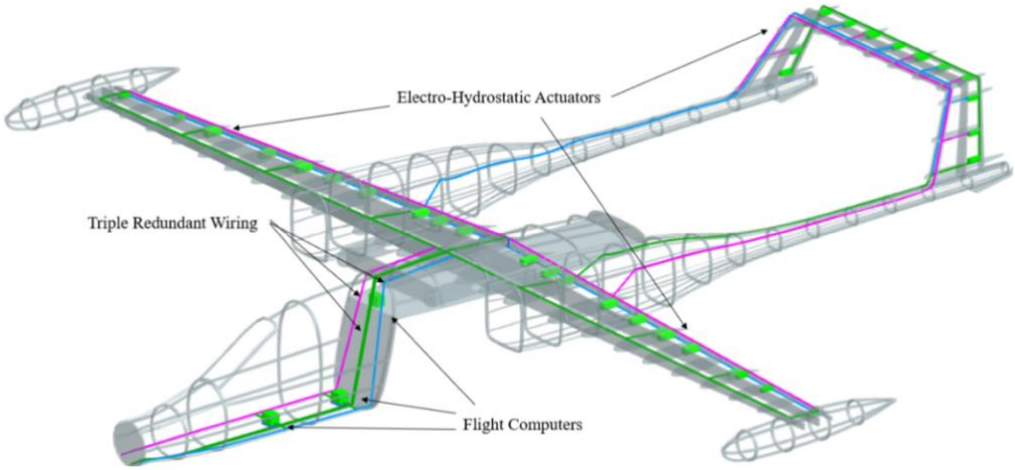

Figure 12.1: Layout of Wiring and Placement of Flight Computers and Control Surface Actuators

Each control surface will be controlled by 3 actuators. This feature provides the system with redundancy in case any of the actuators fails. In the case of an actuator failure, the attach point of the actuator to the wing structure will be designed to fail at a stress, in both tension and compression, that two together can provide and that an individual actuator cannot provide. This stress will be caused at a moment 40% higher than the individual actuator provides. Table 12.1 shows the required moments that each actuator must provide to the control surfaces in the worst-case scenario. The moments specified for the sizing of actuators was chosen so that the same actuator could be used for multiple control surfaces when the requirements were reasonably close.

Table 12.1: Control Surface Actuator Requirements

	Total Required Moment Provided by Actuators (lb-in)	Individual Actuator Moment (lb-in)	Actuator Attach Point Failure Moment (lb-in)
Inboard Aileron	515	425	595
Outboard Aileron	823	275	385
Inboard Flap	888	500	700
Outboard Flap	949	500	700
Elevator	236	125	175
Rudder	709	425	595

12.1.2 Electrical Requirements

The electrical power requirements of the aircraft are met through a triple redundant system of the Auxiliary Power Unit (APU) and excess power from the aircraft engines. For startup, the APU is powered by a battery. The APU then starts the engines pneumatically. The APU, a Honeywell Micro Power Unit, is the main power source for the systems before flight, providing the APU size requirements. For the cockpit air conditioning and heating systems, the primary source of power will be provided directly from the APU mechanically. The engines will provide backup power, using converters to convert shaft horsepower into electrical power.

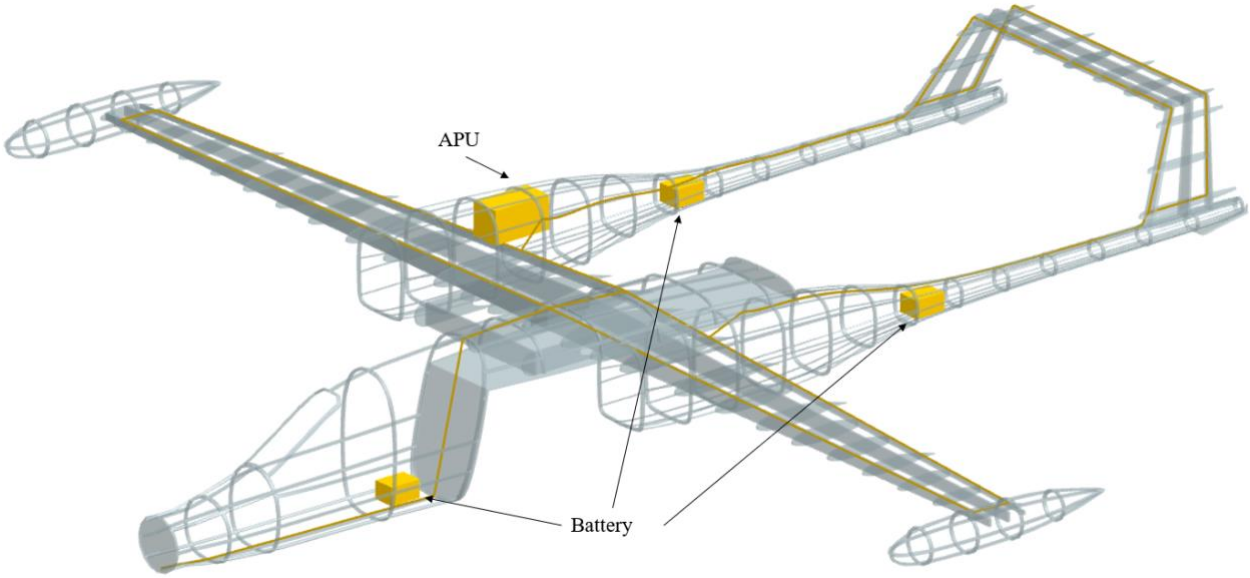

Figure 12.2: Electrical System Layout

Table 12.2: Electrical Requirements

	Ground Loading		Takeoff/Climb		Cruise/Loiter	
	K.V.A.	**%**	**K.V.A.**	**%**	**K.V.A.**	**%**
Lighting	0.52	6.57 %	0.77	7.68 %	0.04	0.48 %
De-icing	4.00	50.57 %	4.00	39.88 %	4.00	48.45 %
Gun	0.00	0.00 %	0.00	0.00 %	0.75	9.04 %
Flight Control	0.25	3.16 %	0.40	3.99 %	0.40	4.84 %
Avionics	1.06	13.40 %	1.48	14.76 %	1.45	17.56 %
Fuel	0.00	0.00 %	1.30	12.96 %	1.30	15.75 %
Hydraulic	1.76	22.25 %	1.76	17.55 %	0.00	0.00 %
Environmental	0.32	4.05 %	0.32	3.19 %	0.32	3.88 %
Total	**7.91**		**10.03**		**8.26**	

12.2 Fuel System

The fuel system for the aircraft holds 385 gallons of fuel as required for completing the design mission. Single point refueling is accomplished on the right wing of the aircraft as can be seen in Figure 12.3. Sumps are located in the inboard wing fuel tank as well as the tip tanks, and scavenging pumps are located throughout the tanks to make sure all the fuel is usable. Since the aircraft is meant primarily for combat, all fuel tanks are self-sealing.

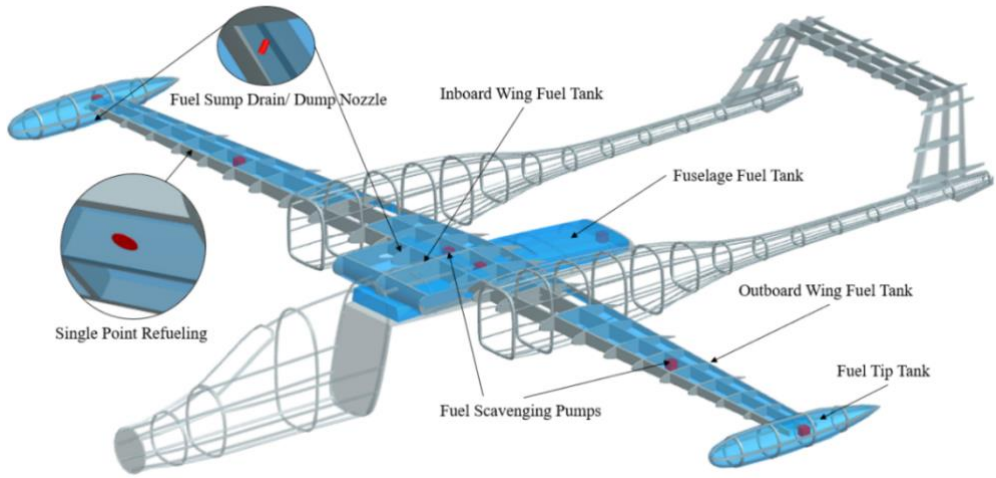

Figure 12.3: Fuel System Layout

12.3 Hydraulic System

The hydraulic system is used for the extension and retraction of landing gear seen in Figure 12.4. It is sized from the hydraulic pressure required by the main landing gear oleo struts when the aircraft is sitting on the ground. The hydraulic system will be sized to 4000 psi to provide pressure to both main landing gear and the nose landing gear.

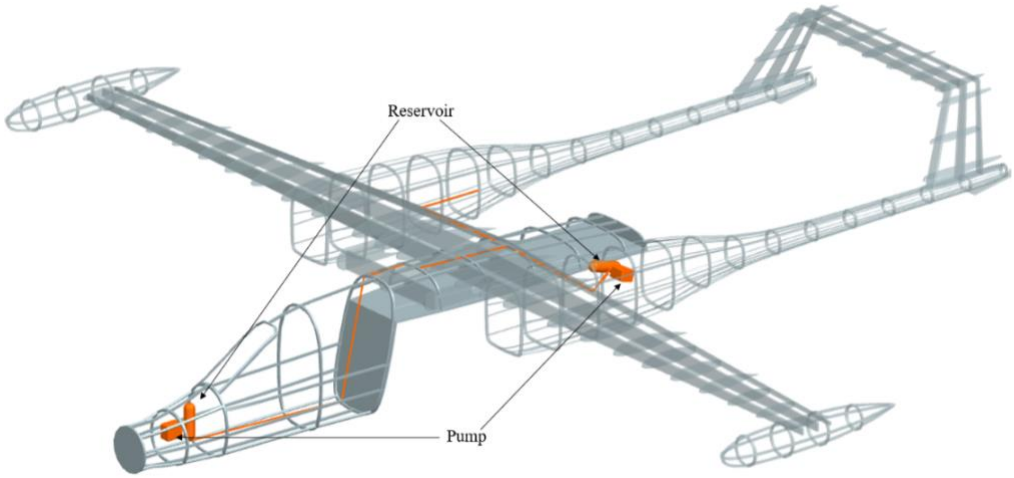

Figure 12.4: Hydraulic System Layout

12.3.1 Main Landing Gear Actuators

The main landing gear has two hydraulic actuators, a retraction strut for extending and retracting the landing gear and an oleo-strut for helping absorb shocks on the austere during takeoff and landing. The oleo-strut and retraction

strut hydraulic requirements are sized by the fully extended and fully retracted states, respectively. Pressure requirements for the gear can be seen in Table 12.3. The oleo-strut also allows the aircraft to "squat" while it is on the ground so that the aircraft's pod can be easily replaced. This method will be shown in further detail in section 12.12.

Table 12.3: Main Landing Gear Pressure Requirements

	Pressure Extended (grounded)	Pressure Extended (in flight)	Pressure Halfway Extended	Pressure Retracted
Oleo-strut	1276 psi	-44 psi	35 psi	85 psi
Retraction strut	20 psi	20 psi	41 psi	91 psi

Since a "negative" pressure was initially calculated for the main landing gear oleo-strut when they are extended in flight, a spring system was specified to bring the required pressure to zero. In addition to fixing the problem of negative pressure, the spring system allows the gear to be extended in flight even if the hydraulic system fails due to combat, etc. A spring system was also created for the retraction strut to provide this same feature to extend the system fully if hydraulics are no longer functioning. In the case of a hydraulic failure, the oleo-strut can be latched into place until the system is repaired and can once again support the aircraft and its squatting mechanism.

Table 12.4: Main Landing Gear Pressure Requirements with Spring System

	Pressure Extended (grounded)	Pressure Extended (in flight)	Pressure Halfway Extended	Pressure Retracted
Oleo-strut	1320 psi	0 psi	84 psi	121 psi
Retraction strut	0 psi	0 psi	16 psi	79 psi

12.4 Targeting Systems and Optics

Dragoon uses the Wescam MX-20D airborne targeting solution made by L3Harris. The AT6 Wolverine light attack aircraft also uses an L3Harris targeting solution, but it uses the smaller Wescam Mx-15D system. The MX-20D system's ball turret has a 21.1 in diameter and a total system height of 26.5 in. It has a 360° azimuth range and a +90° to -120° elevation range with a 320W average power draw and a 1000W maximum power draw. The entire system is comprised of eight sensors listed in Table 12.5. The targeting system is mount on the nose facing forwards to help keep the airflow of the aircraft as streamline as possible and reduce drag. The placement is

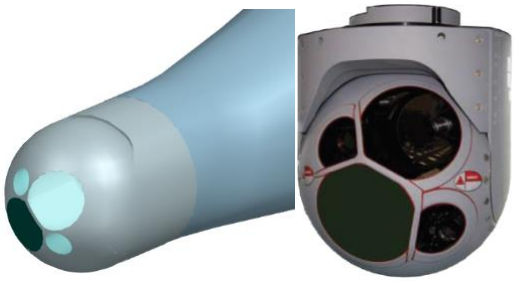

Figure 12.5: Wescam MX-20D

(Manufacturer Photo and CAD) [176]

Table 12.5: Wescam MX-20D Sensors

640 x 512 resolution thermal imager
1280 x 1024 resolution thermal imager
megapixel color low-light continuous zoom camera
2-megapixel color daylight spotter
2-megapixel low light spotter
Narrow or ultra-narrow 860 nm laser illuminator
1064/1570 nm selectable 30 km laser designator/rangefinder code compatible with U.S. and NATO laser guided munitions
1064 nm laser spot tracker compatible with U.S. and NATO laser guided munitions

also to ensure clean weapons egress from the pod rotary system, as a bottom mounted version may collide or have an increased amount of vision reduction due to the smoke trails left by rockets or missiles.

12.5 Cockpit Instrumentations, RF, and Sat Coms

The layout of the cockpit has been setup into a tandem for purposes of reducing the cross-sectional area of the fuselage and drag. Where the pilot will sit front seat and the WSO in the back. The primary instrumentation for the aircraft is all done through glass panels, each seat with four displays seen in Figure 12.6. Each of the display panels can be set to display any critical flight data in the case of one screen possible failure. In addition to the primary display panels a flat targeting panel is in place to ensure no distortion when firing in strafe mode. The instrumentation onboard the Dragoon also includes the most up to date radio frequency and satellite communications technologies to ensure fast and secure uplinks to headquarters and ground personnel. This also allows for the long-distance unmanned ferry mission of the aircraft if every needed to be transported.

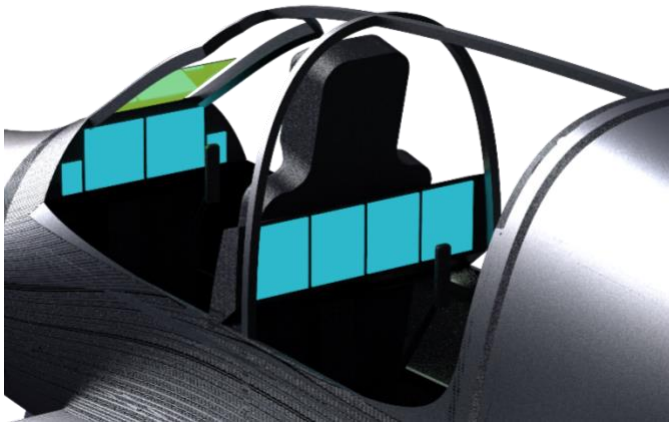

Figure 12.6: Cockpit Instrumentation Layout

12.6 De-Icing and Anti-Icing Systems, Window Rain, Fog, and Frost Control

The de-icing system for the aircraft will use bleed air from engines to de-ice the stators and ducted fans. This system can be turned on or off by the pilot to reduce the IR signature of the aircraft as much as possible because the

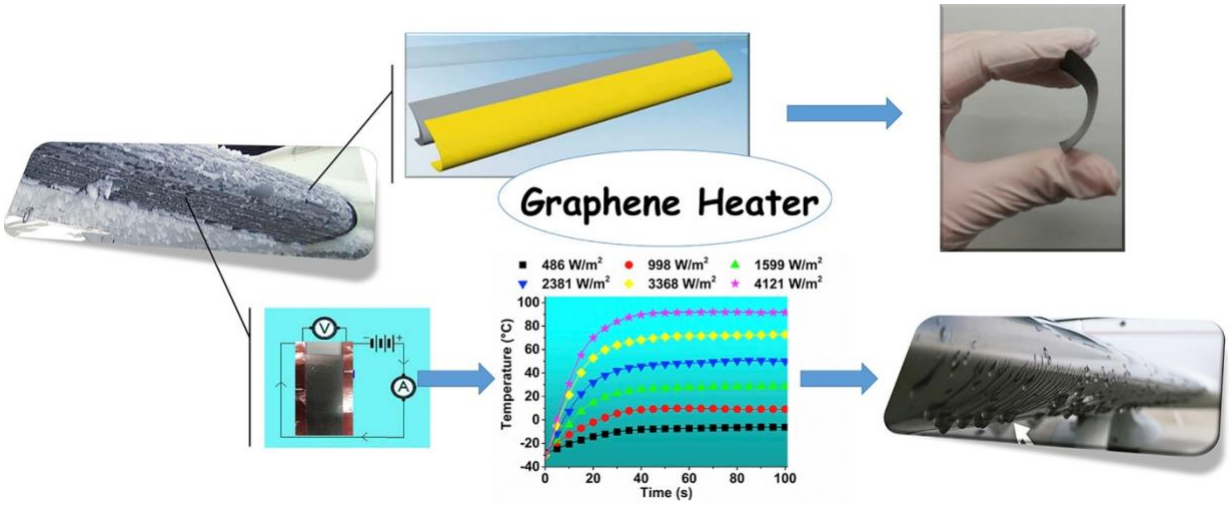

Figure 12.7: Graphene De-icing System [178]

hot air will run only when needed. The slats of the aircraft will have de-icing provided by running a current through graphene, which creates a resistance heater. The graphene will be a component of the leading-edge slats. When the heater is turned on from the cockpit, the ice that has built up on the surface will melt, causing the rest of the ice build-up to fall off. This will have a low IR signature because the ice will only need to be heated to just above freezing and the heater can be turned off when ice is not present.

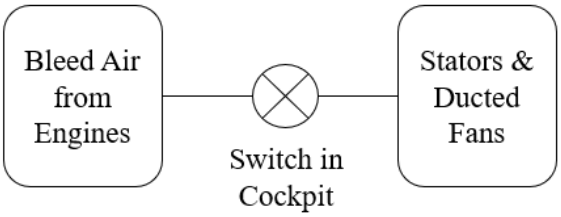

Figure 12.8: Bleed Air De-icing System

The rain, fog, and frost on the window will be controlled using windshield wipers. As a supplement for fog and frost control, the heater and air conditioning system for the cabin will have vents routed to the windows. These vents will be able to melt frost and clear fog once the APU is running.

12.7 Gun System, Round Handling and Loading

12.7.1 Gun Platform Options

During the initial design of the Dragoon, a variety of gun platforms were considered for application as the onboard gunnery system. This list included calibers varying in size from 0.50 BMG rounds up to 25mm cannon shells. While smaller calibers were not considered in the primary gun selection as their effectiveness degrades at long distance, mounting the gun in the munitions pod allows for the implementation of any available smaller caliber gun platforms at the discretion of the user. Additionally, rounds larger than 25mm were not considered as the recoil forces present in gun platforms firing large-caliber shells exceeded the airframe capabilities of the Dragoon. Table **12.6** shown above, displays the range of gun platforms considered.

Table 12.6 Gun Platforms Considered for Use in Design [34,36,38,39,41,179,180,181]

Gun Platform	Diameter	Weight (lbs.)	Length (in.)	Rate of Fire
M2 Browning	12.7mm	83.7	65.1	450-600
GAU-19	12.7mm	138	53.9	1,000-2,000
M39	20mm	178.5	72.05	1,500
M197	20mm	132	71.93	1,500
M61	20mm	248	71.39	6,000
Sky Viper	20mm	Classified	Classified	Classified
GAU-12	25mm	270	83.2	1,800-4,200
GAU-22	25mm	230	83.2	3,200
M242	25mm	262	105.2	1-200

When selecting gun platforms, there are several characteristics considered that impact the size of shells deployed, including effectiveness against various targets, cost of shells, weight of shells, and the number of rounds required to kill targets. The first of these characteristics, target effectiveness, is a function of both size and type of shells used. As shown in Figure 10.3 in a previous section of this report, aerial gunnery rounds, including those fired by the gunnery

platforms shown in Table **12.6**, have varying effectiveness against armored targets. Table 12.7 below examines the effectiveness of common shells compatible with the gun platforms considered for use onboard the Dragoon.

Table 12.7 Shell Effectiveness Against Targets Based on Armor Level

Shell Type	Personnel	Unarmored Vehicles	Light (0-0.5 in.) Armored Vehicles	Armored (0.5-1.5 in.) Vehicles	Heavy (1.5+ in.) Armored Vehicles	Helicopters
12.7mm Ball	High	Medium	Limited	None	None	Medium
12.7mm AP	High	High	Medium	None	None	Medium
PGU-28A/B	High	High	Medium	Limited	None	High
M56A3/A4	High	High	Medium	Limited	None	High
PGU-32	High	High	Medium	Limited	None	High
25mm APEX	High	High	High	Limited	None	High
BASS2081	High	High	High	High	High	High
BASS2083	High	High	High	Limited	None	High
BASS2581	High	High	High	High	High	High
BASS2583	High	High	High	High	Limited	High

Advances in smart munitions, including laser guided bombs, missiles and rockets, has, in recent years, thrown into question the need for gun platforms onboard aircraft. While air superiority fighters like the F-22 Raptor and F-35 Lightning II rely primarily on air-to-air missiles for engagements with enemy aircraft, the designers of these aircraft have included provisions for onboard gunnery systems, and with good reason. Lessons learned by Air Force pilots in Vietnam have influenced the designs of aircraft and aerial gunnery systems have been retained as last a backup for self-defense on board fighters. Onboard ground attack aircraft, the inclusion of gun platforms has been driven by cost factors. This data is presented in Table **12.8**, tracking the cost of shells and other mechanisms.

Table 12.8 Kill Mechanism Costs

Kill Mechanism	Cost Per Shot
12.7mm Ball	~$2.00[182]
12.7mm AP	~$3.00[182]
PGU-28A/B	~$30.00[183]
M56A3/A4	~$12.00[183]
PGU-32	~$23.00[183]
25mm APEX	~$148.00[183]
BASS2081	~$30[184]
BASS2083	~$30[184]
BASS2581	~$30[184]
BASS2583	~$30[184]
M780 30mm	~$125 [184]
Hellfire	~$150,000 [55]
Mk. 82	~$3,000 [50]

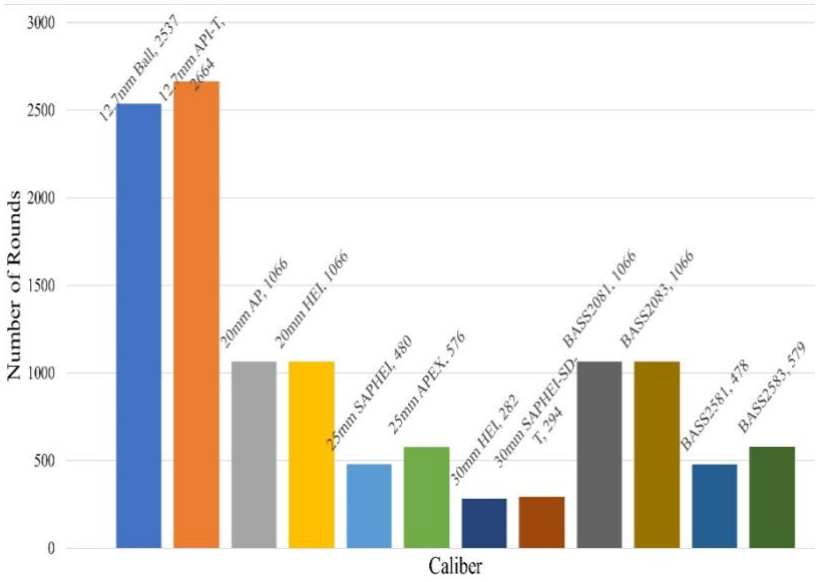

Figure 12.9: Number of Rounds Carried VS Caliber

Figure 12.9 shows the number of rounds capable of being carried into the air plotted against caliber. Based on the information in this Chapter and in Chapters 9 and 10 of this report, in addition to advice received from subject matter experts the integrated gun platform selected for the Dragoon is the M242 Bushmaster 25mm chain gun. Chosen for its extreme reliability, with a mean rounds between failure of 22,000, this cannon also features a unique dual feed system shown in Figure 12.10 allowing gunners to switch rounds mid-engagement by selecting the upper or lower feed belt, shown here loaded with BASS 2581 AP rounds on the top and BASS 2583 HE rounds on the bottom [178].

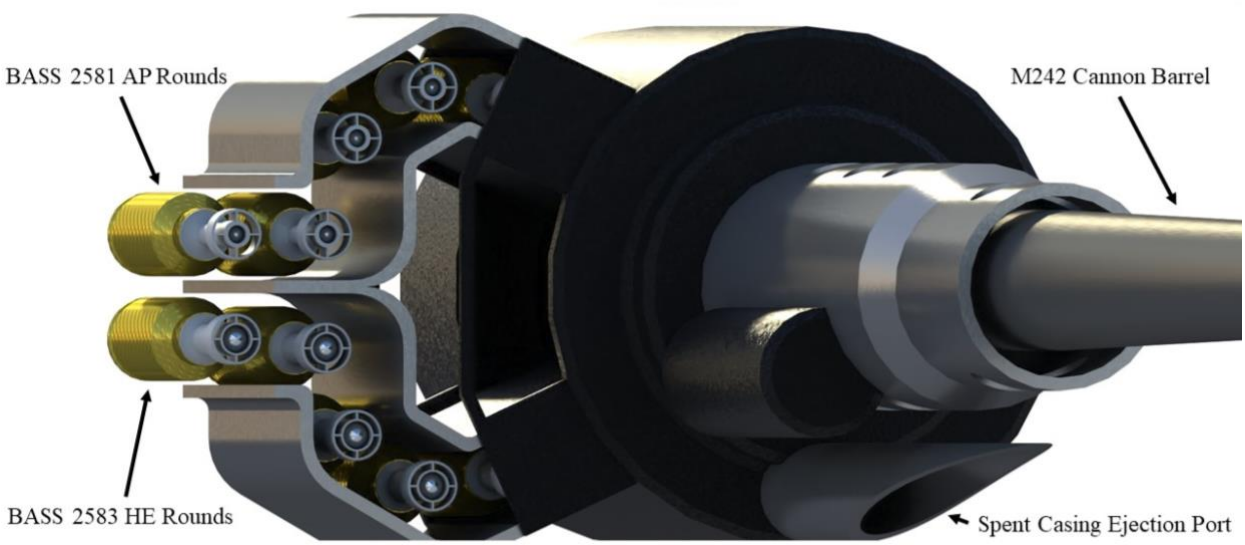

Figure 12.10 M242 Bushmaster Dual Feed System

12.7.2 Gun Positions

As outlined in Chapter 10 of this report, the integrated gun system onboard Dragoon is configured to fire in both strafing engagements and in orbital engagement styles. The M242 cannon shown in Figure 12.11 used in the Dragoon is mounted in a modified ball turret under the left-side wing on the forward bulkhead of the removable munitions pod. This turret allows the cannon to rotate ninety degrees aft to align with the wing, and to pivot from a horizontal firing arc to a maximum depression angle of 45 degrees below horizontal.

A major issue present in many aerial gunnery systems is gun gas ingestion into the engines and optical system fouling due to exposure to gun gas. The chemicals in gun gasses are extremely corrosive, and the effects of ingestion into engines can be seen in the A-10 program, which has seen countless engine fans replaced due to corrosion. The integration of the M242 cannon onboard the Dragoon minimizes the effects of ingesting gun gas by mounting the engine high on the wing and the cannon low on the fuselage as shown in Figure 12.12 below.

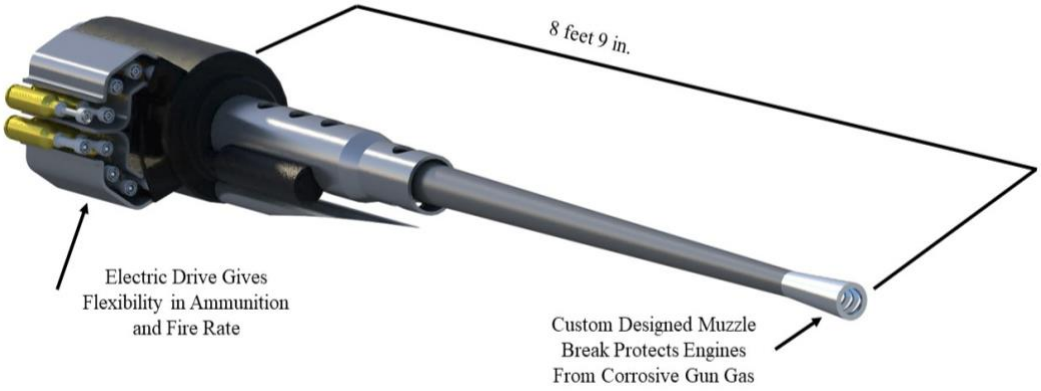

Figure 12.11 M242 Bushmaster 25mm Chain Gun

Figure 12.12 M242 Bushmaster Cannon Placement for Strafe Engagements

Additionally, the M242 mounted to the Dragoon is fitted with a uniquely designed muzzle break, shown in detail in Figure 12.13, designed to divert gun gasses away from the engine intakes by diverting them both up and down around the ducted fan disk. The integration of the M242 cannon and muzzle break also serves to protect the optical sensor pod from exposure to corrosive gun gasses by diverting the gasses away from the sensor. The asymmetrical design of the muzzle break will impart a side force on the barrel. This is avoided in orbit mode by locking the muzzle break in place and slewing only the barrel and shroud which can be seen in following figures in this section. The single barreled nature of the M242, discussed in depth later, allows it to be mounted to the aircraft in a manner designed to protect the cockpit crew and adjacent structures from the muzzle blast. This is accomplished in the strafe mode by locking the cannon into an armored trough running along the fuselage seen in Figure 12.13. The design of the trough provides increased strength for the mounting system discussed below.

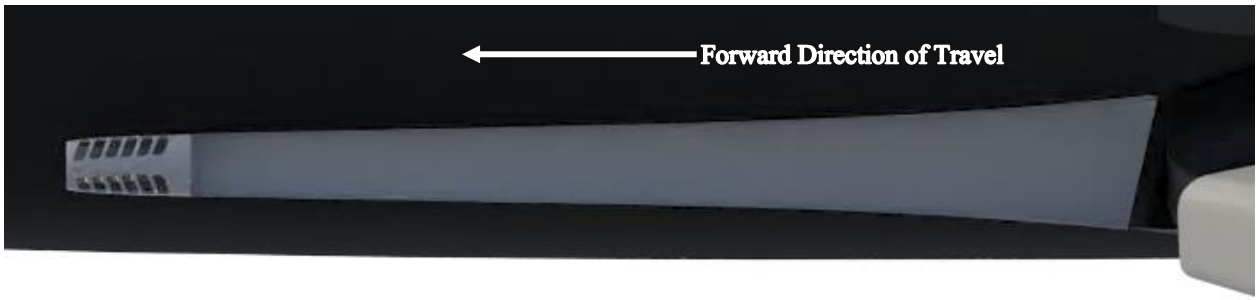

Figure 12.13 M242 Strafe Mode Armored Trough with Integrated Muzzle Break

While multi-barreled weapons like the GAU-12 and M61 Vulcan enjoy a superior rate of fire over the single barreled M242, the lower rate of fire is seen as beneficial as it allows the aircraft to conserve ammunition while firing. This lower rate of fire also reduces the recoil forces, thereby reducing the error in targeting induced by recoil. The single barrel design also allows the M242 to lock into a forward bracket mounted to the nose structure while in the strafe configuration. This reduces sway in the barrel due to aerodynamic forces and recoil by transferring the forces into the structure of the aircraft on both ends of the cannon.

When transferred into the orbit mode, the cannon will experience greater CEP and barrel whip due to the lack of forward support. The error will be exacerbated by aerodynamic forces on the barrel. The aerodynamic shroud shown in Figure 12.14 on the next page is designed to reduce the aerodynamic forces on the barrel. Mounted internally in this shroud, a barrel tuner serves to mitigate barrel whip by absorbing the vibrations caused by firing the cannon.

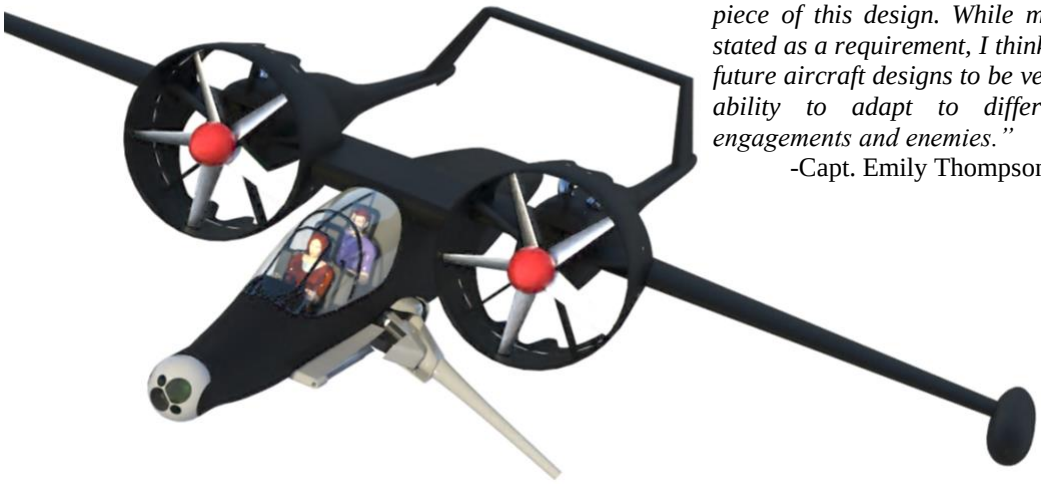

"This team nailed the versatility and flexibility piece of this design. While maybe not explicitly stated as a requirement, I think it's crucial for our future aircraft designs to be versatile and have an ability to adapt to different environments, engagements and enemies."

-Capt. Emily Thompson, USAF, F-35 Pilot

Figure 12.14 M242 Bushmaster Aerodynamic Shroud Shown in Orbit Mode

In addition to reducing aerodynamic forces on the barrel, the shroud surrounding the M242 onboard the Dragoon serves to reduce the overall drag on the aircraft caused by slewing the cannon into the orbit configuration. The integrated muzzle break also serves as a flash hinder, designed to reduce the flash of the muzzle blast while firing, helping to reduce the observables presented by the aircraft to ground observers. The shroud around the cannon also provides structure to tie the barrel cooling system into as shown in Figure 12.15. Similar to the system onboard the A-10, a tank of deionized water is carried onboard the aircraft, and as the cannon fires, a small amount is sprayed out onto the barrel to cool it.

The final issue considered while integrating the M242 cannon was the facilitation of spent casing ejection and avoidance of ingestion of casings into the engine. As shells are fired, the spent casing is extracted from the cannon and ejected from the aircraft, via the coaxial ejection port standard on the M242, shown in Figure 12.16 below. As the firing cannon is always aligned to prevent firing shells into the engine intake, the ejection port will also be aligned to prevent introducing debris into the intakes.

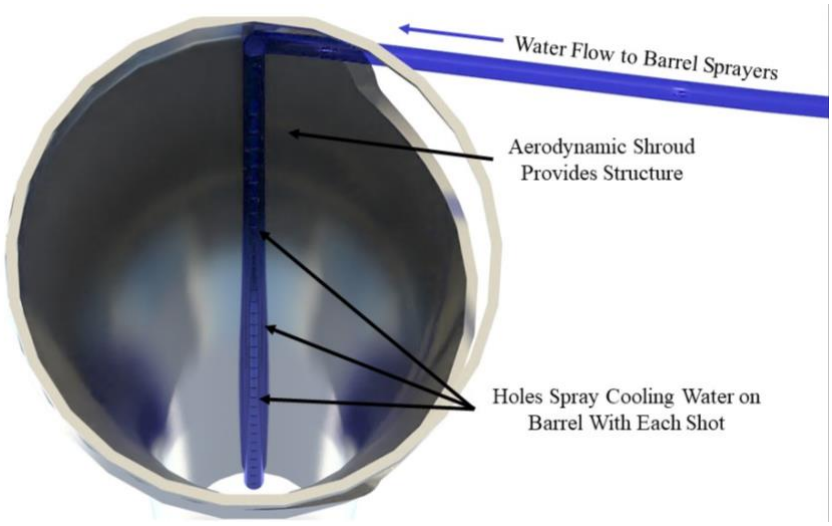

Figure 12.15: Water Based Barrel Cooling System

12.7.3 Selected System Integration

As mentioned previously in this chapter, the M242 used in the Dragoon aircraft is mounted to the removable munitions pod at the rear of the aircraft. Figure 12.16 below shows the mounting location low on the left side of the aircraft, as well as the spent casing ejection port.

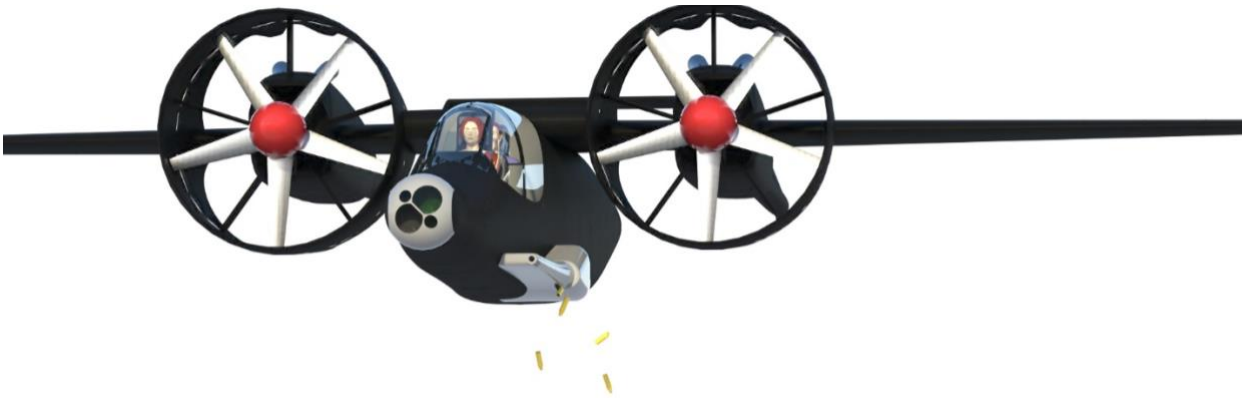

Figure 12.16 M242 Bushmaster Integration and Spent Casing Ejection

12.7.4 Weapon Loading

The Dragoon is designed to facilitate quick turns on the ground before returning to combat, attained using a removable pod system rather than conventional line loading the aircraft. While the aircraft can be re-armed according to conventional methods, the primary method is accomplished in the manner outlined in Table 12.9, requiring 22 minutes total. Note: this chart does not include the re-fueling, which is assumed to occur simultaneously.

Table 12.9: Combat Turn Rearmament Time Budget

Number	Description	Time
1	Landing and Taxi to Depot	5 minutes
2	Decompress Rear Suspension and Kneel Aircraft	1 minutes
3	Release Empty Pod to Gurney and Remove	5 minutes
4	Lift Loaded Pod into Place and Attach	5 minutes
5	Recompress Rear Suspension and Stand Aircraft	1 minutes
6	Taxi and Takeoff	5 minutes
Sum	**Total Time for Rearmament**	**22 minutes**

After empty pods are removed from aircraft, they are returned to depot hangars where Loadmasters and weapon crews can reload the pods while the aircraft return to the battlefield.

12.7.5 Operational Characteristics and Features

The design integration of the M242 cannon onboard the Dragoon in addition to facilitating ease of reloading, allows for ease of maintenance, repair, and overhaul. The M242 is notoriously reliable, as mentioned before, and this long deployment time means that the Dragoon will have an increased Mean Time Between Overhaul than many competitors. Similar to the reloading procedure, overhaul of the munitions pod is completed independent of the aircraft

at depot. Gun cleaning is accomplished in depot and is facilitated by removing the aerodynamic shroud fitted to the cannon.

12.8 Missile Accommodation, Loading and Launch

12.8.1 Missile Options

As covered in Chapter 2 of this report, the Dragoon has been designed to accommodate the AGM-114 Hellfire series as the primary missile system for engaging targets. While the weapons bay is large enough to accommodate other missiles, including the AGM-64 Maverick series, the line is being phased out of use in the United States military. Depending on the user's inventory and intended targets, the internal weapons bay can carry and deploy a variety of missiles up to a length of 90 inches. Chapter 12.8.2 will address flexibility options allowing for external missile stores.

As mentioned in Chapter 12.7.1, guided missiles have rapidly grown in popularity with the military in recent years as they allow for precision targeting of enemies, thereby reducing the potential for accidental friendly fire or non-combatant engagements. The AGM-114 Hellfire series is an air to ground laser guided missile, capable of engaging a wide variety of ground targets, ranging from personnel and unarmored vehicles to tanks and armored personnel carriers. With a price tag of around $150,000, Hellfire missiles are a staple in the United States and allied country's air to ground missile inventories [55].

Used by most Western air superiority fighters, the AIM (Air Intercept Missile)-9 Sidewinder, has been in service with the United States and Allied armed Forces since its adoption by the Navy in 1956. The AIM-9 has been used in many variations as updates have continually been made to the system to maintain a competitive edge. The short-range missile operates via an infrared homing guidance system and has remained popular despite attempts to replace it due to low cost, versatile deployment options, and reliable nature. Carrying a price tag of roughly $400,000, the Sidewinder has secured its place in the United States armories at least until 2055, when Boeing will conclude a contract secured in 2010. The AIM-9 is too long to be carried internally onboard the Dragoon, but optional external pylons allow for aircraft configurations including self-defense or anti-helicopter missions [185].

In the general-purpose mixed loadout, the internal rotary munitions rack onboard the Dragoon carries four AGM-114s, but at the discretion of the user, the rotary rack can be re-configured to carry up to 14 missiles internally. The details of missile egress and loading from the munitions pod will be discussed below in Chapters 12.10 and 12.8.3 respectively.

12.8.2 Missile Positions

The primary method of carrying and deploying missiles from the Dragoon is via the rotary munitions rack installed in the removable munitions pod. When the aircraft is not engaging a target with Hellfires or other missiles stored internally, the munitions rack is contained completely within the aft mounted pod, protecting the missiles from ground debris and reducing overall drag. When engaging a target, the pod doors open, and the munitions rack is extended downwards on the set of screw jacks. This process exposes the missiles to the open airstream, allowing the Hellfire's nose mounted laser seekers to arm and also facilitates rail launches. The full mechanics of internal stores deployment will be covered in Chapter 12.10.

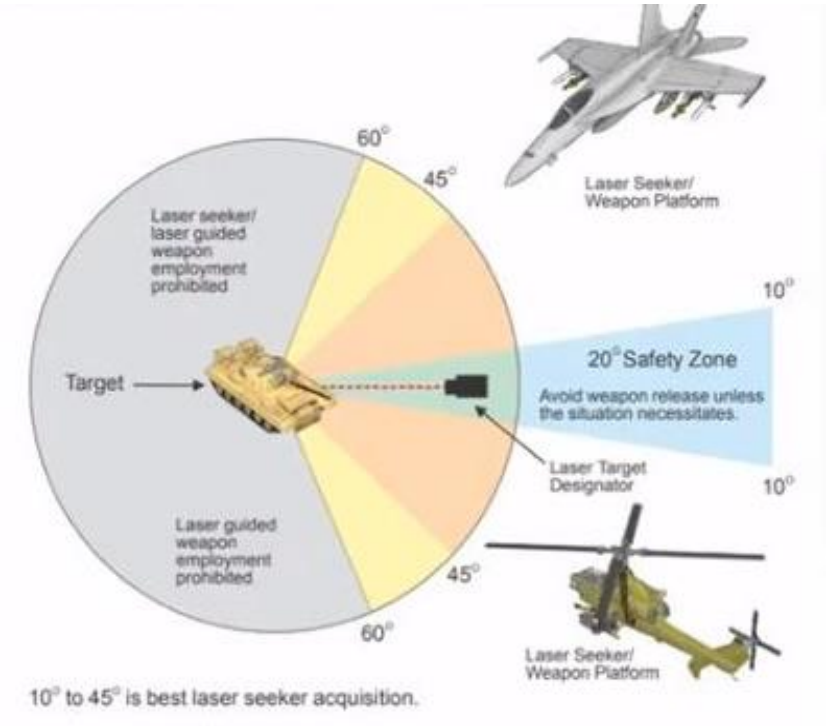

Figure 12.17: Boresight Dynamics for Laser Guided Weapons [186]

The aft mounted munitions pod serves to protect the forward mounted optical suite from the corrosive exhaust of the missiles at launch, placing the body of the aircraft between the sensitive electrics and the missile exhaust. The location of the missiles at launch also serve to improve launch dynamics with respect to the local structure. The rotary rack is mounted at an angle within the fuselage. This configuration ensures that upon launch, the missiles begin their flight with a nose-down flight attitude, facilitating an easier exit of the boundary layer airflow around the body of the aircraft. This effect is more critical for gravity weapons and will be discussed in further detail in Chapter 12.10.

When engaging targets with laser guided munitions, there are regions of target engagement around the launching aircraft that impact the shot dynamics of laser guided missiles. Figure 12.17 shows the fields of fire delineated into boresight and off-boresight shots, as well as fields of fire outside of the operational characteristics of the AGM-114.

In addition to the impact of the firing aircraft location, the location of the target designator can influence the dynamics of the target engagement. Hellfires and other laser guided munitions are guided by a laser designator fired at the target which reflects off the target. This reflection is absorbed by the targeting suite in the Hellfire's nose, and

the guidance system then homes in on the reflection. The optical suite onboard the Dragoon contains a laser designator, allowing the CSO to self-designate targets, or if working in multiple aircraft flights, to designate targets for allied aircraft. Targets can also be designated by other friendly aircraft or ground forces in addition to the individual operation capabilities.

Finally, the design of the Dragoon utilizes the internal munitions storage to meet the desired performance capabilities. The internal storage was a driving design decision because it reduces the drag on the aircraft and reduces the radar cross section by eliminating sharp corners from the visible area. Reducing drag increases the L/D ratio, and thereby increases the range of the aircraft. However, the designers of the aircraft recognize that in some missions, the need for increased range is diminished, and the ability to carry additional stores is more important than the slight increase in observables. In these cases, the Dragoon can be fitted with wing mounted rails shown in Figure 12.18 allowing the aircraft to carry missiles on external hardpoints. As mentioned before, the AIM-9 Sidewinder is too long to fit within the internal weapons bay, but these rails allow the Dragoon the ability to carry them for self-defense or anti-helicopter missions. The depicted loadout is comprised of one AIM-9 Sidewinder and three additional AGM 114 Hellfires per wing, though per user discretion these can be swapped for a combination of other missiles.

"I like very much the versatility of your internal carriage design and love that you mentioned the wing mounted options for A-G and A-A! No fighter pilot will ever turn down the ability to protect themselves, their formation, and their aircraft. I think this is essential to a design for a light attack aircraft and applaud you for including it in yours." -Capt. Emily Thompson, USAF, F-35 Pilot

Figure 12.18: Optional External Missile Hardpoints

12.8.3 Weapon Loading

Internal missile stores are reloaded in the same manner as outlined in the gun loading section, the aircraft decompresses the rear landing gear, allowing the empty pod to be removed and taken to depot for re-armament while a loaded pod replaces it on the aircraft. For optional external stores, the decompression of the main landing gear lowers the wing hardpoints to a level accessible by ground personnel, allowing for armorers to team-lift the missiles onto the launch rails.

12.8.4 Operational Characteristics and Features

Similar to the maintenance and overhaul procedures outlined in Chapter 12.7.5 of this report, the maintenance procedures for internally stored missiles are accomplished by removing the pod and returning it to depot for teardown and overhaul while the aircraft returns to combat with a new munitions pod. One major advantage that underwing stores have over internally carried stores is the ability to arm and activate underwing stores as soon as the aircraft enters a combat zone, while internally carried stores require the bomb bay doors to open and the munitions rack to extend before the missiles can be armed and activated. There is a trade-off for this handicap as the sealed pod storage protects the missile optics from potential damage due to bird strikes, ground debris, and gun gas emissions.

12.9 Bomb Accommodation, Loading and Launch

12.9.1 Bomb Options

As covered in Chapter 2 of this report, the Dragoon has been designed to accommodate all current US employed bombs in the 250- and 500-pound nominal weight classes. The internal rotary weapons rack designed for use in the aircraft can be configured to carry numerous combinations of munitions per user discretion, provided that the desired weapons fit within the confines of the fuselage bomb bay, but the general-purpose load includes two Mk 81 250-pound and three Mk82 500-pound bomb derivatives.

Capable of carrying a variety of gravity weapons including the unguided Mk 81 and Mk 82 bombs, the Dragoon also facilitates deployment of precision guided munitions including the GBU-29 series of 250-pound laser guided bombs, the GBU-39 series of 250-pound precision glide bombs, the BLU 100 series of low collateral damage 500-pound unguided bombs, and the GBU-38 series of all-weather precision guided 500-pound bombs.

12.9.2 Bomb Positions

As outlined in Chapter 17.8.2 of this report, the primary munitions storage is facilitated via the use of an internally mounted rotary weapons rack. Carrying bomb stores internally again serves to reduce drag on the aircraft to increase range and to reduce the radar cross section. In the same manner as the missiles discussed previously, bombs are deployed by opening the bomb bay doors, rotating the munitions rack to center the desired bomb, then lowering the rack on the screw jacks to expose the bomb to freestream air before release. The deployment location of the bomb bay serves to reduce the likelihood of released munitions from coming into contact with any aircraft structure as the only structure aft of the bomb bay is mounted well above the release point of the bomb. Of special note is the nose-down attitude of the bombs upon release, which helps gravity weapons escape the boundary layer air.

The rotary munitions rack allows the Dragoon to employ a variety of gravity weapons and to deploy them as necessary depending on the type of munition. For unguided and laser guided bombs, the aircraft can conduct standard level flight or shallow dive releases to deliver munitions on target. In cases where the aircrew needs to maintain distance from the target, glide-bombs, which are designed to deploy wings after being dropped to increase the range of travel, can be deployed from the rotary munitions rack. If glide-bombs are not available, aircrews can initiate a "toss-bombing" maneuver shown in Figure 12.19. This maneuver allows the aircraft to remain at lower altitude and longer range, allowing delivery of munitions to well defended positions while avoiding anti-air fire.

Unlike missiles, the Dragoon carries all bomb loads internally with a rotary munitions rack, designed primarily to reduce the drag on the aircraft and to minimize radar cross section. The wing design is capable of supporting the point loads caused by missiles but cannot carry point loads attributed to Mk. 81 or Mk. 82 bombs.

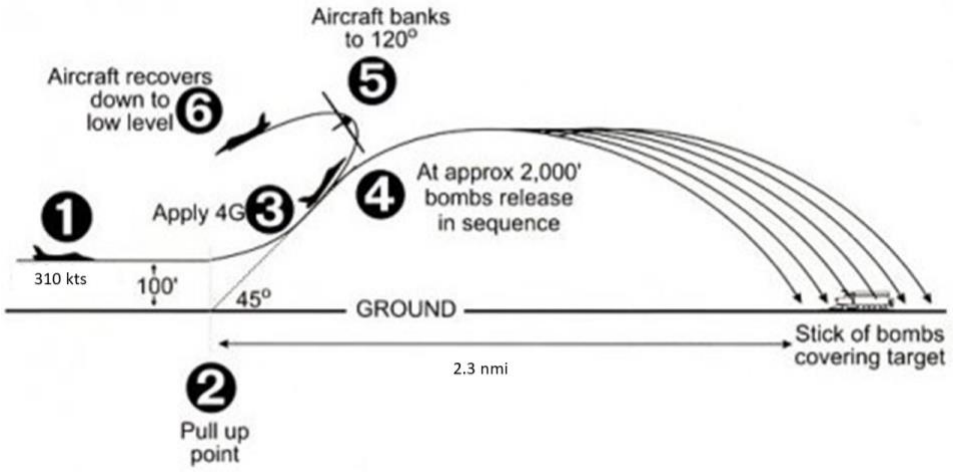

Figure 12.19: Toss Bombing Engagement Diagram [187]

12.9.3 Weapon Loading and Short Ground Turn

Bomb loading is accomplished in the same manner as the gun, whereby the aircraft decompresses the rear landing gear allowing ground personnel to remove the munitions pod. The empty pod is returned to depot for re-armament while a loaded pod takes its place on the Dragoon. Figure 12.20 on the next page illustrates the quick turn procedure using the munitions pod system.

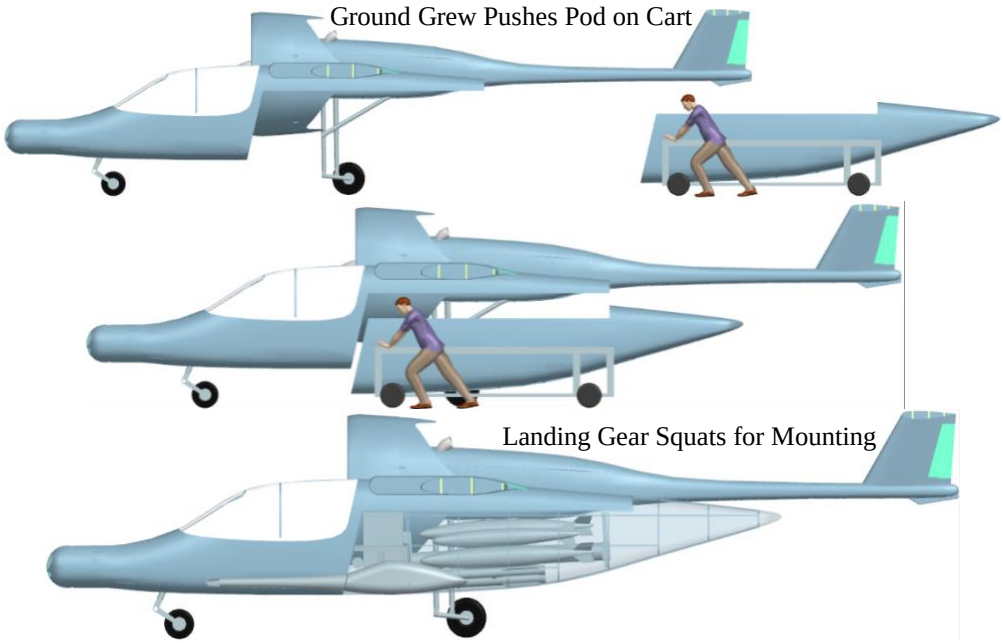

Figure 12.20 Ground Turn Pod Loading

12.9.4 Operational Characteristics and Features

Maintenance and overhaul procedures for bombs are the same as those discussed in Chapter 12.8.4. The advantages of internal bomb stores are similar to internal missile stores, as the body of the aircraft protects the optics and guidance components of the munitions. The trade-off of internal stores is the same as with missiles, in that the weapons cannot be armed and activated until after being extended from the bomb bay on the rotary munitions rack.

12.10 Internal Weapon Release and Egress

As outlined in previous chapters of this report, the Dragoon carries all of its design payload, and most of its potential payload internally onboard a rotating munitions rack installed in the aft mounted pod. The use of this pod reduces the time spent on the ground between sorties to a fraction of the time required to line load a conventionally configured aircraft. However, internal stores while beneficial in drag and radar cross section, do pose some potential

difficulties upon egress. The design of the Dragoon's weapons pod addresses the difficulties of weapons egress in three significant ways. First, the rotary munitions rack is mounted to a set of jackscrews, allowing it to be lowered from the aircraft, presenting the munitions to freestream air upon release. Second, the jackscrew and rotary rack are mounted at an angle inside the fuselage, meaning that internal stores leave the aircraft with a nose down trajectory. Finally, ejection charges are used to force internal stores clear of the airframe. Figure 12.21 shows a pair of engagements using internal stores highlighting the deployment process.

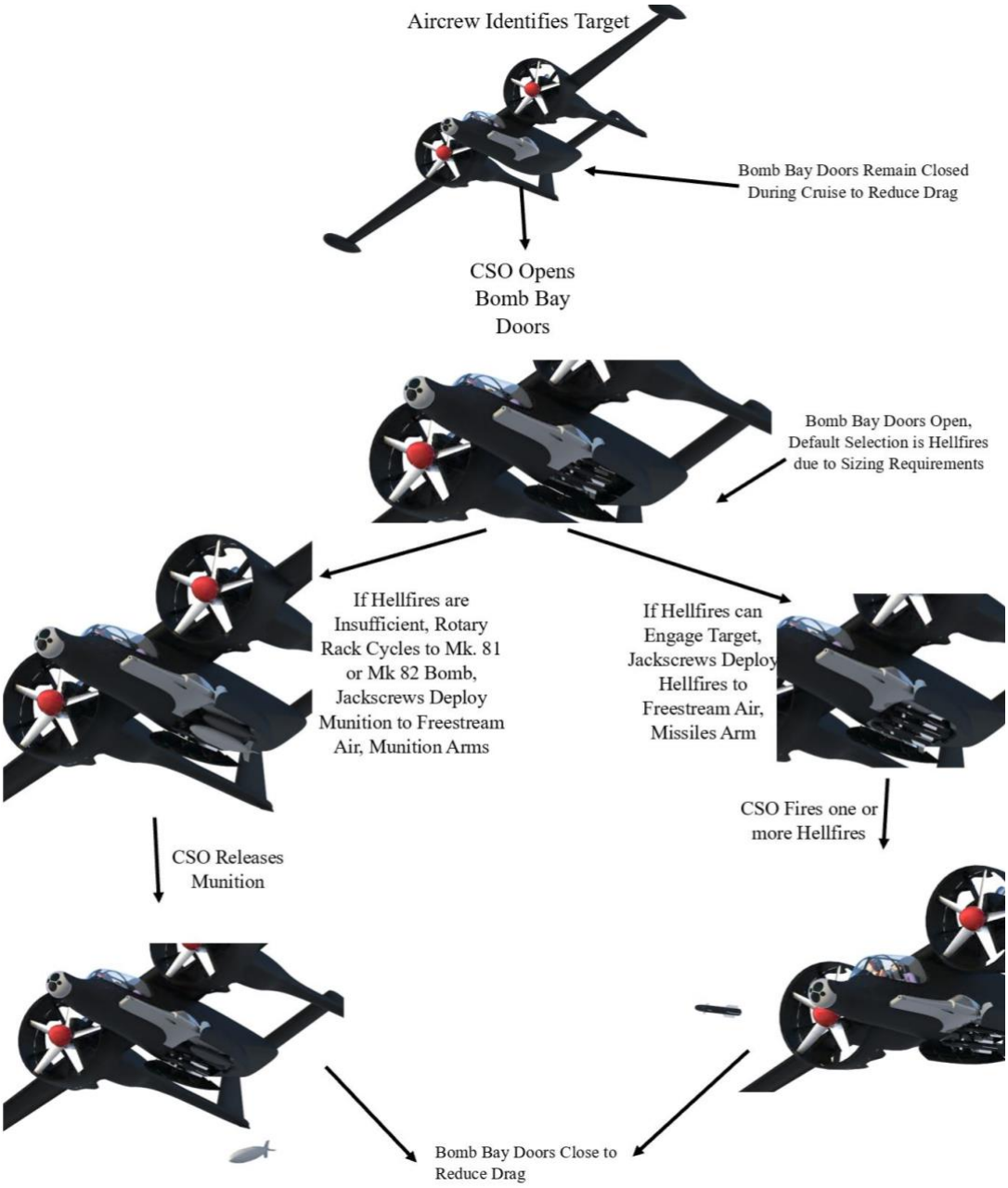

Figure 12.21 Internal Stores Egress Diagram

12.11 Safety and Survivability: Fault-Tree Analysis, Ejection Seats, Crashworthiness and Armor

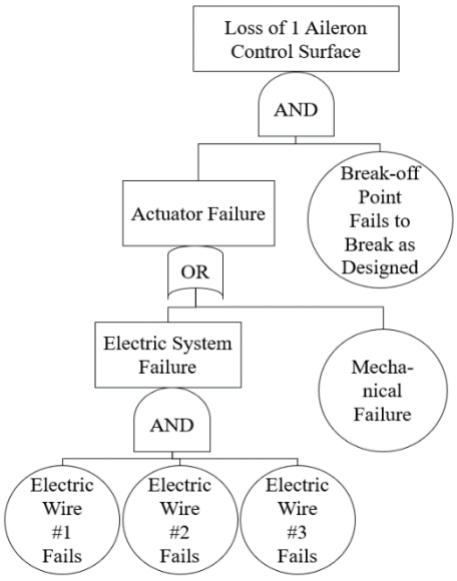

Figure 12.22: Example Fault Tree Analysis Diagram

Safety is an important factor in all aircraft, but especially in combat aircraft. This section provides an example fault tree analysis and specifies the ejection seats for the aircraft along with a brief discussion of crashworthiness and armor.

One way that safety can be measured for aircraft is by creating a fault-tree analysis. This fault tree uses Boolean algebra to measure the probability of an undesirable event. Loss of an aileron control surface is such an event, so a fault tree was created to analyze the probability of losing one of the aircraft's ailerons. The specified probabilities for the individual events that could cause the loss of an aileron are shown in Table 12.10, along with the probability that one of the aileron control surfaces will be lost.

Table 12.10: Single Aileron Control Surface Fault Tree Analysis Probabilities

Event	Probability	Event	Probability
Break-off Point Failure	10^{-5}	Wire #3 Failure	10^{-2}
Mechanical Failure	10^{-4}	Electric System Failure	10^{-6}
Wire #1 Failure	10^{-2}	Actuator Failure	10^{-4}
Wire #2 Failure	10^{-2}	**Loss of Control Surface**	**10^{-9}**

Given the inherent dangers of a light attack aircraft in the field of duty a variety of systems have been put into place to safeguard the success of the mission. Standard flares and chaff will be carried to provide alternate targets for enemy missiles. Martin-Baker 0-0 ejection seats will be integrated into the cockpit to provide ejection capabilities in case the crew needs to get out of the airplane Figure 12.23. These ejection seats are designed to work at 0 altitude and 0 velocity. This ensures that the crew can eject at any flight speed and altitude, including on the ground if necessary. The cockpit is surrounded in a titanium bathtub for protecting the crew members during strafing runs. Additionally, the inboard section of the ducts have been reinforced as a

Figure 12.23: Armored Cockpit & Ejection Seats

precautionary measure to ensure the pilot and WSO safety in case of an engine blade separation. The bulkhead aft of the cockpit is also doubled up and reinforced from the weapons and fuel bay. As the aircraft requires tip tanks due to the high aspect ratio, additional armoring was provided to mitigate the risk of potential ground fire. As described earlier in Chapter 12.1, the flight control and electrical systems are triply redundant and independent from one another, featuring three batteries, flight computers, and wiring schemes. The wiring itself is then insulated and runs along the structure of the aircraft to minimize the risk of damage by ground fire. The hydraulic system is the one system that is not triply redundant, but the risk inherent with that system is mitigated by the spring system that allows the gear to be lowered without hydraulic pressure as mentioned in Chapter 12.3.1. Additionally, since the aircraft will be flying above 30,000 ft, the crew will be provided with an oxygen system that they can use when at high altitudes.

12.12 Ground Equipment, Ergonometrics and Vehicle Compatibility

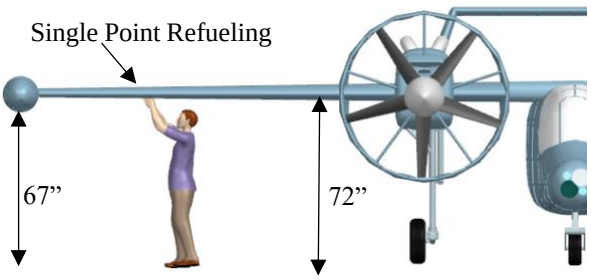

Figure 12.24: Refueling Reach

Figure 12.25: Engine Reach

To ensure the ease and quick ground turnaround times the Dragoon was designed for ground personnel to be able to access the needed refueling and maintenances area without much complication. As seen in Figure 12.24 and Figure 12.25 the refueling process and engine maintenance can be performed without the need for a step stool. The single point refueling was also placed on the right wing of the aircraft to leave room for other ground personnel to check the engines, secure the pod, and preflight gun testing. Additionally, it was placed outside of the optional external hard point locations if the mission should require. Its placement also allows for a hot refueling process with the engines still running. As for the pod loading it can be seen in Figure 12.25 that just a single person is able to push into place for mounting. If other means are available, the pod can also be towed into position via tug/vehicle as the Dragoon has 9.2 ft of vertical clearance from the vertical tail. Figure 12.26 to the below shows a possible scenario on the ground, as all services are able to happen simultaneously without conflict ensuring a fast turnaround.

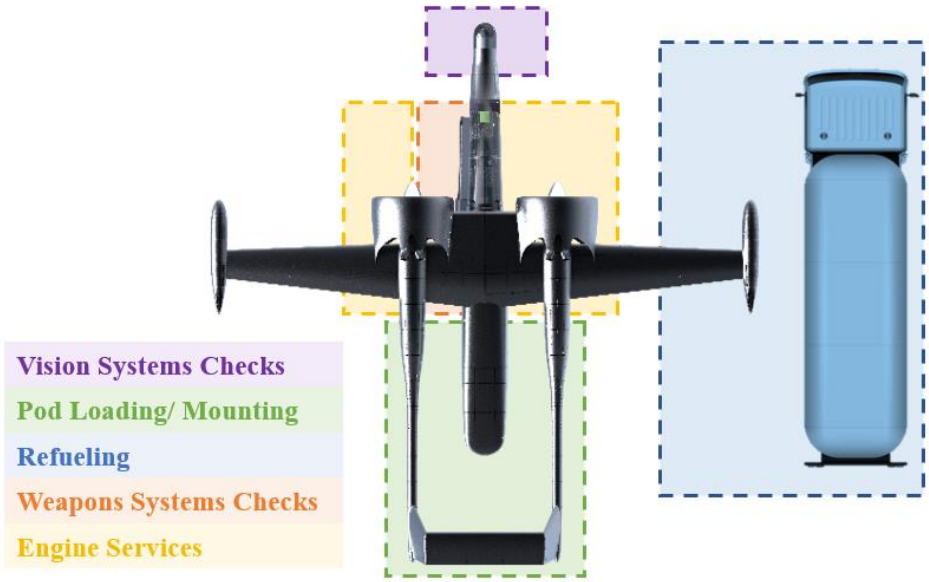

Figure 12.26: Ground Services

13 Class II Landing Gear

The determination of the landing gear strut sizing followed the methods presented in Aircraft Design: Part IV [190]. The updated tire selection and strut sizing are presented in the following tables (Table 13.1, Table 13.2 , and Table 13.3). Overall, the sizing and designs of the struts were closely modeled after the OV-10 due to its success and high-performance capabilities working in austere field conditions.

Table 13.1: Landing Gear Strut and Tire Load Force and Ratios

	Static Strut Load (lb_f)	Static Strut Load (x1.25) (lb_f)	Dynamic Strut Load (lb_f)	Dynamic Strut Load (x1.25) (lb_f)	Load Ratio	Tire Load (lb_f)
Nose Gear	1,120	1,401	1,625	2,031	0.12	1,401
Main Gear	8,427	10,534	12,218	15,274	0.88	5,267

Table 13.2: Salient Tire Characteristics

Location	Goodyear Tire Model	D_t (in.)	W_t (in.)	Rated Load	Rated Inflation (psi)	Loaded Radius (in.)	Rated Speed (mph)	V_{sL} (mph) Req.	V_{sTO} (mph) Req.
Nose Gear	505T08-1	15.0	6.0	2150	88	5.7	190	140	140
Main Gear	650T26-2	20.3	7.0	5750	120	9.1	160	122	122

A load factor of 7g and vertical touch down rate of 15 ft/s was assumed for both the nose and main landing gears for the austere conditions. Shock absorber deflection (S_t), shock absorber stroke (S_s), and shock absorber diameter (D_s) are then presented below in Table 13.3.

Table 13.3: Landing Gear Strut Sizing

	S_t (in.)	S_s (in.)	D_s (in.)
Nose Gear	2.5	3.11	1.84
Main Gear	1.7	3.24	2.67

14 Class II Performance

This section provides a Class II performance analysis. Methods from *Airplane Design Part V* [177] and *Airplane Design Part VII [192]* were used to predict the performance characteristics of the aircraft as dictated by the RFP.

14.1 Takeoff

The mission specification calls for a takeoff ground run under a 4,000 ft over a 50 ft obstacle. The takeoff performance of the airplane was checked with the following equation from Ref. [192], and a ground run under 2,300 ft over a 50 ft obstacle is predicted.

$$S_{TOG} = \left(\frac{V_{LOF}^2}{2g}\right) * \left[\left(\frac{\overline{T}}{W}\right)_{TO} - \mu'\right]^{-1} = \mathbf{2,293\ ft < 4,000\ ft}$$

$V_{LOF} = 1.1 * V_{s_{TO}}$ for Military Airplanes, $\quad \overline{T} = 5.75 P_{TO} \left\{\frac{\sigma N D_p^2}{P_{TO}}\right\}^{\frac{1}{3}}$, $\quad \mu' = \mu_g + 0.72\left(\frac{C_{D_o}}{C_{LmaxTO}}\right)$

14.2 Climb

No climb requirements are specified in the RFP; however, the rate of climb envelope shown in Figure 14.1 predicts a service ceiling up to 45,000 ft taken at the 100-fpm rate of climb line.

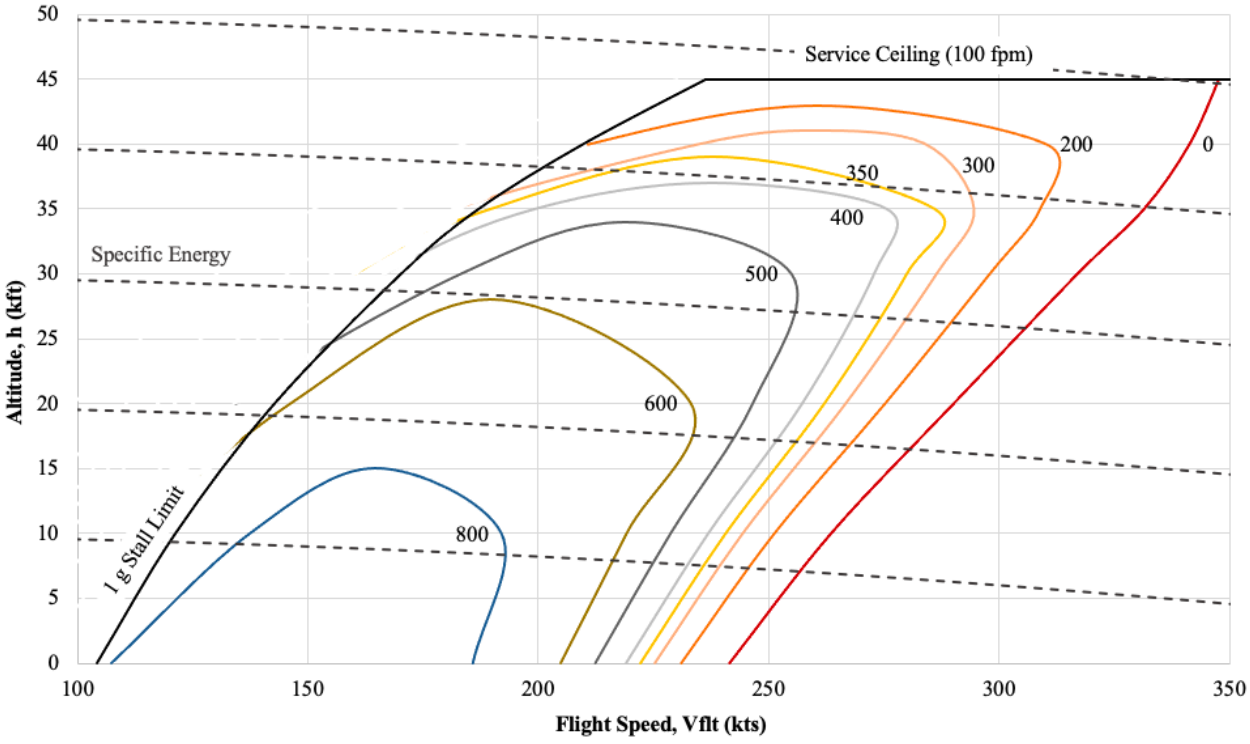

Figure 14.1: Rate of Climb Envelope

14.3 V-n Diagram

The flight envelope for the military type aircraft is shown in Figure 14.2. The maximum positive and maximum negative load factors are attack aircraft values drawn from Table 4.1 of *Airplane Design Part V* [177]. The design airplane can fly in any of the load conditions and speeds enclosed by the solid lines of the figure. The maximum positive load factor was achievable at 170 KEAS, and the maximum negative load factor is achievable at 160 KEAS. The diagram presents two vertical speed lines: V_H, maximum level speed, at 320 KEAS, and V_L, maximum design speed, at 400 KEAS.

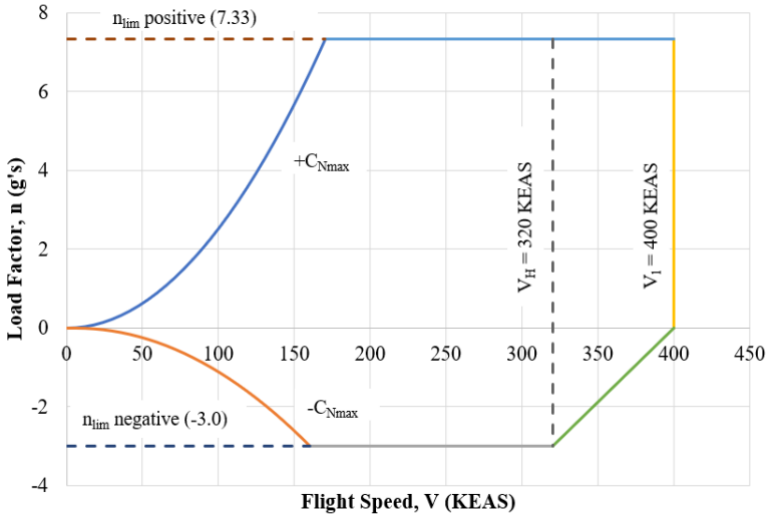

Figure 14.2: V-n Diagram

14.4 Payload-Range Diagram + Utilization Analysis

Figure 14.3 shows the relationship between the maximum payload weight loaded onto the design aircraft and the range the aircraft is capable of flying. To understand the range capabilities of the aircraft, the MTOW of the aircraft was kept constant, but payload was replaced by fuel of corresponding weight. Replacing the munitions entirely with fuel more than triples the range of the aircraft. Furthermore, if a remote crew is utilized, meaning both crew members were removed and replaced with their equivalent weight in fuel, the aircraft could fly an additional 1,000 nmi. The pod architecture proposed allows for increased flexibility in the design of the chosen configuration, meaning it would be possible to create a massive fuel tank pod capable of holding 3,400 lbf of avgas.

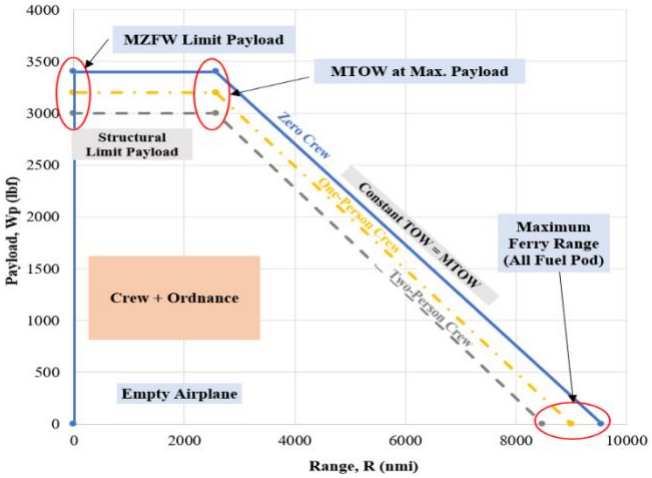

Figure 14.3: Payload-Range Diagram

14.5 Maneuvering

Figure 14.4: Sustained Turn Rate shows the maneuvering diagram generated for the design to visualize the airworthiness of sustained maneuvers such as pull-ups and level turns. During combative situations, the aircraft would be capable of a maximum sustained turn rate just under 3g's at a radius no greater than 1,000ft. This would occur at an approximate airspeed of 170 kts.

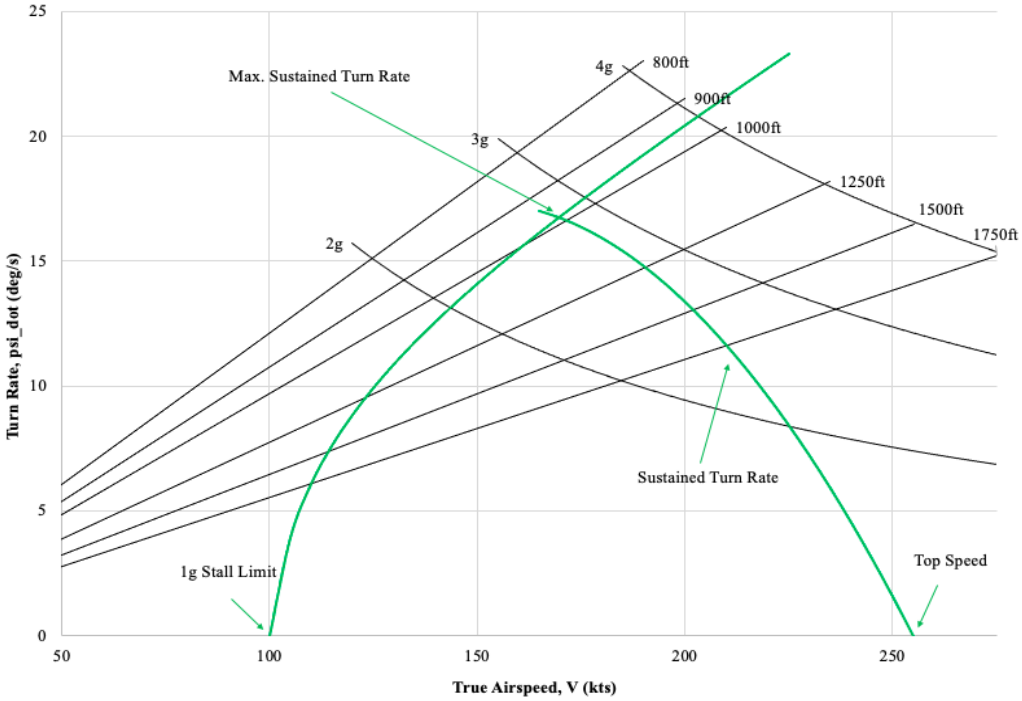

Figure 14.4: Sustained Turn Rate

14.6 Landing

Similar to takeoff, the airplane must be able to land with a ground run less than 4,000 ft over a 50 ft obstacle. The following calculation from *Airplane Design Part VII* (REF) predict a landing ground run just over 2,600 ft.

$$s_L = s_{AIR} + s_{LG} = \mathbf{2,613\ ft < 4,000ft}$$

$$s_{AIR} = \left(\frac{1}{\bar{\gamma}}\right)\left\{\frac{V_A^2 - V_{TD}^2}{2g} + h_L\right\}, \qquad s_{LG} = \frac{\{V_{TD}^2\}}{2\bar{a}}$$

15 Class II Weight and Balance

This section presents a Class II weight and balance analysis for the design aircraft. General values initially estimated in the Class I weight and balance were further analyzed using methods from *Airplane Design Part V: Component Weight Estimation* [177]. Table 15.1 shows weight, weight percentages, and center of gravity locations for all components in the following aircraft conditions: empty, operational empty, and takeoff.

Table 15.1: Class II Component Weight Breakdown

#	Component	Weight (lbf)	Weight Fraction	Xcg (in.)	Ycg (in.)	Zcg (in.)
1	Wing	557.95	5.84%	280	0	83
2	Empennage	64.01	0.67%	510	0	107
3	Fuselage	242.61	2.54%	280	0	60
4	Nacelle	245.05	2.57%	260	0	82
5	Nose Gear	41.40	0.43%	125	0	44
6	Main Gear	372.57	3.90%	335	0	83
	Structure Total	**1523.58**	**15.96%**	**298.33**	**0**	**76.50**
7	Engine	548.00	5.74%	280	0	83
8	Fuel System	154.07	1.61%	280	0	80
9	Propeller	347.22	3.64%	240	0	82
10	Propulsion	96.01	1.01%	275	0	83
	Power Total	**1145.30**	**12.00%**	**268.75**	**0**	**82**
11	Avionics	78.36	0.82%	170	0	53
12	Surface Controls	182.50	1.91%	315	0	80
13	Hydraulic System	100.00	1.05%	230	-37	60
14	Electrical Systems	101.20	1.06%	325	0	65
15	AC/Anti-ice	146.97	1.54%	270	0	83
16	Oxygen	47.60	0.50%	230	0	41
17	APU	75.00	0.79%	310	65	84
18	Furnishings	102.40	1.07%	230	0	41
19	Armor	200.00	2.10%	230	0	63
20	Aux. Gear	38.19	0.40%	200	0	41
21	Other	28.64	0.30%	230	0	63
	Fixed Total	**1100.87**	**11.53%**	**249.09**	**2.55**	**61.27**
	EMPTY	**3769.75**	**39%**	**272.06**	**0.85**	**73.26**
22	**Trapped Fuel and Oil**	**48.00**	**0.50%**	**300**	**0**	**80**
23	**Pilot**	**200.00**	**2.10%**	**160**	**0**	**58**
24	**WSO**	**200.00**	**2.10%**	**180**	**0**	**58**
	OPERATIONAL EMPTY	**4217.75**	**44%**	**228.01**	**0.21**	**67.31**
24	**Max. Fuel**	**2328.39**	**24.39%**	**280**	**0**	**80**
25	Gun	270.00	2.83%	230	-20	45
26	Hard Launched	730.00	7.65%	240	0	59
27	Pod	100.00	1.05%	300	0	59
28	Gravity Weapons	1900.00	19.90%	290	0	55
	Payload	**3000.00**	**31.43%**	**265**	**-5**	**54.5**
	TAKEOFF	**9546.14**	**100%**	**257.67**	**-1.60**	**67.27**

The CG excursion diagram shown in Figure 15.1 estimates that the largest CG excursion occurs when all munitions are dropped an all fuel is spent during a mission.

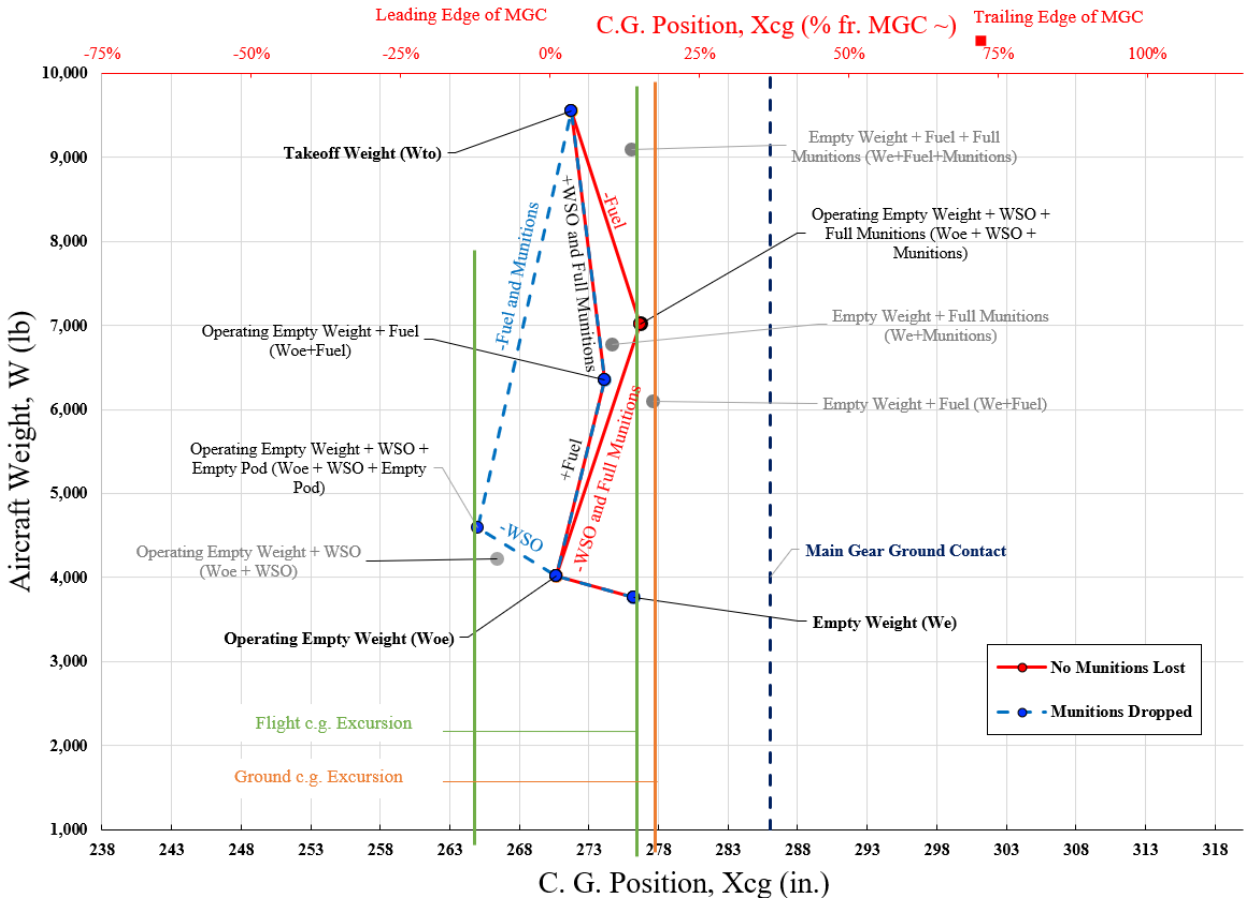

Figure 15.1: Class II Center of Gravity Excursion Diagram

16 Class II 3-View, Advanced CAD, Situational Rendering, and Exploded Views

The purpose of this chapter is to display 3-view, an exploded view, and situational view of the Dragoon, shown in Figure 16.1, Figure 16.2, and Figure 16.3.

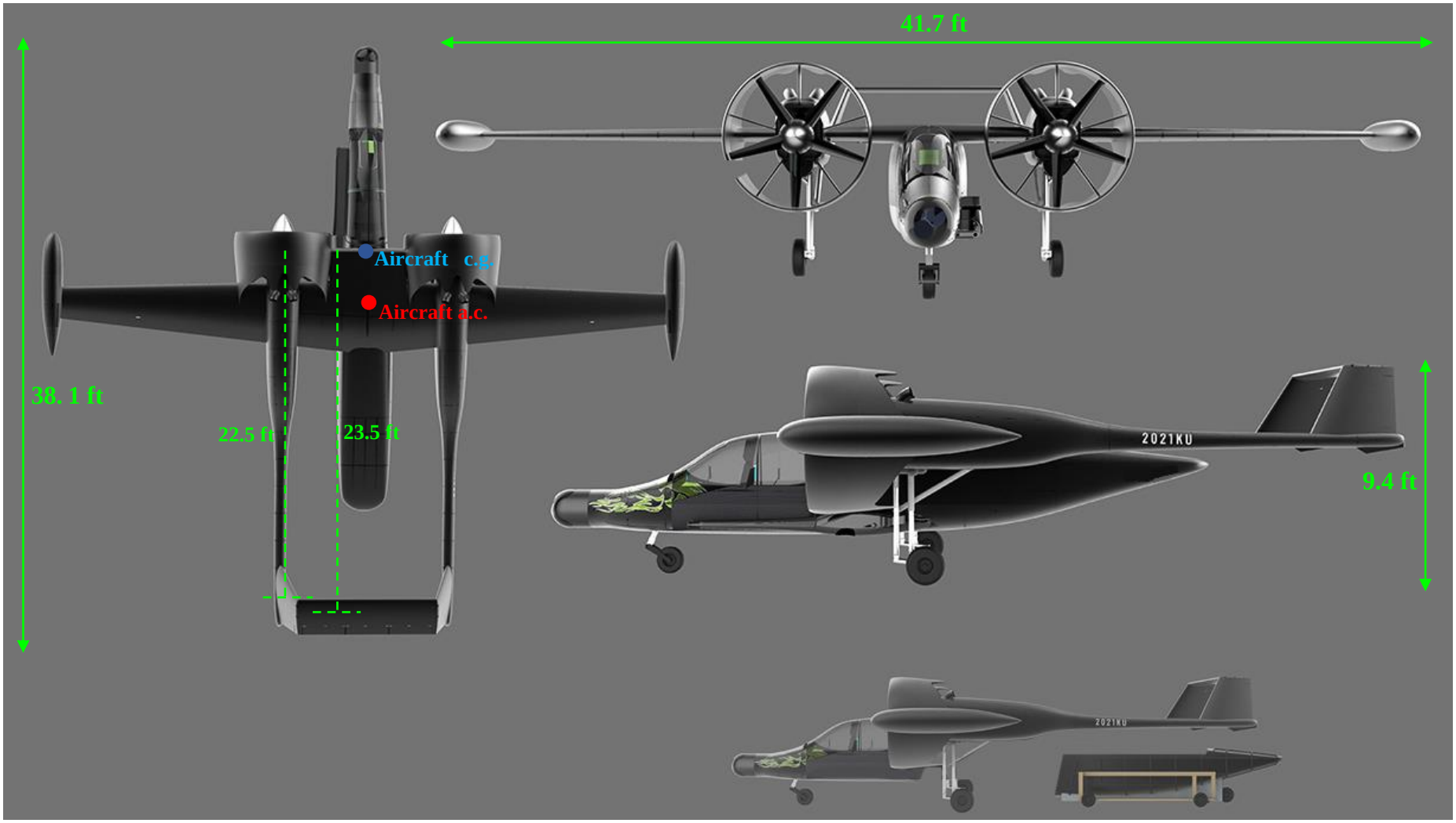

Figure 16.1: 3-View

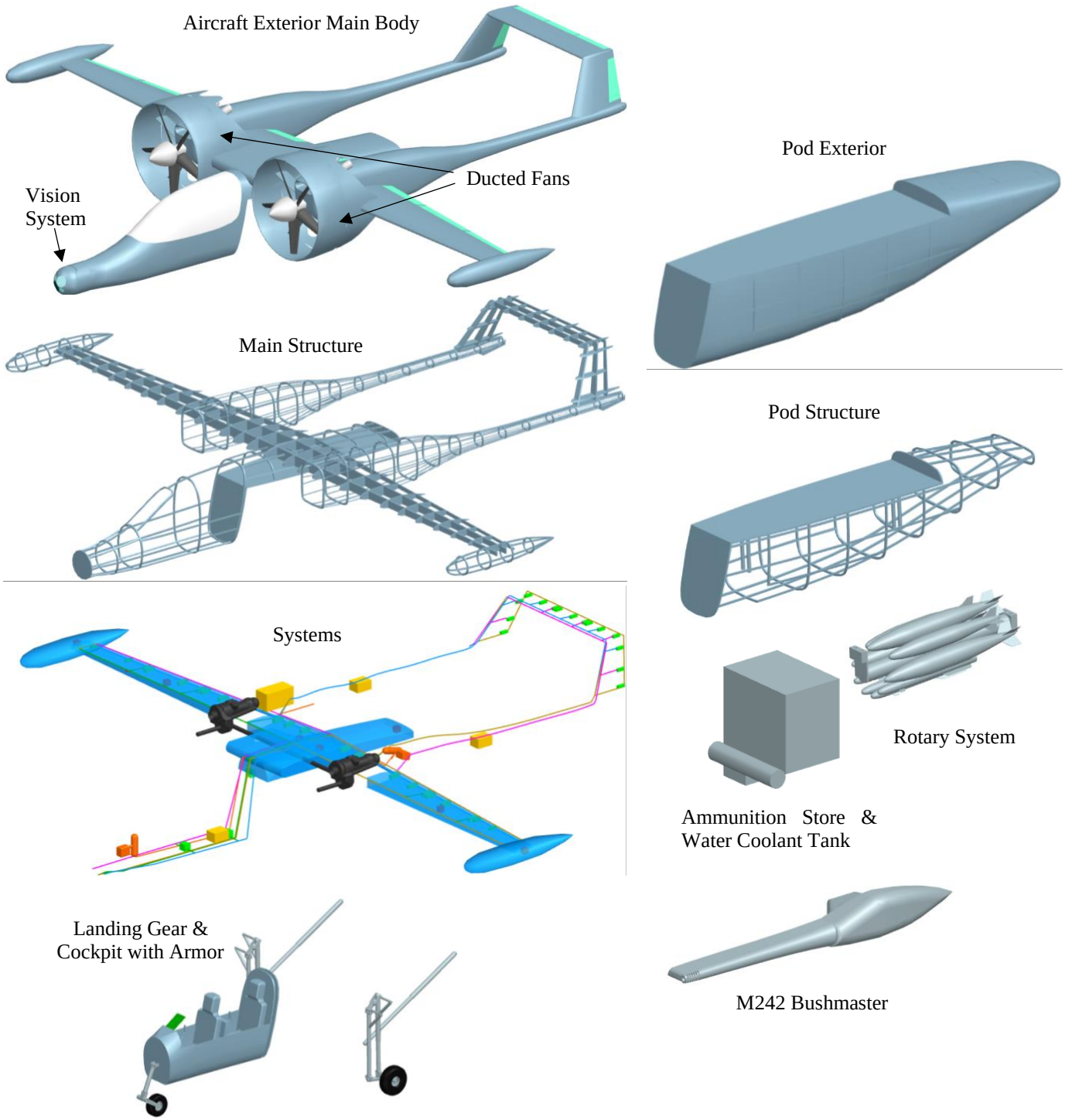

Figure 16.2: Dragoon Exploded View

Figure 16.3: Situational Rendering at a Remote Airbase

17 Advanced Technologies and Risk Mitigation

This section outlines advanced technology utilized by the Swift Dragoon Aircraft as well as details the various risk mitigation design choices prescribed by the aircraft. One of these design choices was to design a spring system that will allow the landing gear to lower even in the circumstance that hydraulic pressure is lost.

17.1 Remote Crew

"A single pilot is already doing it on the A-10. You should be working toward one pilot and possibly less considering the current climate" – **Richard Bramlette**, senior engineer, NextGen Aeronautics

Based on subject matter expert feedback it is believed that there is no need to have two crew members in the aircraft for most missions. Modern ground attack aircraft like the A-10 operate successfully with a single pilot and competitor aircraft like the AT-6 Wolverine and Super Tucano were built initially as trainers and have retained the back seat primarily due to this initial role. However, due to the unique strafing or orbiting fire mode we do believe that the pilots load may be relieved by having a virtual co-pilot to support in CAD, JTAC, and suppressing fire missions especially when in an orbiting fire mode. This would be facilitated using a secure data link similar to modern drones operated in the Middle East. There would be a slight delay, but one would have the pilot for any immediate feedback required by the aircraft and the delay should not hinder virtual CAD or JTAC operations. Consequently, the Dragoon aircraft will have a single seat version with remote crew capabilities. The equipment required for the virtual co-pilot would simply be placed where the current co-pilot sits with the weight and power requirements being negligible compared to an in-person crew member.

"In a counter-insurgency mission, … I believe it could be single-piloted. But, a back-seat operator does add some mission capability and help for situational awareness." – **James Allen**, retired naval aviator and former ISR contract pilot OEF

"I believe a virtual co-pilot is definitely on the table." –**Dr. Lauren Schumacker**

17.2 Observables Mitigation

Reduction of observables for attack aircraft helps to reduce the risk inherent within every mission that the aircraft performs. For the Dragoon infrared (IR) signatures and noise were deemed the most important for reduction. IR signatures were mitigated by blowing the exhaust from the engines over the top of the wings and by specifying de-

icing measures that are capable of being turned on and off. These precautions help reduce the chance that IR-seeking weapons will target the Dragoon. Noise mitigation is important so that the aircraft will not be heard by opposing ground forces, and this was achieved by increasing the size of the propeller as much as possible in addition to using ducts with chevrons to surround the propeller.

Figure 17.1: Aircraft Exhaust and Chevrons

17.3 MASS Rounds

Maneuvering Aeromechanically Stable Sabot ammunition rounds are another advanced technology that the Dragoon will be capable of accommodating in the future. MASS ammunition are the next technological advancement after BASS ammunition. The capabilities of the Dragoon to handle these rounds will allow aircrews to have their hands on the latest hard launched ammunitions as they seek to dominate the skies.

17.4 Pod

The pod architecture integrated into the aircraft design allows for increased mission flexibility and weapons configurations. Essentially, the internal structure of each pod can be customized for a variety of attack and ferry missions. Breaking the main aircraft structure and the cargo pod into two separate entities eases maintenance and overhaul of both structures as well as decreases the time required to refit the aircraft for a different mission while on the ground. Potential future pod configurations include only fuel for ultra-long-range ferry missions, allowing the aircraft to be deployed without disassembly into a cargo aircraft. Additionally, pods could be created to deliver hardware to soldiers in the field. Sniper teams could also be delivered using a specially created pod. The pod provides an enormous amount of flexibility to the aircraft and allows for a large number of uses while having a quick ground turn time to keep control of the skies.

17.5 Cross-shafting

Since combat aircraft are often under fire from enemy aircraft and ground forces, there is a possibility of the engines

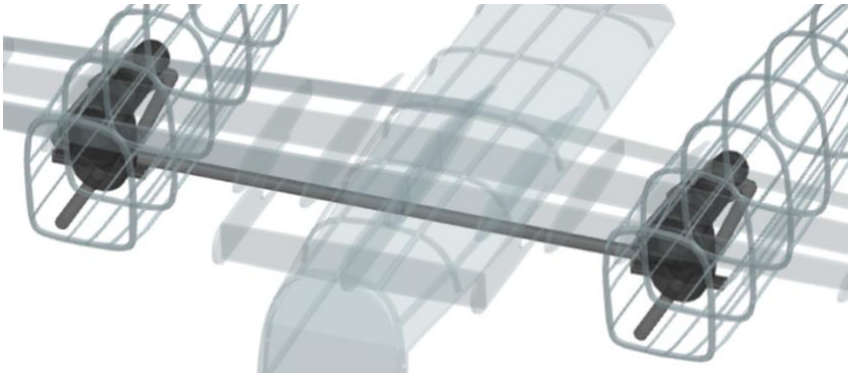

Figure 17.2: Cross-Shafted Engines

becoming damaged. When an aircraft with two engines loses power to one of them, the propeller for that one engine stops rotating. This creates an adverse yawing moment because thrust is only provided on one side and the non-rotating propeller causes drag on the other, making the single engine-out condition very dangerous for all on board. To prevent this from happening on the Dragoon, cross-shafting of the engines was employed. This allows power from one engine to be directed to both propellers in the case that one of the engines loses power. Additionally, the cross-shafting mechanism allows for one engine to start the other, thus the APU only needs to be able to start one engine.

18 Class II Cost Analysis

The purpose of this chapter is to present the costs associated with the Swift Dragoon Program. The cost analysis detailed by Roskam in *Airplane Design Part VIII: Airplane Cost Estimation: Design, Development, Manufacturing and Operating* [63] was used to assess the total costs. Research, development, test and evaluation costs are given in Table 18.1. Manufacturing, acquisition, operating, and total life cycle costs are given in Table 18.2. An estimated price per plane based on production runs is shown in Figure 18.1.

Table 18.1: RDT&E Costs

	Cost (Million $)
Airframe Engineering Design	38.73
Development and Support	9.18
Flight Test Aircraft	198.33
Flight Test Operations	13.95
Test and Simulation Facilities	72.27
RDT&E Profit	16.26
Cost to Finance RDT&E Phases	12.65
RDT&E Total Cost (50 Units)	**7.3**

Table 18.2: Manufacturing, Acquisition, Operating, and Life Cycle Costs (50 Units)

	Cost ($)
Total Manufacturing	**462.7 Million**
Total Acquisition	**509.0 Million**
Estimated Price per Airplane	19.0 Million
Fuel, Oil, and Lubricants	160.8 Million
Direct Personnel	2,811 Million
Indirect Personnel	1,380 Million
Consumable Materials	240.8 Million
Operating Cost (1,200 Hrs.)	**6,901 Million**
Operating Cost per Hour	**3,962**
Life Cycle Cost	**8,721 Million**

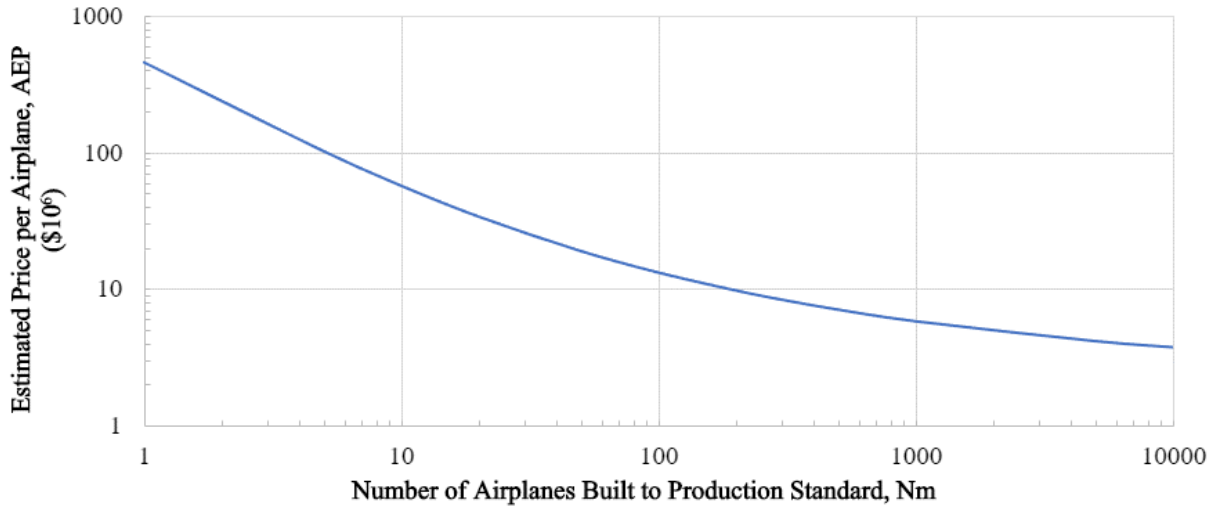

Figure 18.1: Aircraft Production Unit Costs

19 Manufacturing Plan

The purpose of this chapter is the outline a brief manufacturing plan for the Swift Dragoon aircraft. Provided are material selections and flow charts detailing the steps for component manufacturing and subsequent aircraft assembly. It is assumed that the final assembly of the aircraft will be done in a single, well established and accessible location, so as to reduce complexity and mitigate any risks associated to parts time and travel. To save on costs, manufacturing and acquisition of aircraft structural and electrical components will be outsourced to companies across the globe.

The wing substructure and skin will be manufactured primarily of graphite PEEK composites, largely to save on weight. Wing control surfaces including the ailerons, flaps, and leading-edge slats will consist of Kevlar.

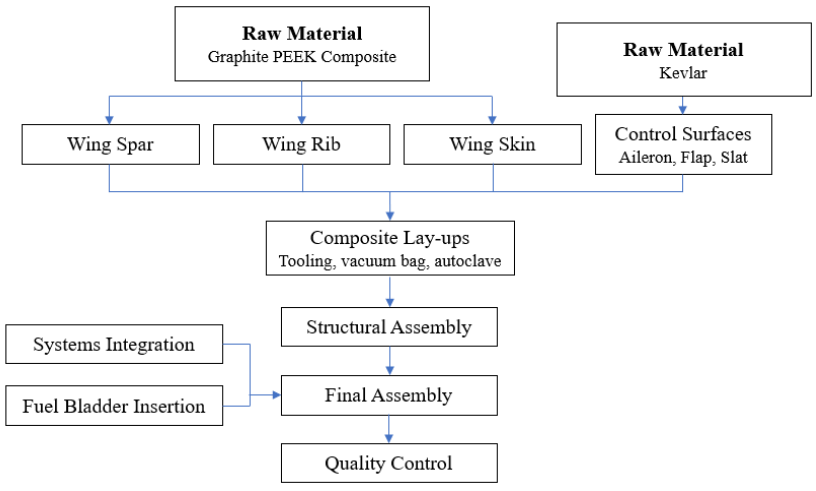

Figure 19.2: Wing Assembly Flow Chart

Table 19.1: Wing Material Selection

Component	Material
Spar	Graphite PEEK Composite
Rib	Graphite PEEK Composite
Skin	Graphite PEEK Composite
Aileron	Kevlar
Flap	Kevlar
Slat	Kevlar

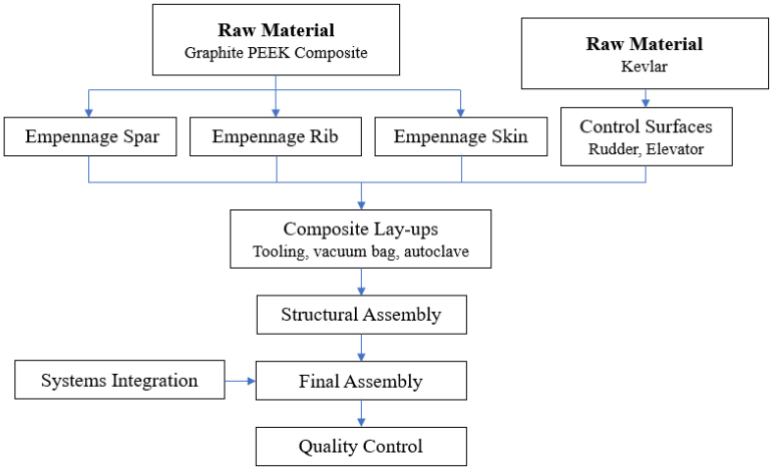

Figure 19.3: Empennage Assembly Flow Chart

Similar to the wing, the empennage substructure and skin will be manufactured out of graphite PEEK composites. And the empennage control surfaces including the elevators and rudders will be made of Kevlar.

Table 19.2: Empennage Material Selection

Component	Material
Spar	Graphite PEEK Composite
Rib	Graphite PEEK Composite
Skin	Graphite PEEK Composite
Elevator	Kevlar
Rudder	Kevlar

Similar to the rest of the aircraft, the fuselage substructure and skin will consist of graphite PEEK composites, and the armor surrounding the cockpit will consist of Kevlar. The simplicity of the material selection will mitigate any risks associated to material compatibility; however, the design relies largely on the availability of the two primary materials.

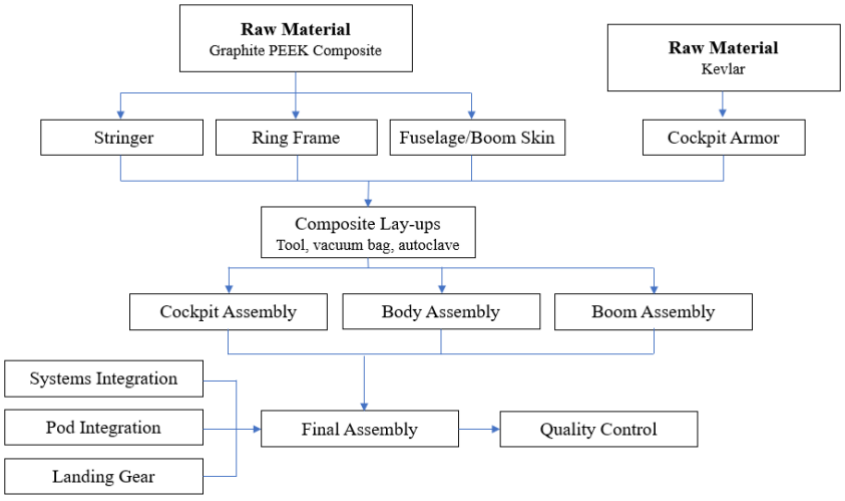

Figure 19.4: Fuselage Assembly Flow Chart

Table 19.3: Fuselage Material Selection

Component	Material
Ring Frame	Graphite PEEK Composite
Longeron	Graphite PEEK Composite
Stringer	Graphite PEEK Composite
Skin	Graphite PEEK Composite
Cockpit Armor	Kevlar

A detailed flow chart of the final aircraft assembly can be seen in Figure 19.5.

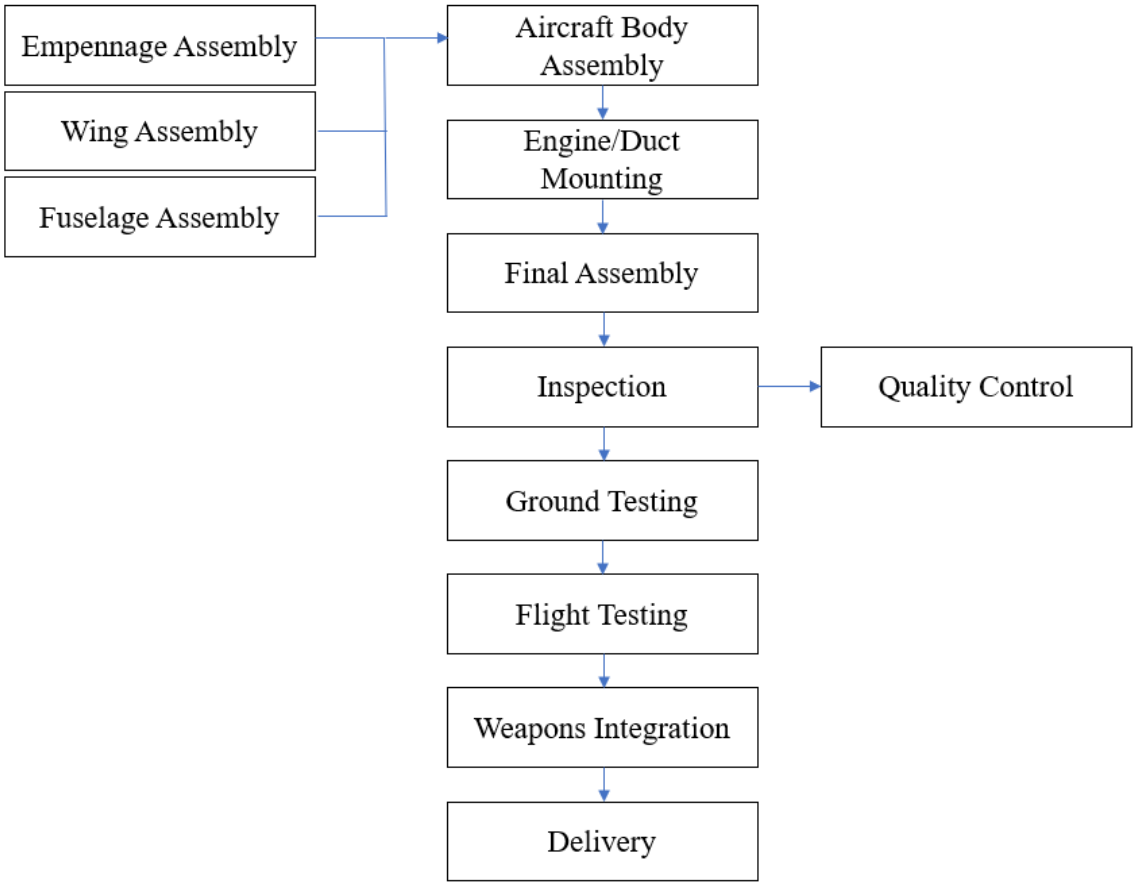

Figure 19.5: Aircraft Final Assembly Flow Chart

20 Compliance to Design Specification and TRL Considerations

The purpose of this chapter is to verify the compliance of the Swift Dragoon aircraft to the requirements and objectives outlined in the RFP, including TRL considerations. Table 20.1 shows the compliance matrix.

Table 20.1: Specification Compliance Matrix

Requirements: [R] = Mandatory Requirement, [O] = Goal	Specification of Requirement	Objective Met? (Chapter #)
[R] Austere Field Performance	Takeoff and landing over a 50 ft obstacle in ≤ 4,000 ft when operating from austere fields at density altitude up to 6,000 ft with semi-prepared runways such as grass or dirt surfaces with California Bearing Ratio of 5	Yes (14.1, 14.6)
[O] Survivability	Consideration for survivability, such as armor for the cockpit and engine, reduced infrared and visual signatures, and countermeasures	Yes (12.11, 17.2)
[R] Payload	3,000 lbs of armament	Yes (15)
[O] Weapons Provisions	Provisions for carrying/deploying a variety of weapons, including rail-launched missiles, rockets, and 500 lb (maximum) bombs	Yes (12.8, 12.9, 12.10)
[R] Gun	Integrated gun for ground targets	Yes (12.7)
[R] Service Life	15,000 hours over 25 years	Yes (18)
[R] Service Ceiling	≥ 30,000 ft	Yes (14.2)
[R] Crew	Two, both with zero-zero ejection seats	Yes (8.1, 12.11)
[R] Design Mission	Complete design mission with full payload requirement	Yes (5.26.1)
[R] Ferry Mission	Complete ferry mission with full crew and 60% payload	Yes (14.4)

Since TRL considerations were specifically mentioned in the RFP, the Dragoon uses critical technologies that are at TRL-8 or above. Table 20.2 shows critical technologies and their TRL.

Table 20.2: TRL for Critical Aircraft Systems

Technology	TRL	Technology	TRL
Graphite PEEK Composite	9	M242 Bushmaster	9
BASS Rounds	8	Gears for Cross-Shafting	9
Allison M250	9	Wescam MX-20D	9

References

1. Anon., “Austere Field Light Attack Aircraft; Request for Proposal,” 2020-2021 AIAA Foundation Undergraduate Team Aircraft Design Competition, pp. [online RFP], 1-6, URL: https://www.aiaa.org/get-involved/students-educators/Design-Competitions
2. Anon, “The Junkers Ju 87 Stuka. Part 2: Development,” *Aircraft Nut* [aircraftnut.blogspot.com/] 30 April, 2014.
3. Anon., “Junkers Ju 87,” *Wikipedia* [https://en.wikipedia.org/].
4. Srecko, “Henschel Hs 129 colors” *LETLETLETWARPLANES* [www.letletlet-warplanes.com/] 30 January, 2015.
5. Anon., “Henschel Hs 129,” *Wikipedia* [https://en.wikipedia.org/].
6. Anon., “Curtiss P-36 P-40 series drawings,” *Soyuyo* [soyuyo.main.jp/].
7. Anon., “Curtiss P-40 Warhawk,” *Wikipedia* [https://en.wikipedia.org/].
8. Anon., “Republic P-47 Thunderbolt,” *Aviastar* [www.aviastar.org/].
9. Anon., “Republic P-47 Thunderbolt,” *Wikipedia* [https://en.wikipedia.org/].
10. Anon., “Hawker ‘Typhoon’,” *War in the Skies*[www.warintheskies.com/].
11. Anon., “Hawker Typhoon,” *Wikipedia* [https://en.wikipedia.org/].
12. Anon., “Ilyushin Il-2 single-seater with VYa-23 guns (Il-2 model 1942)” *altervista* [https://massimotessitori.altervista.org/].
13. Anon., “Ilyushin Il-2,” *Wikipedia* [https://en.wikipedia.org/].
14. Gohin, Nicholas, “A-1H Skyraider,” *HyperScale* [www.hyperscale.com/].
15. Anon., “Douglas A-1 Skyraider,” *Wikipedia* [https://en.wikipedia.org/].
16. Armstrong, Ric, “Your Top 3 Aircraft,” *FlightAware Discussions* [https://discussions.flightaware.com/]
17. Anon., “North American Rockwell OV-10 Bronco,” *Wikipedia* [https://en.wikipedia.org/].
18. Anon., “Fairchild A-10 Thunderbolt II,” *Gaetan Marie’s Aviation Profiles* [www.gaetanmarie.com/]
19. Anon., “Fairchild Republic A-10 Thunderbolt II,” *Wikipedia* [https://en.wikipedia.org/].
20. Anon., “Embraer EMB 312 Tucano,” *Gaetan Marie’s Aviation Profiles* [www.gaetanmarie.com/]
21. Anon., “Embraer EMB 314 Super Tucano,” *Wikipedia* [https://en.wikipedia.org/].
22. Anon., “5.56x45mm NATO,” *Wikipedia* [https://en.wikipedia.org/].
23. Anon., “XM214 Microgun,” *Wikipedia* [https://en.wikipedia.org/].
24. Anon., “M60 machine gun,” *Wikipedia* [https://en.wikipedia.org/].
25. Anon., “Minigun image,” *PNGWING* [pngwing.com].
26. SoloA2., “Aircraft’s cannons,” *Deviant Art* [deviantart.com].
27. Anon., “Extremely Rare General Electric GAU-12/U 25mm Equalizer Desk Top Model, C. 1978,” *Worth Point* [worthpoint.com].
28. Anon., “NavWeaps Bofors 40mm,” *NavWeaps* [navweaps.com].
29. Murphy, Michael., “M102 105mm Towed Light Howitzer 1,” *flickr* [flickr.com]
30. Anon., “7.62x51mm NATO,” *Wikipedia* [https://en.wikipedia.org/].
31. Anon., “M134 Minigun,” *Wikipedia* [https://en.wikipedia.org/].
32. Anon., “M240 machine gun,” *Wikipedia* [https://en.wikipedia.org/].

33. Anon., ".50 BMG," *Wikipedia* [https://en.wikipedia.org/].
34. Anon., "M2 Browning," *Wikipedia* [https://en.wikipedia.org/].
35. Anon., "Profense PF 50," *Wikipedia* [https://en.wikipedia.org/].
36. Anon., "M39 cannon," *Wikipedia* [https://en.wikipedia.org/].
37. Anon., "20mm caliber," *Wikipedia* [https://en.wikipedia.org/].
38. Anon., "M61 Vulcan," *Wikipedia* [https://en.wikipedia.org/].
39. Anon., "M197 electric cannon," *Wikipedia* [https://en.wikipedia.org/].
40. Anon., "25mm caliber," *Wikipedia* [https://en.wikipedia.org/].
41. Anon., "GAU-12 Equalizer," *Wikipedia* [https://en.wikipedia.org/].
42. Anon., "GAU-8 Avenger," *Wikipedia* [https://en.wikipedia.org/].
43. Anon., "M230 chain gun," *Wikipedia* [https://en.wikipedia.org/].
44. Anon., "Shell Sizes," *Pinterest* [https://www.pinterest.com/pin/815081232537556103/].
45. Anon., "Mk44 Bushmaster II," *Wikipedia* [https://en.wikipedia.org/].
46. Anon., "Bofors 40mm gun," *Wikipedia* [https://en.wikipedia.org/].
47. Anon., "M102 howitzer," *Wikipedia* [https://en.wikipedia.org/].
48. Anon., "Mark 81 bomb," *Wikipedia* [https://en.wikipedia.org/].
49. Anon., "GBU-39 Small Diameter Bomb," *Wikipedia* [https://en.wikipedia.org/].
50. Anon., "Mark 82 bomb," *Wikipedia* [https://en.wikipedia.org/].
51. Anon., "Joint Direct Attack Munition," *Wikipedia* [https://en.wikipedia.org/].
52. Anon., "Zuni (rocket)," *Wikipedia* [https://en.wikipedia.org/].
53. Anon., "Hydra 70," *Wikipedia* [https://en.wikipedia.org/].
54. Anon., "Advanced Precision Kill Weapon System," *Wikipedia* [https://en.wikipedia.org/].
55. Anon., "AGM-114 Hellfire," *Wikipedia* [https://en.wikipedia.org/].
56. Anon., "AGM-65 Maverick," *Wikipedia* [https://en.wikipedia.org/].
57. Anon., "Harpoon (missile)," *Wikipedia* [https://en.wikipedia.org/].
58. Anon., "AGM-84H/K SLAM-ER," *Wikipedia* [https://en.wikipedia.org/].
59. Anon., "AGM-88 HARM," *Wikipedia* [https://en.wikipedia.org/].
60. Anon., "Penguin (missile)," *Wikipedia* [https://en.wikipedia.org/].
61. Anon., "AGM-176 Griffin," *Wikipedia* [https://en.wikipedia.org/].
62. Anon., "AGM-179 JAGM," *Wikipedia* [https://en.wikipedia.org/].
63. Roskam, J., *Airplane Design Part VIII: Airplane Cost Estimation: Design, Development, Manufacturing and Operating*, DARcorporation, Lawrence, KS, 2018.
64. Anon, "AT-6 Wolverine" [https://defense.txtav.com/].
65. Mease, Nigel, "Too Little for Too Much? Or A Lot for A Little? The Air Force OA-X Light-Attack Program," *CSIS: Center for Strategic & International Studies*, [https://www.csis.org/too-little-too-much-or-lot-little-air-force-oa-x-light-attack-program].

66. Mattock, Michael G., Beth J. Asch, James Hosek, and Michael Boito, *The Relative Cost-Effectiveness of Retaining Versus Accessing Air Force Pilots*, Santa Monica, CA, RAND Corporation, 2019 [https://www.rand.org/pubs/research_reports/RR2415.html. Also available in print form].
67. Roskam, J., *Airplane Design Part I: Preliminary Sizing of Airplanes*, DARcorporation, Lawrence, KS, 2018.
68. Barrett, R., "AE 522 Lecture Powerpoint Slides," Lawrence Kansas, 15 February, 2021.
69. Anon., "North American A-36 Apache," *Wikipedia* [https://en.wikipedia.org/].
70. Anon., "Bell P-39 Aircobra," *Wikipedia* [https://en.wikipedia.org/].
71. Anon., "Bell P-63 Kingcobra," *Wikipedia* [https://en.wikipedia.org/].
72. Anon., "Vought F4U Corsair," *Wikipedia* [https://en.wikipedia.org/].
73. Anon., "Breda Ba.64," *Wikipedia* [https://en.wikipedia.org/].
74. Anon., "A-36 Apache," *world war photos* [https://worldwarphotos.info/].
75. Anon., "Prototype Breda Ba.64," *SECRET PROJECTS* [https://www.secretprojects.co.uk/].
76. Fowles, Curtis, "The A-36," *MustangsMustangs* [mustangsmustangs.net/].
77. Osborn, Bill, "CONDOR 1:72 A-36 APACHE," *OoCities* [oocities.org/].
78. Anon., "Bell P-39 Airacobra," *Aviastar* [aviastar.org/].
79. Budge, Kent, "P-39 Airacobra, U.S. Fighter," *The Pacific War Online Encyclopedia* [pwencycl.kgbudge.com/].
80. Anon., "Bell P-63A Kingcobra," *Yanks Air Museum* [yanksair.org/].
81. Rickard, J., "Bell P-63 Kingcobra," *History of War* [historyofwar.org/].
82. Anon., "Free 3-View! Bell P-63 Kingcobra," *Flight Journal* [flightjournal.com/].
83. Anon., "Vought F4U1 'Corsair'," *War in the Skies* [warintheskies.com/].
84. Linn, James, "'Angels of Okinawa': The F4U Corsair," *National World War II Museum* [nationalww2museum.org/].
85. Anon., "F4U Performance," *WWII Aircraft Performance* [wwiiaircraftperformance.org/].
86. Anon., "Photos of the Cessna A-37 Dragonfly," *Photos of the Cessna A-37 Dragonfly* [www.tomhildrethphotos.com].
87. Anon., "Cessna A-37 Dragonfly," *Weapons and Warfare* [https://weaponsandwarfare.com/] 7, January 2021.
88. Anon., "Douglas A-4 Skyhawk," *Wikipedia* [https://en.wikipedia.org/].
89. Anon., "McDonnell Douglas A-4 Skyhawk," *Virtual Aircraft Museum* [www.aviastar.org/].
90. Anon., "A-4 Skyhawk," *FAS Intelligence Resource Program* [https://fas.org/].
91. Anon., "A4D (A-4) Skyhawk," *GlobalSecurity.org* [https://www.globalsecurity.org/].
92. Anon., "OV-10 Bronco," *FAS Intelligence Resource Program* [https://fas.org/].
93. Anon., "North American Rockwell OV-10 Bronco," [httpw://www.militaryfactory.com/].
94. Goebel, Greg, "The Rockwell OV-10 Bronco," [www.airvectors.net/].
95. Anon., "File:Fairchild A-10 Thunderbolt.svg," [https://commons.wikimedia.org/].
96. Wilkinson, Stephen, "A-10 Warthog: The Warplane Nobody Wanted," *HISTORYNET* [https://www.historynet.com].
97. Anon., "Virtual Aircraft Museum," *Embraer EMB-312 Tucano* [www.aviastar.org/].

98. Anon., “AD/A-1 SKYRAIDER ATTACK BOMBER,” *Boeing* [boeing.com/].
99. Goebel, Greg, “The Douglas AD / A-1 Skyraider,” *Air Vectors* [airvectors.net] 1, November 19.
100. Anon., “Cessna A-37 Dragonfly,” *Wikipedia* [https://en.wikipedia.org/].
101. Anon., “Embraer Super Tucano,” *aircraftcompare.com* [https://www.aircraftcompare.com].
102. Anon., “EMB-314 Super Tucano / ALX Trainer and Light Attack Aircraft,” *Airforce Technology* [https://www.airforce-technology.com/].
103. Anon., “Douglas AD-1 ‘Skyraider’,” *War in the Skies* [warintheskies.com/],
104. Anon., “KAI T-50 Golden Eagle,” *Wikipedia* [https://en.wikipedia.org/].
105. Anon., “Lockheed Martin T50 Golden Eagle,” *aircraftcompare.com* [https://www.aircraftcompare.com/].
106. Anon., “KAI T-50 Golden Eagle Bluepring,” *Blueprints* [https://drawingdatabase.com/].
107. Anon., “Designing the P-47 Thunderbolt,” *Air Force Magazine* [https://www.airforcemag.com/].
108. Anon., “aircraft minimum take off distance,” *WW2AIRCRAFT.NET* [https://ww2aircraft.net/].
109. Anon., “P-47 Thunderbolt, U.S. Fighter,” *The Pacific War Online Encyclopedia* [pwencycle.kgbudge.com/].
110. Anon., “Republic P-47 ‘*Thunderbolt*’” *WAR IN THE SKIES* [https://www.warintheskies.com/].
111. Anon., “Aermacchi MB-339,” *Wikipedia* [https://en.wikipedia.org/].
112. Anon., “Alenai Aermacchi M-346 Master,” *the-blueprint.com* [https://www.the-blueprints.com/].
113. Kaltokri, “MB-339 Basic Course (DCS),” *Open Flight School* [https://www.openflightschoole.de/].
114. Anon., “McDonnell Douglas AV-8B Harrier II,” *Wikipedia* [https://en.wikipedia.org/].
115. Anon., “AV-8B Harrier,” *FAS Military Analysis Network* [https://fas.org/].
116. Anon., “AV-8B Harrier,” *GlobalSecurity.org* [https://globalsecurity.org/].
117. Anon., “Alenia Aermacchi M-346 Master,” *Wikipedia* [https://en.wikipedia.org/].
118. Anon., “Alenia Aermacchi M-346,” *aircraftcompare.com* [https://www.aircraftcompare.com/].
119. Anon., “M-346 Master,” *GlobalSecurity.org* [https://www.globalsecurity.org/].
120. Anon., “The Flying Tank: Why One of the Most Produced Aircraft Just Disappeared After WWII,” *WAR HISTORY ONLINE* [https://www.warhistoryonline.com/].
121. Anon., “Sukhoi Su-25,” *Wikipedia* [https://en.wikipedia.org/].
122. Anon., “Su-25 (Su-28) Frogfoot Close-Support Aircraft,” *Airforce Technology* [https://www.airforce-technology.com/].
123. Anon., “Specifications Su-25,” *MILAVIA* [https://www.milavia.net/].
124. Anon., “AMX International AMX,” *Wikipedia* [https://en.wikipedia.org/].
125. Anon., “AMX Alenai AMX,” *SKYbrary* [https://www.skybrary.aero/].
126. Anon., “LTV A-7 Corsair II,” *Wikipedia* [https://en.wikipedia.org/].
127. Anon., “Ling-Temco-Vought (LTV) A-7E “Corsair II,” *MAPS AIR MUSEUM* [https://mapsairmuseum.org/].
128. Anon., “Henschel Hs 129,” *wikia.org* [https://world-war-2.wikia.org/].
129. Anon., “Henschel Hs 129,” *Virtual Aircraft Muesuem* [www.aviastar.org/].
130. Anon., “Henschel Hs 129,” *Henschel Hs 129* [www.historyofwar.org].
131. Anon., “Grumman A-6 Intruder,” *Wikipedia* [https://wikipedia.org].

132. Anon., “Grumman A-6 Intruder Attack Bomber,” *aerospaceweb.org* [www.aerospaceweb.org/].
133. Anon., “CASA C-101,” *Wikipedia* [https://wikipedia.org/].
134. Anon., “Casa C 101 Aviojet,” *BlueprintBox* [https://blueprintbox.com].
135. Anon., “Blackburn Buccaneer,” *BAE SYSTEMS* [https://wikipedia.org/].
136. Anon., “Blackburn Buccaneer,” *Wikipedia* [https://wikipedia.org/].
137. Anon., “Messerschmitt Bf 110,” *Wikipedia* [https://wikipedia.org/].
138. Anon., “Messerschmitt Bf 110,” *Virtual Aircraft Museum* [www.aviastar.org/].
139. Anon., “Douglas A-26 Invader,” *Wikipedia* [https://wikipedia.org/].
140. Anon., “Douglas A-26 Invader PDF ebook & Manuals,” *AIRWINGMEDIA.COM* [https://airwingmedia.com/].
141. Anon., “Hawker ‘Typhoon’,” *WAR IN THE SKIES* [www.warintheskies.com/].
142. Anon., “Ilyushin Il-10,” *Wikipedia* [https://wikipedia.org/].
143. Anon., “Ilyushin Il-10 Stormovik,” *the-blueprints.com* [https://www.the-blueprints.com/].
144. Anon., “Martin AM Mauler,” *Martin AM Mauler* [https://wikipedia.org/].
145. Anon., “SEPECAT Jaguar,” *SEPECAT Jaguar* [https://wikipedia.org/].
146. Anon., “SEPECAT Jaguar,” *SEPECAT Jaguar* [www.aviastar.org].
147. Anon., “Sukhoi Su-24,” *Wikipedia* [https://wikipedia.org/].
148. Anon., “Sukhoi Su-24 Fencer A,” *the-blueprints.com* [https://www.the-blueprints.com/].
149. Anon., “McDonnell Douglas F-4 Phantom II,” *Wikipedia* [https://en.wikipedia.org/].
150. Anon., “Mikoyan MiG-27,” *Wikipedia* [https://en.wikipedia.org/].
151. Anon., “Mikoyan MiG-27 Blueprint,” *Blueprints* [https://drawingdatabase.com].
152. Anon., “Breguet 693,” *Wikipedia* [https.//en.wikipedia.org/].
153. Anon., “IAT-93 Vultur,” *Wikipedia* [https://en.wikipedia.org/].
154. Anon., “IAR-93 Vultur,” *the-blueprints.com* [https://www.the-blueprints.com].
155. Anon., “Breda Ba.88,” *Wikipedia* [https://en.wikipedia.org/].
156. Anon., “Airplane and Helicopter Plans,” *Airplane and Helicopter Plans – Multi-View’s* [target4today.com].
157. Anon., “Martin Maryland,” *Wikipedia* [https.//en.wikipedia.org/].
158. Anon., “Martin 167 Maryland,” *the-blueprints.com* [https://www.the-blueprints.com/].
159. Anon., “Martin AM Mauler,” *Military Weapons* [https://www.militaryfactory.com/].
160. Anon., “Martin Baltimore,” *Wikipedia* [https://en.wikipedia.org/].
161. Anon., “Martin Baltimore,” *Military Weapons* [https://www.militaryfactory.com/].
162. Anon., “Soko G-2 Galeb,” *Wikipedia* [https://en.wikipedia.org/].
163. Anon., “FMA IA 58 Pucara,” *Wikipedia* [https://en.wikipedia.org/].
164. Anon., “Soko G-4 Super Galeb,” *Wikipedia* [https://en.wikipedia/].
165. Anon., “SOKO G-4 Super Galeb,” [www.aviaster.org/].
166. Anon., “IA-58 Pucara,” *AeroFred* [https://aerofred.com].
167. Anon., “Beechcraft T-6 Texan II,” *Wikipedia* [https://en.wikipedia.org/].
168. Anon, “Curtiss P-40 Tigershark-AVG-Tomohawk” *Fiddlersgreen* [www.fiddlersgreeen.net/].

169. Anon, “Warhawk,”Curtiss P-40 Wayhawk” *Military Factory* [https://www.militaryfactory.com/].
170. Anon., “NAMMO AMMUNTION HANDBOOK Edition 5, 2018”
171. Barrett, R., “AE 522 Lecture Powerpoint Slides,” Lawrence Kansas, 25 February 2021.
172. Hess, Derek, “PGU SERIES 20MM AMMUNITION FOR THE F-15,” Eglin AFB Florida
173. Anon., “M3 .50 Caliber Machine Gun,” *GlobalSecurity.org* [https://www.globalsecurity.org/].
174. Anon., “GAU-8 Avenger,” *FAS Military Analysis Network* [https://fas.org/].
175. Barrett, Ronald M. & Schumacher, Lauren N., “Maneuvering Aeromechanically Stable Sabot System.” International Patent WO2020/217227 A2. October 29, 2020.
176. Anon., “Wescam MX-20D Fully Digital High Definition”
177. Roskam, J., *Airplane Design Part V: Component Weight Estimation*, DARcorporation, Lawrence, KS, 2018.
178. L. Vertuccio, F. De Santis, R. Pantani, K. Lafdi, L. Guadagno, “Effective De-icing Skin Using Graphene-Based Flexible Heater,” *Composites Part B: Engineering*, Volume 162, Pages 600-610, April 1, 2019 [https://doi.org/10.1016/j.compositesb.2019.01.045].
179. Anon., “M242 Bushmaster,” *Wikipedia* [https://en.wikipedia.org/].
180. Anon., “GAU-19,” *Wikipedia* [https://en.wikipedia.org/].
181. Tegler, E., “Northrop-Grumman’s Sky Viper Chain Gun May Get A Shot At The Army’s FARA Helicopter,” [https://forbes.com].
182. Anon., “In Stock 50 BMG Ammo,” *Wikiarms* [https://www.wikiarms.com/group/50BMG].
183. Anon., “Exhibit P-40, Budget Line Item Justification: PB 2019 Air Force,” *Department of the Air Force* [https://www.dacis.com/].
184. Barret, Ronald M., Technical Conversation, Lawrence, KS, April 15, 2021.
185. Anon., “AIM-9 Sidewinder,” *Wikipedia* [https://en.wikipedia.org/].
186. Borys, D., Technical Conversation, Lawrence, KS, March 26, 2021.
187. Anon., “South African Missiles/Rockets/PGM’s-Prototypes, Projects, Concepts, etc.,” *Secret Projects* [https://www.secretprojects.co.uk/].
188. Roskam, J., *Airplane Design Part II: Preliminary Sizing of Airplanes*, DARcorporation, Lawrence, KS, 2018.
189. Roskam, J., *Airplane Design Part III: Layout Design of Cockpit, Fuselage, Wing, and Empennage: Cutaways and Inboard Profiles*, DARcorporation, Lawrence, KS, 2018.
190. Roskam, J., *Airplane Design Part IV: Layout Design of Landing Gear and Systems*, DARcorporation, Lawrence, KS, 2018.
191. Roskam, J., *Airplane Design Part VI, Preliminary Calculation of Aerodynamic, Thrust, and Power Characteristics*, DARcorporation, Lawrence, KS, 2018.
192. Roskam, J., *Airplane Design Part VII: Determination of Stability, Control and Performance Characteristics: FAR and Military Requirements*, DARcorporation, Lawrence, KS, 2018.
193. Rolls-Royce, “M250 Turboprop,” [M250 turboprop – Rolls-Royce]